~~B. I. SPINRAD
AUG 1960
DIRECTOR
REACTOR ENGINEERING DIVISION~~

ANL-6145

Return

0391

Argonne National Laboratory

CHEMICAL ENGINEERING DIVISION SUMMARY REPORT

January, February, March, 1960

ANL-6145
Chemistry - Separation Processes
for Plutonium and Uranium
(TID-4500, 15th Ed.)
AEC Research and
Development Report

0391

ARGONNE NATIONAL LABORATORY
9700 South Cass Avenue
Argonne, Illinois

CHEMICAL ENGINEERING DIVISION SUMMARY REPORT

January, February, March, 1960

Stephen Lawroski, Division Director
W. A. Rodger, Associate Division Director
R. C. Vogel, Associate Division Director
V. H. Munnecke, Assistant Division Director

Preceding Quarterly Reports:
ANL-6101 October, November, December, 1959
ANL-6068 July, August, September, 1959
ANL-6029 April, May, June, 1959

Operated by The University of Chicago
under
Contract W-31-109-eng-38

TABLE OF CONTENTS

LIST OF TABLES

LIST OF TABLES

LIST OF TABLES

LIST OF FIGURES

LIST OF FIGURES

LIST OF FIGURES

LIST OF FIGURES

CHEMICAL ENGINEERING DIVISION
SUMMARY REPORT

January, February, March, 1960

SUMMARY

I. Chemical-Metallurgical Processing (pages 19-89)

A direct-cycle fuel-reprocessing plant using pyrometallurgical procedures is being designed as part of the Experimental Breeder Reactor No. II (EBR-II) project. A Laboratory and Service Building, construction of which is very nearly complete, is also included. Melt refining, liquid metal extraction, and processes involving fractional crystallization from liquid metal systems are being examined for the recovery and purification of EBR-II fuels. Based on these studies, process equipment is being designed and tested.

Construction of the EBR-II Fuel Cycle Facility Building, which stopped in December and will resume with the first ground thaw, is about 8 per cent complete as of March 15, 1960. Construction of the Laboratory and Service Building is 95 per cent complete.

Twenty-four more enriched fuel ingots for EBR-II fuel manufacture have been produced in the Mark-V mock-up furnace. Fifty-eight ingots have been produced to date.

Preparations for demonstrating the melt-refining process to be used for recovery of EBR-II fuel with highly irradiated fuel material continued. Equipment to be used in these runs has been put through 200 hours of dummy runs and all components have operated satisfactorily. Prolonged air exposure of the pins will be avoided, since this was shown to affect yields adversely.

Oxidation of melt-refining skulls by an oxygen-argon mixture is a convenient and efficient method of removing them from the zirconia melt-refining crucibles. The product of the oxidation treatment is a free-flowing powder which can be poured from the crucible. Laboratory studies have shown that complete oxidation is accomplished in 5 to 6 hours at temperatures above 700 C.

The reduction of uranium oxide has been investigated, using pure magnesium and solutions of magnesium in zinc and cadmium. At higher magnesium concentrations, and with the addition of zinc to the system, high reduction yields were demonstrated. A high yield was also obtained when pure magnesium was used as the reducing agent at a temperature of 850 C. Fused-salt fluxes have frequently been used to promote mixing of the uranium oxide and liquid metal and to remove the magnesium oxide product from the system. These fluxes have consisted primarily of chloride salts. Brief studies of metaphosphate fluxes indicated that they are unattractive for use in this application.

Cadmium solutions of uranium were shown to be stable in Types 405 and 410 steel containers at temperatures of up to 550 C. At a temperature of 700 C, uranium was removed from cadmium solution, presumably by interaction with the steel. Graphite similarly scavenged uranium from a cadmium solution. Cadmium solutions of uranium exposed to nitrogen were unaffected.

The liquid metal corrosion loop in which a uranium-magnesium-cadmium alloy is being circulated at 550 C has now been in trouble-free operation for 3000 hours. Over this period, the uranium concentration has dropped from about 0.94 to 0.85 per cent.

Recovery of plutonium from magnesium solution by distillation of the magnesium, the final step of a blanket process, was demonstrated on a 1-g plutonium scale.

Fundamental physicochemical data are lacking for many liquid metal systems of interest. For example, the solubilities of a number of elements in liquid metal systems are unknown and must be measured.

The solubility of thorium in liquid cadmium was measured over the temperature range from 325 to 600 C.

The solubility of cobalt in liquid cadmium was found to range from 1.9×10^{-3} per cent at 348 C to 1.8×10^{-2} per cent at 658 C.

The solubility of manganese in liquid cadmium was found to range from 0.27 per cent at 414 C to 1.43 per cent at 661 C.

The solubility of nickel in liquid cadmium has been measured, most of the data being obtained above the incongruent melting point of the γ-brass phase. The new data indicate this incongruent melting point to be 496 C.

Additional studies of the niobium-zinc system in the range from 428 to 750 C have indicated the existence of three (possibly four) intermetallic compounds.

The compound in equilibrium with the melt in the range from 478 to 750 C has been identified as $NbZn_3$.

The partition of uranium between liquid aluminum and liquid cadmium has been studied as a function of uranium concentration. The distribution coefficient (atom per cent uranium in cadmium-rich phase/atom per cent uranium in aluminum-rich phase) varied from 2.8×10^{-5} to 4.6×10^{-5} as the concentration in the aluminum phase varied from 0.57 to 0.13 atom per cent. The activity coefficient of uranium in pure aluminum is about 1.29×10^{-3} at 688 C.

The reaction of solid aluminum with a liquid cadmium solution containing uranium, zirconium and cerium was studied. The concentrations of both uranium and zirconium were reduced practically to zero within a few hours of reaction, while the cerium concentration was only decreased by about 16 per cent.

The free energy of formation of the uranium-lead intermetallic compound UPb_3 was measured between 374 and 846 C by means of a galvanic cell method.

Magnetic susceptibility measurements on the intermetallic compound $CeCd_{11}$ have been made over a range of temperature from 4 to 295 K.

II. Fuel Cycle Applications of Volatility and Fluidization Techniques (pages 90-133)

The volatilities of uranium and plutonium hexafluorides are the bases for various volatility schemes proposed for processing irradiated fuels. These schemes include a Direct Fluorination Process, the Aqueous Dissolution Fluorination (ADF) Process and the Fused Fluoride Volatility Process. A firm knowledge of the chemistry of fluorine and fluorine compounds, fluidization and volatility separations techniques are important in the development of the separation processes. Application of fluidization techniques is also being made to preparation of uranium compounds.

The Direct Fluorination Process is currently aimed toward the processing of the Zircaloy-clad, uranium dioxide fuel typical of the Dresden Reactor. Equipment has been constructed from which information can be obtained to substantiate a process flowsheet in regards to plutonium hexafluoride transfer, fluorination of uranium and plutonium oxide mixtures, and separation of uranium and plutonium hexafluorides. The use of sulfur tetrafluoride as a fluorinating agent is being investigated in reactions with uranium tetrafluoride, uranium dioxide, U_3O_8, uranium trioxide, uranyl fluoride, plutonium dioxide, and plutonium tetrafluoride.

One approach to the separation of this hexafluoride utilizes the preferential reduction of the more chemically reactive plutonium hexafluoride by sulfur tetrafluoride.

The direct fluorination of dense uranium dioxide pellets submerged in an inert fluidized medium was carried out in a 3-inch reactor at 500 C at fluorine concentrations up to 30 per cent. Negligible fines were produced with a 3-inch pellet bed under the conditions used, although substantial amounts of fines were found in deeper beds. Uranyl fluoride was identified as the major species in the fines. The reaction rate was found to be directly proportional to fluorine concentration. The concentration of unreacted fluorine in the offgas decreased approximately exponentially with bed height, with corresponding increase in overall fluorine efficiency. The formation of solid intermediate uranium compounds was observed in the case of pellet beds deeper than three inches.

Experimental work has continued to determine the mechanism of the nickel-fluorine reaction. As a means of checking the validity of the experimental method, both oxidation and fluorination reactions have been used. The results indicate that the mechanism for the nickel-fluorine reaction is one in which fluorine migrates through the nickel-fluorine film.

In the development of the ADF process, current emphasis is being directed toward recovery of uranium from low uranium-Zircaloy-2 fuel alloys. Major process steps are aqueous dissolution of the fuel, fluid-bed drying of the solution to a dry powder, and fluorination of the powder to remove and recover the uranium as the hexafluoride. The use of additional anhydrous hydrogen fluoride as part of the fluidizing gas during drying did not lower the residual oxygen and water contents of the dryer products, whereas a separate hydrofluorination step carried out at slightly higher temperatures (450 C) eliminated about two-thirds of these components. A jet-target grinder capable of higher attrition rates than the ordinary attrition jets was successful in stabilizing the particle size distribution during the recent dryer studies.

A new 2-inch diameter, 6-foot tall, static-bed fluorination reactor was installed and operated to gain additional information on the effects of powder (cake) depth on fluorine efficiency and pressure drop. Other experiments explored alternate "dry" fluorination processes, such as direct contact of the metal with gaseous reactants to eliminate the aqueous dissolution step. A mixture of hydrogen fluoride and hydrogen chloride appears promising for gas-phase conversion of zirconium-base fuels to fluoride compounds.

A series of four dissolutions was carried out semicontinuously in the graphite pilot plant dissolver according to the Fused Salt Fluoride Volatility Process flowsheet. In this process uranium-zirconium matrix fuel is dissolved in molten fluoride salts at 600 to 700 C with a hydrogen fluoride sparge. Partial salt transfers and salt makeup are carried out between dissolutions. Dissolution rates up to 2.3 mg/(min)(sq cm), or about 9 mils/hr, were obtained. Zirconium-uranium plate-type fuel elements were carried to 90 per cent dissolution in as little as six hours. Graphite heaters and other components functioned satisfactorily.

Additional studies of the one-step fluid-bed process for the conversion of uranium hexafluoride to uranium dioxide with steam and hydrogen confirmed the fact that this gas-gas reaction is very rapid and that it results in the formation of intermediate fluoride solids. Current uranium hexafluoride feed rates are up to 60 g/min [equivalent to 105 lb uranium/(hr)(sq ft reactor cross section)]. Material of lower residual fluoride content is produced when greater excesses of reactants, higher temperatures and longer residence times are used.

A method for achieving controlled downward transport of solids in multistage fluidized bed reactors using external vibrators without the use of internal downcomers is being investigated in a six-inch diameter, 3-stage Pyrex and metal unit. The effects of induced vibrational frequency, type of frequency transmitter, vibrator on-time, feed particle size and particle size distribution on throughput using an air-glass bead system were determined.

III. Reactor Safety (pages 134-175)

The oxidation, ignition, and combustion processes of uranium, zirconium, thorium, and plutonium are being studied in order to provide information leading to an understanding of the reactions. This knowledge should make it possible to minimize the hazards associated with handling these nuclear reactor materials.

Since one of the most common hazards involves the ignition and burning of chips and turnings from machining operations, considerable effort has been directed toward understanding the combustion processes. Although chips and turnings have irregular cross sections and are not uniform along their lengths, it has been demonstrated that comparable results are obtained with either turnings or foil strips. Studies of the propagation of burning along foil strips have provided a method for more carefully appraising the effects of many variables on the combustion process.

Although gas contaminants of moisture, carbon dioxide, and ozone have very limited effects, the character of burning propagation of both uranium and zirconium in air is considerably altered by the presence of 5 per cent chlorobromomethane or chlorodifluoromethane (Freon 22). For 0.13-mm thick uranium, the propagation rate, the extent of reaction, and the burning temperature are all markedly reduced. Pure zirconium foil, 0.13-mm thick, would not sustain burning in air contaminated with these agents. Even the 14.9 atom per cent titanium-zirconium alloy foil, which normally burned rapidly in air, would not sustain burning in air contaminated with 5 per cent Freon 22 and showed considerably reduced propagation rate, burning temperature, and burning zone length in air contaminated with 5 per cent chlorobromomethane. The effects of uranium combustion were shown to be uniformly dependent on the concentration of the agent present in the range up to 9 per cent. In an effort to identify more precisely the mechanism by which these halogenated compounds lower the burning propagation rate of uranium, several other agents such as carbon tetrachloride, dibromomethane, ethyl bromide, and difluoridibromomethane were also studied.

Because of the common use of aluminum and silicon in conjunction with uranium in nuclear reactors, the study of the effect of small quantities of these elements in uranium was extended. The ignition temperatures in oxygen of 8.5-mm uranium cubes containing greater than 75 parts per million of either aluminum or silicon or as a combined total are markedly decreased.

Preliminary ignition experiments with plutonium demonstrated that useful ignition data for plutonium and its alloys can be obtained by burning-curve or shielded ignition experiments. Burning-curve experiments in air and in oxygen on samples with varied impurity content indicate a gradual increase of ignition temperature with increasing purity below approximately 1000 ppm. The ignition temperature of plutonium appears not to be strongly influenced by iron content but is strongly influenced by carbon content.

Because of the importance of uranium powders and the need for extension of the specific area relationship, an investigation of the ignition of metal powders is being carried out. Ignition temperatures of specially prepared uranium powder which has essentially spherical particles confirm the strong dependence on specific area or particle size and to a lesser extent on sample weight. The agreement of the data for samples greater than 0.5 gram with ignition temperatures calculated on the basis of equations derived from bulk oxidation data, heats of formation, and particle size indicates the possibility of defining a fundamental relationship.

Ignition temperatures of a variety of metal foils have been determined by shielded ignition experiments. The relationships between the logarithm of the specific area and the reciprocal ignition temperature for titanium, iron, and molybdenum in addition to uranium and zirconium appear to follow the equation

$$\log S = \log I + (E/2.3\ RT).$$

Further consideration of how values of I are related to oxidation kinetic data and thermal and physical properties of the metals should result in a more general understanding of metal-ignition behavior.

The experimental program to determine rates of reaction of molten reactor fuel and cladding metals with water is continuing. The principal laboratory-scale method involves the rapid melting and dispersion of metal wires in a water or steam environment by a surge current from a bank of condensers. A series of runs with 30-mil uranium wires was completed. Runs up to initial temperatures of 2200 C showed relatively slow rates of pressure rise and up to 20 per cent reaction. Runs with initial temperatures above 2500 C showed an explosive pressure rise and up to 30 per cent reaction. The change in character of the reaction rate of uranium was not as abrupt as for zirconium. The data for extent of reaction as a function of initial temperature for 30-mil wires were nearly identical to those reported previously for 60-mil wires. This suggests that a linear rate law may be applicable.

A second laboratory-scale method involves the rapid contact of steam with heated metal. In this method, the metal receives a "pressure pulse" of water vapor. A series of preliminary runs with liquid zirconium in the range from 1850 to 2100 C and water vapor at 20 mm was completed. Tentative results indicated that the liquid metal followed the parabolic rate law.

A series of twelve experiments has been conducted in the TREAT reactor. In these experiments, a stainless steel autoclave containing a fuel pin, gold foils, helium and water was subjected to a short burst of neutrons. The pins were 20 per cent enriched uranium completely clad in Zircaloy-2 cans. Small defects in the form of 3- and 15-mil holes were introduced into the clad before the runs. Reactor transients up to 60 megawatt-seconds caused partial melting of uranium and bursting or bulging of the Zircaloy can. More energetic transients caused up to 20 per cent of the uranium to be dispersed into fragments and fine particles. Very energetic transients in the range from 90 Mw-sec to 175 Mw-sec caused complete melting of the core and cladding and extensive spraying of metal and fine particle production. Up to 10 per cent of the uranium reacted with water under these conditions.

A relation between the total energy of the reactor transient and the energy absorbed by the pin was derived from the data. A preliminary correlation of all the TREAT runs to date is presented. This correlation will be the basis for a more extensive analysis on the analog computer.

IV. Reactor Chemistry (pages 176-191)

Data are being obtained on the neutron capture cross sections of uranium-236 as a function of neutron energy.

Work continues on development of a Boiling Slurry Reactor concept (described in ANL-6101, page 160). Problems being examined include preparation of spherical thoria-urania particles and determination of physical properties of thoria-urania materials.

The Reactor Decontamination Program is directed principally to boiling water reactors. It is concerned with the consequences of a fuel element rupture; how much and what types of fission products will be expected to be deposited on the internal surfaces of the reactor system, and what methods are available for removing these deposited activities should this become necessary.

A stainless steel loop simulating the action of a boiling water reactor has been operated with yttrium-90 and cesium-137 tracer activities. Activity deposted is monitored internally on metal samples removed following operation, and externally with a gamma scintillation spectrometer coincident with operation. The latter allows study of the time parameter. Runs to date have been made principally at 200 psig with steam velocities of 0.8 and 1.2 feet per second of from 4.5 to 144-hour duration. A minimum of activity deposition occurs consistently at elevations of 35 to 45 inches above the liquid level.

Laboratory studies are being directed toward corrosion behavior of the alkaline permanganate-citrate procedure toward turbine and other materials, and the selection and evaluation of adequate foaming agents for the transportation of liquid decontaminants with foam techniques. Recent experiments have shown that an overpressure of either hydrogen or oxygen (considerably in excess of that to be expected in reactor operation) during the contamination cycle reduces the decontamination obtained with the alkaline permanganate-citrate procedure.

A program of research directed toward the selection and evaluation of materials for nuclear superheaters has been initiated. Fundamental studies have begun of the corrosion of metals in superheated steam at temperatures up to 560 C and pressures up to 65 atm. Initial phases of the work will concentrate on the effects of simulated radiolytic hydrogen and oxygen in the steam phase.

V. Routine Operations (page 192)

The operation of the radioactive waste-processing facility and the gamma-irradiation facility continued without incident.

I. CHEMICAL-METALLURGICAL PROCESSING

A direct cycle fuel-reprocessing plant using pyrometallurgical procedures is being designed as part of the Experimental Breeder Reactor No. II (EBR-II) project. A Laboratory and Service Building, construction of which is very nearly complete, is also included. Melt refining, liquid metal extraction, and processes involving fractional crystallization from liquid metal systems are being examined for the recovery and purification of EBR-II fuels. Based on these studies, process equipment is being designed and tested.

Preparations are being made for resuming construction of the EBR-II Fuel Cycle Facility building. Construction stopped in December and will resume with the first ground thaw.

The Model 8 manipulator being built by AMF for the Junior Caves of the Laboratory and Service Building was inspected and tested. Eight of the 12 units ordered are promised for shipment by the last of March. The six Junior Cave windows for the Laboratory and Service Building were inspected in January. In February the windows were shipped to Idaho and are presently in storage at the site.

The five-ton cranes for the Fuel Cycle Facility were inspected and tested the last of February. A number of features were unacceptable; these will be corrected by the manufacturer, after which the cranes will be inspected and tested again. Bids for the eight operating manipulators have been received and are being evaluated.

Glass production work for the Fuel Cycle Facility process cell windows is entering the last phase. Work is about 80 per cent complete. Steel fabrication work for window components was recently set back by the discovery of some porous welds, which will require rework for correction. All of the wall mounts for the cell lighting luminaires have been completed. Inspection revealed minor defects which will be corrected. A number of miscellaneous equipment items for the Fuel Cycle Facility are being worked on. Design of a degassing furnace has been completed. The fuel transfer coffin design is underway. All preliminary sketches for the induction-heating motor-generator installation have been completed.

MI cable samples with ceramic end seals have been irradiated to 1.18×10^{10} rad. The tests have been terminated and the insulation resistance is still greater than 200 megohms. Irradiation tests of the 54-conductor manipulator power cable have started. The cable is being irradiated in small dose increments and is being stressed between doses.

Some remote-maintenance procedures for the operating manipulator have been demonstrated in the EBR-II mockup area. All motor-drive units have been removed and replaced, using another manipulator. A number of minor flaws have developed in the operating manipulator in the mock-up area. These are being corrected and the experience gained is being applied to the design of the units for the plant.

Twenty-four more enriched fuel ingots for EBR-II fuel manufacture have been produced in the Mark-V mockup furnace. Fifty-eight ingots have been produced to date. During these runs, information on the life of components is being acquired.

Preparations for demonstrating the melt-refining process to be used for recovery of EBR-II fuel with highly irradiated fuel material continued. Demonstration runs involving 400-gram batches of fuel irradiated to one per cent burnup will be made in the Senior Cave Facility to confirm fission product behavior. Equipment to be used in these runs has been put through 200 hours of dummy runs and all components have operated satisfactorily. Prolonged air exposure of the pins will be avoided, since this was shown to affect yields adversely. Equipment is under construction for studying the release of gaseous fission products from highly irradiated fuel material during heating and melting.

By avoiding all exposure of sodium-coated pins to air, oxide films and pin shells were eliminated on melting. This is an encouraging result which indicates that, under the expected inert atmosphere conditions in the plant, the pin shell problem may not exist.

Silicon carbide powder (1000-mesh) and carbon black were found to be highly effective insulating materials for use in a melt-refining assembly. Both are compatible with a graphite susceptor and would be superior to the presently used zirconia grain which reacts with graphite to produce carbon monoxide.

Oxidation of melt-refining skulls by an oxygen-argon mixture is a convenient and efficient method of removing them from the zirconia melt-refining crucibles. The product of the oxidation treatment is a free-flowing powder which can be poured from the crucible. Laboratory studies have shown that complete oxidation is accomplished in 5 to 6 hours at temperatures above 700 C. The rate of the reaction is easily controlled by dilution of the oxygen with argon. During the oxidation, over 50 per cent of the molybdenum present is volatilized, probably as the trioxide, at temperatures exceeding 850 C. Ruthenium is also volatilized under similar conditions, but only in a flowing stream of oxygen. Earlier results which indicated that ruthenium was not volatilized during the oxidation were found to be erroneous, due to a sampling problem.

The reduction of uranium oxide has been investigated, using pure magnesium and solutions of magnesium in zinc and cadmium. One of the principal problems encountered in a study of the system is the difficulty in finding suitable analytical methods for following the reduction yields. In cadmium solutions containing low magnesium concentrations, impurities such as iron, nickel, silicon and aluminum result in precipitation of the uranium in the form of intermetallic compounds. These impurities are introduced by container materials in many instances. At higher magnesium concentrations, and with the addition of zinc to the system, high reduction yields were demonstrated. A high yield was also obtained when pure magnesium was used as the reducing agent at a temperature of 850 C. Fused-salt fluxes have frequently been used to promote mixing of the uranium oxide and liquid metal and to remove the magnesium oxide product from the system. These fluxes have consisted primarily of chloride salts. Brief studies of metaphosphate fluxes indicated that they are unattractive for use in this application.

Cadmium solutions of uranium were shown to be stable in Types 405 and 410 steel containers at temperatures of up to 550 C. At a temperature of 700 C, uranium was removed from cadmium solution, presumably by interaction with the steel. Graphite similarly scavenged uranium from a cadmium solution. Cadmium solutions of uranium exposed to nitrogen were unaffected.

Construction of the full-scale distillation equipment was continued. Construction of a smaller unit for testing some of the design concepts was completed. Experiments were conducted which showed close agreement between the temperature at the surface of a boiling metal and that calculated from the pressure in the condenser.

Retorting studies have shown that little difficulty is encountered in removing uranium from ceramic retorting crucibles or ceramic-coated graphite of metal crucibles.

Equipment items for liquid metal service tested during the last quarter include a fixed liquid-level probe, autoresistively heated transfer lines, and samples.

The liquid metal corrosion loop in which a uranium-magnesium-cadmium alloy is being circulated at 550 C has now been in trouble-free operation for 3000 hours. Over this period, the uranium concentration has dropped from about 0.94 to 0.85 per cent.

Recovery of plutonium from magnesium solution by distillation of the magnesium, the final step of a blanket process, was demonstrated on a 1-g plutonium scale. Runs at a 100-gram scale will be carried out next quarter.

Fundamental physicochemical data are lacking for many liquid metal systems of interest. For example, the solubilities of a number of elements in liquid metal systems are unknown and must be measured. The solubility of thorium in liquid cadmium was measured over the temperature range from 325 to 600 C. The data fit the equation

$$\log\,(\text{atom per cent thorium}) = 9.620 - 15.358\,\frac{10^3}{T} + 3.175\,\frac{10^6}{T^2}\;.$$

The solubility of cobalt in liquid cadmium was found to range from 1.9×10^{-3} per cent at 348 C to 1.8×10^{-2} per cent at 658 C.

The solubility of manganese in liquid cadmium was found to range from 0.27 per cent at 414 C to 1.43 per cent at 661 C.

The solubility of nickel in liquid cadmium has been measured, most of the data being obtained above the incongruent melting point of the γ-brass phase. The new data indicate this incongruent melting point to be 496 C.

Additional studies of the niobium-zinc system have indicated the existence of three (possibly four) intermetallic compounds. Solubilities for two of the compounds may be represented by the equations

$$(428 \text{ to } 478\,\text{C})\ \log\,(\text{atom per cent niobium}) = 5.029 - (4.749 \times 10^3/T)$$

$$(478 \text{ to } 750\,\text{C})\ \log\,(\text{atom per cent niobium}) = 5.925 - (10.938 \times 10^3/T) + 4.142\ 10^6\ T.$$

The compound in equilibrium with the melt in the range from 478 to 750 C has been identified as $NbZn_3$.

The partition of uranium between liquid aluminum and liquid cadmium has been studied as a function of uranium concentration. The distribution coefficient (atom per cent uranium in cadmium rich phase/atom per cent uranium in aluminum rich phase) varied from 2.8×10^{-5} to 4.6×10^{-5} as the concentration in the aluminum phase varied from 0.57 to 0.13 atom per cent. The activity coefficient of uranium in pure aluminum is about 1.29×10^{-3} at 688 C.

The reaction of solid aluminum with a liquid cadmium solution containing uranium, zirconium and cerium was studied. The concentrations of both uranium and zirconium were reduced practically to zero within a few hours of reaction, while the cerium concentration was only decreased by about 16 per cent.

The free energy of formation of the uranium-lead intermetallic compound UPb_3 was measured by means of a galvanic cell method. The values between 374 and 846 C may be represented by the equation

$$\Delta F = -23{,}460 + 21.61\,T - 1.899\ 10^{-2}\,T^2 + 9.721\ 10^{-6}\,T^3\ \text{cal/mole.}$$

Magnetic susceptibility measurements on the intermetallic compound $CeCd_{11}$ have been made as a function of temperature. The reciprocal of the susceptibility contributed by the cerium atoms was found to be approximately linear with absolute temperature. The effective number of Bohr magnetrons (M_{eff}) computed from the slope was 2.58, which may be compared with a theoretical value of 2.56 for a Ce^{+3} ion in a $^2F_{5/2}$ state. Examination of the temperature dependence suggests that the Curie law holds above 77 K, but that a more complex relation may hold at lower temperatures.

The rotating bomb calorimeter has been calibrated with two different bombs during this period: a platinum-lined bomb for combustions in oxygen and a nickel bomb for combustions of boron in fluorine.

The study of experimental conditions for the satisfactory combustion of tungsten disulfide in oxygen are being continued on a part-time basis. Calorimetric combustions of crystalline boron in fluorine are being carried out and exploratory studies of techniques for burning some soft metals (magnesium, aluminum, zinc and cadmium) in fluorine have been started.

The design, construction, installation and testing of the new fluorine still are complete. Two distillations of fluorine in the still have shown that (1) in a single distillation, fluorine of greater than 99.9 per cent purity can be obtained, (2) the purification can be accomplished in less than 20 hours, and (3) the probable yield of the still will be approximately 75 per cent of the starting material. Each one of these represents considerable improvement over the performance of the first still.

A preliminary series of four calorimetric combustions of zirconium in fluorine has been completed. The data lead to a value for the standard heat of formation of zirconium tetrafluoride of $\Delta H_{f298.15} = -453.8 \pm 0.4$ kcal/mole. The value estimated by Brewer et al.,[1] is -445 ± 30 kcal/mole.

A. Fuel-processing Facilities for EBR-II

1. Design, Development and Construction of Buildings and Equipment

The Fuel Cycle Facility and the Laboratory and Service Building have been described in previous quarterly reports (ANL-5789 and ANL-5820). The former will be used for the processing of EBR-II fuel and the latter will provide radiochemical analytical and related facilities for the entire Idaho Division of Argonne National Laboratory. The architect-engineer is the H. K. Ferguson Company, Cleveland, Ohio.

---

[1] Brewer, L., Bromley, L. A., Gilles, P. W., and N. L. Lofgren, National Nuclear Energy Series, IV-19B, L. L. Quill, Editor, McGraw-Hill Book Company, Inc., New York (1950) p. 76.

a. Status of Laboratory and Service Building Construction and Equipment

(G. J. Bernstein, A. A. Chilenskas, T. W. Eckels)

The building is approximately 95 per cent complete.

The production model of the AMF Atomics Model 8 manipulator was inspected and tested in January 1960. Eight units of the 12 ordered are promised for shipment on March 23, 1960. Fabrication of the acid-fuming scrubber for the Junior Caves is complete and the unit will be tested for efficiency by the Industrial Hygiene and Safety Division The mockup of the Waste Solidification Cell equipment has been tested successfully and equipment items have been shipped to Idaho. A rough draft of a report covering the procedures and the equipment for radioactive waste disposal at the EBR-II site has been completed. Additional information concerning the details of equipment and facilities is being assembled for inclusion in this report.

The six Junior Cave windows were inspected at the vendor's point of assembly in Detroit in January. Light-transmittance measurements were made on four different windows. The minimum value observed was 40 per cent - better than the original estimate of 36 per cent. In February the windows were shipped to the Idaho site in a heated truck and are at present stored in the Laboratory and Service Building. A temperature recorder is monitoring the room temperature and standby heating is available. This precaution is deemed necessary in view of the risk of window breakage due to any drastic temperature changes.

An order has been placed for a wall periscope to be used in existing wall openings in either Cell 5 or Cell 6E of the Junior Cave with delivery requested by August 15, 1960.

b. Status of Fuel Cycle Facility Building Design and Construction

(E. J. Petkus, H. L. Stethers)

Field construction has been deferred during most of this quarter due to winter conditions. The Facility was approximately 8 per cent complete as of March 15, 1960. All of the concrete footings and some of the walls below the first floor level were poured before halting construction in December 1959. The H. K. Ferguson Company has completed the engineering drawings for the Fuel Cycle Facility. A total of 169 Facility drawings have been issued to the construction contractor.

Most of the structural steel drawings of the Facility above the first floor have been submitted for approval. These include the Argon Cell liner and cooling ducts, and Air Cell equipment items, such as the tranfer port and large shielding doors. These are being checked in detail as they are received.

c. Cranes and Manipulators
(J. Graae, G. J. Bernstein)

The five-ton cranes were inspected and tested in Paceco's shop on Febraury 29 and March 1. Load capacity and speeds were acceptable, but a number of items were either missing or not satisfactory. Paceco will correct these items and advise when the cranes are ready for inspection and testing again. Bids for the eight operating manipulators have been obtained and are being evaluated.

Manufacturer's drawings of control equipment are nearing completion. Lifting tools for crane trolleys and manipulator carriages are being redesigned into one common tool to save storage space in the Argon Cell. A requisition has been issued for Model 8 manipulators for the Air Cell. General design and performance specifications follow closely the specifications for the Junior Cave manipulators. Additional features include longer through-tubes with internal shielding.

d. Process Cell Windows
(T. W. Eckels)

About 80 per cent of the glass production work for the Fuel Cycle Facility windows has been completed. Casting is proceeding on the last variation in glass composition, 3.3 density glass containing 2.4 weight per cent ceric oxide. This composition is used for the 31 "A" slabs (hot side). Steel fabrication work had been reported to be approximately 95 per cent complete. However, upon assembly of the first two tank units (which contain four $9\frac{1}{16}$-inch thick slabs of glass and two one-inch cover plates), it was found that oil was seeping through some porous welds. A considerable amount of rework will be necessary to correct the condition. Assembly of glass into fabricated steel frames is about 15 per cent complete and will be delayed somewhat by the reworking of the tank units. All but three of the 32 steel window liners have been delivered to the Idaho site.

e. Cell Lighting
(T. W. Eckels, L. F. Coleman)

All the wall mount units have been fabricated and galvanized. Ten luminaire units have been assembled. A visit was made by Argonne personnel to the vendor's plant on March 15. Work done to date was inspected, the need for a few minor changes discussed, and the changes authorized.

f. Miscellaneous Fuel Cycle Facility Equipment

(G. J. Bernstein, L. F. Coleman, R. Jahnke, M. A. Slawecki, C. M. Putness)

Design of a vacuum degassing furnace has been completed and is being checked. This furnace will be used for degassing crucibles, molds, cans and other small items before transfer into the Argon Cell. The furnace incorporates a bagging device to permit sealing of degassed items without exposure to air.

The Chemical Engineering Division has assumed responsibility for design of the interbuilding fuel transfer coffin. This coffin will be used to transfer fuel subassemblies between the Reactor Building and the Air Cell in the Fuel Cycle Facility. A summary and review of design and performance requirements is now underway.

The layout of a revised melt-refining furnace control panelboard has been completed. The panelboard takes the form of the existing one being used in the J-134 mockup area, except for a few changes which affect only the overall size of the completed cabinet and the layout of the semigraphic furnace vacuum panel. The new vacuum panel is to be built and placed on the existing mockup panelboard for test purposes. Drawings and specifications are being prepared in order that the plant panelboards can be built by a vendor. Formal invitations to bid, however, will not be issued until the vacuum panel has been tested.

All preliminary sketches for the Package 4 induction-heating, motor-generator installation for the Fuel Cycle Facility have been finished, and final drawings are being prepared. This covers control wiring and power distribution wiring from the generator. Certified prints for the units have been received and will be sent to the field for the unit installation which will be handled by the Package 3 contractor.

g. Material Testing

(G. J. Bernstein, A. A. Chilenskas, L. F. Coleman, M. A. Slawecki)

Irradiation testing of a grease designated California Research 159* has been completed. This grease is one of several lubricants being considered for use on cranes and manipulators in a high-gamma field, both in an air and argon environment. The samples of both the grease and the oil base were exposed to gamma radiation while encapsulated in a brass bomb (excluding all but a trace of air) or in an air environment.

---

*Grease Composition:

	83%	C_{16-18} alkyl biphenyl bottoms
	12%	Na-n-octodecyl teraphthalamate
	5%	di-docecyl selenide
	0.1%	quinizarin

The results of the tests indicate that either the air-exposed or the encapsulated samples of grease and oil would be usable as lubricants after receiving 3×10^9 rad of exposure. However, all the samples became somewhat tackier than their unirradiated counterparts. The air-exposed samples were noticeably tackier than the encapsulated samples, indicating that the presence of air hastens the deterioration of these lubricants under irradiation.

The MI cables with ceramic end seals have been irradiated to 1.18×10^{10} rad. Insulation resistance of the samples was greater than 200 megohms. The ceramic was discolored, but this had no effect on insulating properties. Irradiation of these samples has been terminated.

Other MI cable samples are being irradiated. Some have been sealed with Temporell #741 manufactured by Orell, Inc., and some with a varnish manufactured by Sterling Company. They have received a dose of 8.6×10^8 rad and are still reading greater than 200 megohms insulation resistance.

The asbestos-covered alloy wire has been irradiated to a total dose of 7.6×10^9 rad. The insulation resistances of the samples varied between 150 and 200 megohms. The insulation is still powdering, but bending of the samples will not rupture the insulation.

Aluminum-paint samples have received a total dose of 7.6×10^9 rad. They are discolored, but the surface is still protected. The "Silicon White Heat Aluminum Paint" samples have been irradiated to 2.5×10^9 rad and are blistering and pitting badly. It is possible that the paint thickness is too great. Other samples of this paint will be prepared and irradiated, using more care in their preparation.

Three one-foot samples of the 54-conductor manipulator cable have been irradiated to 1.92×10^8 rad in 1.75×10^7-rad increments. After each dose increment the cables are twisted 10° per foot approximately 1500 times. Since the first irradiation period, the cables have given off an extremely pungent odor. They are still flexible, but gradual hardening of the hycar rubber sheath and the natural rubber insulation is evident. The surface of the sheath is sticky and the color coding on the conductors has disappeared. The insulation resistances of the samples are still greater than 200 megohms.

h. Transfer Cell Equipment

(G. J. Bernstein, J. Graae)

Most of the design features have been approved and AMF Atomics has been authorized to proceed with fabrication. Minor drawing modifications still remain to be made.

2. EBR-II Fuel Processing Mockup

a. Manipulator and Manipulator Removal Blister

(J. Graae, D. C. Hampson)

Timken tapered roller bearings, chrome alloy coated or molybdenum disulphide coated or both, have been tested under loads approaching those of actual operation and without any other lubrication than that provided by the coatings. The chrome alloy coating alone flaked off and the bearing froze after only 16 minutes of operation. The molybdenum disulphide coating also flaked off and squeaked considerably, but did not freeze. The bearing which was both chrome alloy and molybdenum disulphide coated stood up much better than the other two. However, it too squeaked and gave indication that the coating was not smooth but grainy.

Rolling contact stresses in the bearings were calculated to be approximately 100,000 psi. The tapered design of the Timken bearings appears to cause wedging when the bearings are subject to axial loads, increasing the rolling contact stresses. There is no "give" or play to allow for minute solid particles or molybdenum disulphide buildup when the bearings are subjected to thrust.

While the above experiments indicate that solid dry lubricants are not practical for rolling contact bearings serving a dual function of absorbing radial and axial loads, it is possible that they might be satisfactory for single-function use. In such cases the bearing must be provided with play to allow the rollers or balls to ride over the minor particles or flakes of the solid lubricant. Radiation-resistant greases are being tested (see page 35) and their use for bearing lubrication on the manipulators is being contemplated.

Part of a program to demonstrate remote maintenance of the operating manipulator has been carried out. The carriage has been remotely removed from the bridge and lowered into the floor stand. All motor drive units have been removed from the carriage and replaced (see Figure 1). The grip drive shielding box has been unbolted, removed, replaced and bolted - all remotely. This has been done while observing through the clear glass window with the aid of temporary mirrors. When viewing mirrors and stands are completed, the operations will be performed from behind the shielding window.

The Manipulator Removal Blister Can has been rewelded, leak checked and shipped to Idaho.

FIGURE I
DRIVE MOTOR REMOVAL FROM MANIPULATOR CARRIAGE

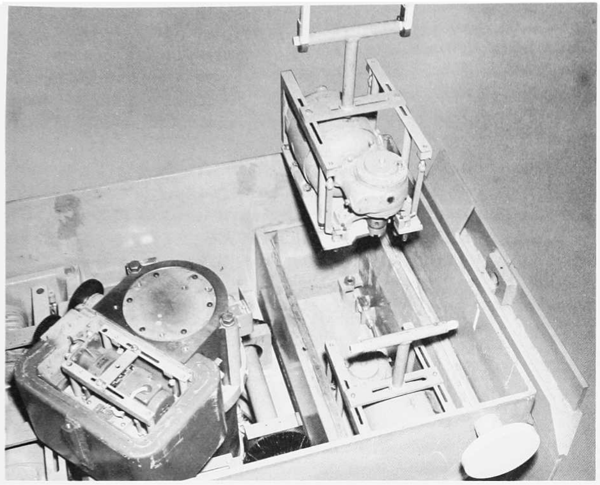

b. Melt-refining Furnaces
(D. C. Hampson, W. E. Miller)

(1) Ingot Preparation

Twenty-four more enriched fuel ingots for EBR-II fuel manufacture were produced in Mark-V processing mockup, bringing the total to date to 58. The average yield for ingots 17 through 58 was 96.6 per cent. The average "fissium" analyses for ingots 17 through 48 inclusive are:

Element	Nominal Composition (wt per cent)	Ingot Analyses (wt per cent)
Molybdenum	2.46	2.31 ± 0.16[a]
Ruthenium	1.96	2.07 ± 0.16
Rhodium	0.28	0.24 ± 0.02
Palladium	0.19	0.19 ± 0.01
Zirconium	0.10	0.13 ± 0.01

---

[a] $$\sigma = \sqrt{\frac{\Sigma(x - \bar{x})^2}{n - 1}}$$

The average isotopic analysis for uranium-235 content for the same batch of ingots was 48.1 per cent, with the high being 48.2 and the low being 47.8. Each isotopic analysis is accurate to ±0.5 per cent. The nominal composition is 48.13 per cent uranium-235.

Ten more normal uranium "fissium" ingots were produced. These ingots are for the production of fuel pins for the natural uranium loading of the EBR-II core. Thirty-one of these ingots were produced prior to February 1959 and manufacture was resumed at the request of the group which is producing the fuel pins from the ingots.

About 150 kilograms of normal "fissium" alloy pins were received for remelting into ingots. Fifteen, 10-kilogram ingots were produced. The average yield was 93.8 per cent with a high of 95.9 and a low of 89.9 per cent.

(2) Equipment Performance

Crucible Failure

During enriched Run No. 55 the crucible cracked and allowed some of the uranium to run out into the susceptor. When the melt was poured, not all of the uranium ran out of the annulus between the crucible and susceptor; after the furnace cooled, the crucible was found to be frozen to the susceptor by uranium metal. This necessitated breaking the susceptor in order to recover the enriched material. The susceptor had served for 38 runs.

During enriched Run No. 57 a $\frac{1}{2}$-in. wide vertical crack opened near the top of the crucible. When the melt was poured, some of the uranium flowed out of this crack into the annulus between the susceptor and crucible and also outside the susceptor into the furnace insulation. Again the susceptor was broken in recovering the enriched uranium. Both cases of crucible cracking are serious in that they produced problems which would be very difficult to cope with in a remotely operated plant. The tendency to formation of vertical cracks has occurred since Norton changed their method of crucible manufacture. The crucibles made by the old method tended to form circumferential cracks where the side wall joined the base. A cooperative investigation with the crucible manufacturer is proceeding to determine the cause of failure and to establish inspection procedures. Production of enriched alloy has been suspended until this problem is solved.

A test to determine the life of a dense graphite mold was interrupted by the uranium spill in enriched Run No. 55. Seven ingots had been poured into this mold with no damage to the surface. The life of a mold made from CS graphite is one to three pours, after which the inside surface, especially the bottom, starts to break away and clings to the ingot when it is removed. More mold-life tests are planned with dense graphite molds and molds dusted with magnesium oxide powder.

Electrical Arcing

As reported last quarter, the coil in the Mark IV furnace failed during tests to examine the compatibility of furnace materials and sodium vapors. Examination showed that an arc formed between the furnace susceptor and the coil, as fused material was found along this path. The coil burnout occurred at a point directly in front of a crack in the outer insulating shell of the furnace. Prior to coil burnout, four sodium vaporization runs were made in the furnace assembly, consisting of a graphite susceptor, zirconia grain insulation and rigid Fiberfrax outer shell and insulator. A large part of the furnace surface was covered with a reacted sodium layer. Some measurements of electrical resistances along surfaces after the runs are listed below.

	Electrical Resistivity (ohms/in. of probe separation)		
Fiberfrax Liner	Outside	Inside	Bottom
Bottom	20,000	50,000	Non-conducting
Middle	50,000	5,000	
Top	100,000	200	

The Fiberfrax liner surface along the path of the fused material had surface-resistance readings of 10 to 20 ohms/inch. The total amount of sodium charged in the furnace for the four test runs was about 400 grams, of which 213 grams was found in the heat shield trap on top of the crucible after the tests were terminated.

Subsequent to the above tests, the Mark IV furnace was rebuilt and used to test the efficiencies of three different types of fume traps. New insulation and a new susceptor were installed. The outer jacket, coil and bottom brick were reused. On two occasions during the course of this work, arcs formed in the furnace. One of these arcs happened on the first run after the furnace had been cleaned and rebuilt. In this run, 85 per cent of the sodium charge (45 of 53 grams) was recovered in the fume trap. Only 8 grams of sodium leaked out into the furnace before the arcing occurred. The second occurrence of arcing took place after the furnace had received considerable use and was contaminated with sodium. In both cases the furnace was shut down within about 20 seconds after the arcing commenced. In the second case, the furnace was restarted after it had cooled from 710 C to 415 C, and the run was completed without further incident (1400 C final temperatures). In both cases, no evidence of arcing could be found when the furnace was examined after cooling.

From experience to date, it appears that arcs can be started in the furnace even when the total amount of metallic vapors in the furnace is low. On the other hand, occasions have been noted when no arc formed even though clouds of heavy sodium vapors were present in the furnace. Evidently, under the proper conditions, very little metallic vapor in the right location in the furnace can promote arc formation. Since it is unlikely in the remote plant that very clean furnace conditions can be maintained over many runs, it may be advisable to include some device in the furnace power electrical circuit which will be actuated by variations in the voltage and/or current and which will initiate furnace shutdown.

(3) Sodium Vapor Fume Traps

Three runs with the susceptor-extension-ring fume trap have shown that essentially all of the sodium evolved from the crucible can be stopped within the enclosure formed by the trap and the furnace susceptor. The final sink for sodium in this design is a Molecular Sieve bed, and the experiments show that, after completion of a run to 1400 C, approximately all of the sodium was on the Sieves. An exact material balance was difficult to make, since the Sieves and sodium pick up weight on exposure to air. Visual observation of the furnace through the sight port during operation indicated that the fume trap does a good job of stopping sodium vapors.

The use of this type of fume trap in a remote plant will require additional remotely operated equipment in the cell to load and unload the Sieves. For this reason a simpler, disposable fume trap is being sought. An absorber-type trap consisting of a crucible of molded Fiberfrax (aluminum silicate ceramic fiber) which is inverted and placed on top of the furnace assembly (see cutaway view in Figure 2) is being tested. The trap works on the principle of absorption and chemical reaction of the sodium with the trap surface. The reacted layer can be seen in Figure 3. Results of the first tests are encouraging, since the weight gain of the Fiberfrax was equal to the sodium charged and essentially no sodium was observed to escape during the runs. This type of fume trap could be baled and is cheap enough to discard after every run.

FIGURE 2
CUTAWAY OF FUME ABSORBER
IN POSITION ON FURNACE

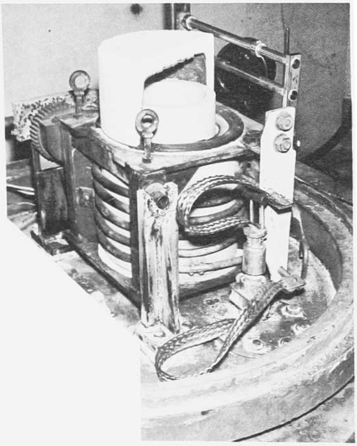

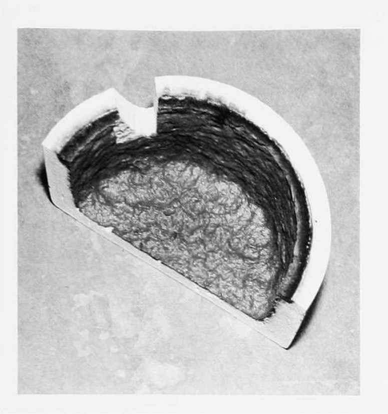

FIGURE 3

SODIUM-FIBERFRAX REACTION LAYER ON ABSORBER

B. Pyrometallurgical Development

1. Melt Refining

(L. Burris, R. K. Steunenberg)

The melt-refining process to be used in the EBR-II fuel processing plant in Idaho involves simple melting of the fuel pins in a zirconium oxide crucible to accomplish fission product removal by volatilization and selective oxidation. The purified material is poured into a mold. The ingot is the starting material for refabrication of fuel. Experimental work on the development of this process was continued in the following areas: (1) preparations for demonstrating fission product behavior with highly irradiated fuel material, (2) development of methods and equipment for studying release of fission product gases during heating and melting of highly irradiated fuel material, (3) melting of oxide-coated fuel pins, and (4) testing of various materials for use in a melt-refining furnace assembly.

a. High-level Demonstration Runs

(V. G. Trice, W. H. Spicer)

Preparations are in progress to demonstrate fission product behavior in the melt-refining process, using a ten per cent enriched uranium-five per cent "fissium" alloy irradiated to one per cent total atom burnup. A small, induction-heated melt-refining furnace has been installed in the Senior Cave. In the first series of three experiments, 400-gram batches of "fissium" alloy will be liquated in zirconia crucibles for three hours at 1400 C. The purified metal will be separated by top pouring and will be sampled to determine the fission product decontamination effected.

Furnace Testing

An endurance test has been completed in which the furnace was subjected to a total of 200 hours of maintenance-free operation. The test program, equivalent to 40 melt-refining experiments, demonstrated satisfactory performance of all components, including the remotely controlled valves, crucible-tilting apparatus and induction-heating facilities.

As a part of the test program, 19 three-hour melt-refining experiments were performed with unirradiated material. Most of these experiments were directed toward determining the conditions producing the highest metal recoveries. Other experiments were devoted to assessing the effect on metal recoveries of holding "fissium" pins in air at temperatures in the range of 110 to 200 C. These latter experiments demonstrated the effect upon yield to be expected from the elevation of surface temperature by the fission product decay heat from the elevation of surface temperature. Metal recoveries from melt-refining experiments with these pins are shown in Table 1.

Table 1

EFFECT OF EXPOSURE OF "FISSIUM" PINS TO AIR AT ELEVATED TEMPERATURES ON METAL RECOVERIES IN MELT REFINING

Melt Refining: Charge, 400 g; Time, 3 hr; Temp, 1400C

Air Temperature (C)	Holding Time (hr)	Metal Recovery (per cent)
(room temperature)	-[a]	89.5[b]
110	65	85.2
150	65	72.3
200	65	46.8

[a] Several days of exposure during normal handling.

[b] Average of six experiments.

Compared to natural uranium, "fissium" alloys show excellent resistance to oxidation. Melt-refining yields, however, are quite sensitive, even to light oxide coatings. As indicated in Table 1, holding "fissium" pins in air at a modest temperature of 110 C causes a significant reduction in the metal recovery obtained in melt refining. Since the Senior Cave Facility is an air cell, procedures are being developed to handle the irradiated fuel pins without prolonged contact with the cell atmosphere.

By carefully controlling the operating variables, reasonably high metal recoveries were achieved in the 400-gram-scale melt-refining experiments with unirradiated fuel alloy. Six experiments performed under optimum conditions produced an average metal yield of 89.5 per cent (with extremes of 88.2 and 91.7 per cent) in the top-poured ingot. In each experiment, 0.6 weight per cent metallic cerium was added to the charge.

Fuel Irradiations

Fuel alloy for two experiments, totalling about 800 grams, is being irradiated in the CP-5 reactor. These irradiations were interrupted by a two-month shutdown of the reactor, which is now back in operation. With continued routine reactor operation, this fuel should reach one per cent burn-up in the first week of May 1960.

Plans have been completed for fuel irradiations in the Materials Testing Reactor in Idaho. Fuel capsules are currently being fabricated, with delivery scheduled for May 1960.

b. Fission Gas Release Investigations

(N. R. Chellew, C C. Honesty, R. L. Kilboy)

Information on the release of xenon-133 and krypton-85 during the heating of highly irradiated uranium-"fissium" alloy pins is important in an evaluation of some problems which may arise in the melt refining of EBR-II fuel. Calculations show that the fuel after two total atom per cent burn-up will contain about 0.27 weight per cent of the noble gases. The volume of these gases, if released quantitatively upon melting of the fuel, would amount to 39 cc per cc of molten metal at STP. A previously reported experiment (ANL-5896, pages 118 to 124) has shown that fission product gas evolution from irradiated uranium (with an initial fission gas concentration of about 0.02 weight per cent) was quantitative near the time of melting. In this experiment there was evidence that spattering of particulate activity occurred, due to the rapid release of the gases. It would be desirable to know whether the evolution rate of the noble gases could be controlled by heating the alloy at appropriate rates. In addition, information on the physical changes of the irradiated alloy which take place on heating and the effects of these phenomena on the coalescence of surface-oxidized fuel pins may be useful in the preparation of process specifications.

The availability of high-burn-up material (see above) should permit realistic studies of problems associated with fission gas release. Equipment for heating small (approximately 7-gram) sections of irradiated alloy under an inert atmosphere is under construction. The main components of the equipment are a resistance-heated tube furnace assembly equipped with view ports for photography of the alloy and a gas-handling system which permits continuous circulation of the active gases between the furnace and a counting chamber. Gamma-ray spectrometry will be used to measure the gaseous activities evolved into the system. The equipment has been designed for use in the Senior Cave Facility.

The effects of gamma radiation on several materials to be used in the apparatus were investigated briefly. Various greases, "Glyptal" enamel and neoprene "O"-rings were exposed to 10^7 rad of gamma activity in the Gamma Irradiation Facility. Types "N" and "T" Apiezon greases, the enamel and the "O"-rings showed little change in their properties, and they are considered suitable for use in the Senior Cave at an exposure level of 10^3 rad per hour for a period exceeding one year. Silicone grease, however, showed a tendency to stiffen and its use is not contemplated.

c. Melt Refining of Sodium-coated Pins

(G. A. Bennett, W. A. Pehl)

Efforts this past quarter on the melt refining of sodium-coated pins were directed primarily toward the completion of experimental runs in which attempts were made to eliminate potential sources of oxygen. In this manner it was hoped to establish definitely whether or not the melting difficulties (pin shells preventing coalescence) which had been experienced previously would persist under conditions similar to those to be maintained in the EBR-II fuel-processing cell. Attention was given also to a promising oxide-reduction technique to be used should these difficulties persist.

(1) Melt Refining under Conditions of Low Oxygen Contamination

In order to eliminate oxygen contamination, a leak-tight bomb was designed for transferring low-oxygen (~10 ppm) sodium from Reactor Engineering to the melt-refining furnace in the Chemical Engineering Division. An aircraft-type mechanical finger was modified so that it could be inserted through the bridge breaker in the furnace in order to transfer within the furnace sodium-coated pins from the coating bomb to the melt-refining crucible. In this manner, all transfer operations were performed under argon,* and the sodium and "fissium" pins were exposed to minimum oxygen contamination for the entire run.

In the first successful run of this type, about 2 kg of five per cent "fissium" pins, injection cast to EBR-II dimensions, were sodium-coated in low-oxygen sodium for $3\frac{1}{2}$ hours at 500 C. About 770 grams were transferred to the melt crucible before a failure of the transfer mechanism occurred. After flashing off the sodium at about 600 C, the pins were melt refined for a period of one hour at 1400 C. At no time during the operation were the charge materials exposed to air.

The resulting yield of 85.9 per cent (Table 2, Run 268) approximates that which would be expected from a similar charge of bare pins, and represents an increase of about three per cent over previous yields (Run 267) which had been obtained with sodium-coated pins on the two-kilogram charge level under less stringent atmosphere control.

---

*Argon impurities as follows: N_2: 300 ppm; O_2: 3.9 ppm; H_2O: 18.3 ppm.

Table 2

EFFECT OF OXYGEN CONTAMINATION ON POURING YIELD

Conditions: Liquation Temperature - 1400 C

	Charge Material			Melting Conditions			Ingot	
Run No.	Surface Condition	Weight (g)	Cerium Content (w/o)	Liquation Time (hr)	Crucible	Calcium Addition (g)	Yield (%)	Cerium Removal (%)
265	Clean	2000	0.00	$\frac{1}{2}$	Degassed ZrO_2	None	91.5	-
266	Clean	2001	0.00	3	Degassed ZrO_2	None	95.0	-
268	Na-coated[a]	767	0.00	1	Degassed ZrO_2	None	85.9	-
267	Na-coated[b]	1977	0.35	3	Degassed ZrO_2	None	82.7	>97.1[c]
264	Na-coated[b]	1871	0.96	3	Degassed $CaO \cdot ZrO_2$	32.5	87.9	64.5[d]

[a] Oxygen contamination kept at minimum.

[b] Oxygen contamination present.

[c] Colorimetric cerium analysis; estimated accuracy ±10 per cent.

[d] Colorimetric cerium analysis; estimated accuracy ±5 per cent.

In addition, there was no evidence of pin shells in the dross. It is planned to check this encouraging result on the two-kilogram scale.

(2) Melt Refining by Oxide Reduction

A previous report (ANL-5959) showed that calcium is an effective reducing agent for the oxide film which is formed on sodium-coated fuel pins. However, no crucible material which was both satisfactorily stable to thermal shock, and which could contain molten uranium, sodium and calcium, had been found. In the last quarter (ANL-6101, page 29), preliminary results obtained with calcium zirconate crucibles indicated this material to be promising. Consequently, the calcium reduction method, using a calcium zirconate crucible, was extended to a 2-kg melt of five per cent "fissium" pins containing sodium. In this run (Table 2, Run 264) the charge material was coated with sodium under conditions which allowed some exposure to air. The coated pins were then charged to the previously degassed calcium zirconate crucible where they were melt refined under argon by means of standard procedures. Analyses of similar pins showed that they contained about 1150 ppm oxygen. At the start of the 1400 C liquation period, 32.5 g of calcium were added to the melt. The resulting ingot was of good quality and was obtained with an 87.9 per cent yield. This is about five per cent higher than that obtained in a similar run without calcium (Run 267). No pin shells were evident in the dross, and the crucible showed no indication of chemical attack.

Although this yield is lower than would be expected with bare pins (Runs 265, 266), the results are nevertheless promising, as the pins were badly oxidized before refining. Cerium removal was

64.5 per cent from an original cerium concentration of 0.96 weight per cent cerium; this is somewhat less than that obtained with zirconia under similar conditions.

d. Study of Alternate Materials and Designs for the EBR-II Melt-refining Furnace

(J. Wolkoff, C. A. Bayens,* M. R. Cusick,* R. E. Nowak)

Additional tests have been made with insulating materials that can be substituted for the zirconia grain now in use in the melt-refining furnace. As previously discussed (ANL-6101, page 29), high-temperature compatibility with graphite, as well as efficient thermal insulation, is being sought. A silicon carbide foam, a fine-grain silicon carbide powder, and a carbon black powder were new materials tested this quarter.

Various types of information were obtained, from which comparison of the various materials may be made. These included steady-state temperatures at selected points for a given power input under both vacuum and argon at one atmosphere pressure, cooling rates, and finally the power input required to produce a temperature of 1400 C inside the crucible.

A representative comparison of the power input required to produce a crucible temperature of 1400 C is shown in Table 3 for the various insulating materials tested. Inasmuch as low coil temperatures are desirable, reflecting jointly the power input and the insulation efficiency, the coil temperatures are also given in Table 3.

Table 3

COMPARISON OF THERMAL INSULATING MATERIALS
FOR MELT-REFINING ASSEMBLY

(Equipment description; ANL-6068, page 44)

Run	High-temperature Thermal Insulation	Grain Retainer	Power Required for Crucible Temp of 1400 C (kw)	Corresponding Coil Temp (C)
20	Zirconia, Type I, 24/40 mesh	Amersil	6.9	508
15	Zirconia, Type I, 24/40 mesh	Rigid Fiberfrax	5.7	473
18	Graphite Powder, 20/100 mesh	Rigid Fiberfrax	5.4	456
22	"Norblack," Carbon Black Powder	Rigid Fiberfrax	4.8	376
21	Silicon Carbide Powder, Type RA, 1000 mesh	Rigid Fiberfrax	4.5	353
19	Foam Silicon Carbide Brick	None	9.6	629

---

*Student Aides from University of Detroit.

The presently used insulating material is zirconia grain of the type used in Run 20. Although a fairly effective insulation, its insulating value drops as sintering of the grain takes place. Furthermore, it reacts with the graphite susceptor to produce carbon monoxide. While this is not a serious problem, its avoidance was sought in the selection of alternate materials by testing only carbides, carbon black, and graphite.

Since the Amersil grain retainer was cracked badly in Run 20, substitution of a rigid, molded Fiberfrax grain retainer was made. This material is in itself excellent insulating material and does not show marked cracking tendencies. A substantial improvement in insulation effectiveness (Run 15) was realized by this simple change. The other insulating powder materials were also tested with the Fiberfrax grain retainer. The Fiberfrax grain retainer for Runs 21 and 22 had a thinner wall ($\frac{3}{8}$-inch) than previously used ($\frac{5}{8}$-inch) in order to decrease the inner surface temperature of the grain retainer.

The inner wall temperature was reduced to less than 875 C. This temperature reduction effected a noticeable improvement in appearance and strength of the retainer, which has been used many times without appreciable deterioration.

Successive increases in insulating effectiveness were realized with graphite powder, carbon black, and silicon carbide powder, the corresponding power requirements for a 1400 C crucible temperature being 5.4, 4.8, and 4.5 kw (Table 3). Coil temperatures were decreased to less than 400 C.

A foam silicon carbide brick which replaced both the grain and grain retainer proved to be very poor insulation. Some degradation of the foam occurred adjacent to the graphite susceptor. No further testing of this material is contemplated.

The highly effective silicon carbide powder (Run 21) was found to be slightly caked in the hottest zones at the end of the run. Therefore, it was subjected to a long-term test in which it was kept at operating temperatures for a total time of 115 hours (Run 23). Cooling to room temperature occurred eight times after successive parts of the run. On the basis of four hours at operating temperature (above 1300 C) for each melt-refining run, an equivalent of almost 29 melt-refining runs was spanned by the test. The insulation was functioning satisfactorily when the run was terminated.

The grain had sintered adjacent to the graphite susceptor to a chalk-hard mass for a thickness of about $\frac{3}{8}$ inch. The remainder of the grain thickness, about $\frac{5}{8}$ inch, was also caked but soft enough to be crumbled by hand. The graphite susceptor was removed from the annular grain with little crumbling. Several surface cracks had formed in the inner surface of the sintered grain.

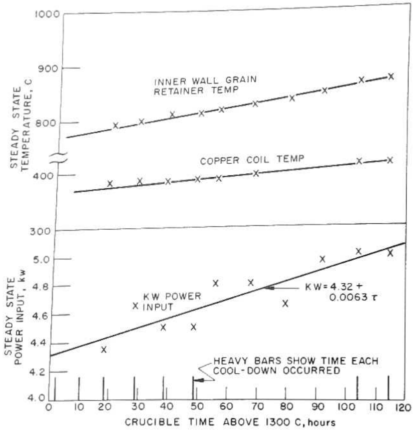

FIGURE 4
SINTERING TEST OF SILICON CARBIDE GRAIN
(RUN 23)

The changes in power input and in other characteristic values that occurred during the run are plotted in Figure 4. The effects of sintering as the run progressed are clear, and deviation from linearity for the selected trends was not obvious in the test time employed. In all cases the values plotted are for the steady state with a crucible wall temperature of 1400 C. Based on a linear fit of the power input, a change of about 0.6-kw input power would occur per 100 hours at operating temperature (approximately 25 melt-refining runs).

There are now available as a zirconia grain replacement insulation compatible with a graphite susceptor, three materials each more effective thermally than zirconia. These are silicon carbide powder (1000-mesh), carbon black (Norblack), and -200 mesh graphite powder. A long-term run with carbon black is planned to determine its sintering tendency. A series of tests are also being started to study the effect of inductor coil modifications on the input power required.

2. Liquid Metal Solvents Process Development

(R. K. Steunenberg, L. Burris)

At the completion of the melt-refining operation, approximately ten per cent of the uranium present in the original charge remains in the zirconia crucible in the form of a "skull" composed of metal and oxide. This material requires processing to recover the uranium and to remove fission products from the fuel cycle in such a way as to maintain the desired equilibrium "fissium" composition in the recycled fuel.

Oxidation by an oxygen-argon mixture converts the skull to a powdered oxide which is easily removed from the zirconia crucible by pouring. Depending on the conditions of oxidation, some fission product ruthenium and molybdenum are volatilized as the oxides.

The skull oxides are reduced by magnesium dissolved in liquid zinc or cadmium. By proper adjustment of the composition of the magnesium alloy, the metallic uranium produced by the reduction reaction can either be precipitated or held in solution. Fused salt flux may be employed to promote mixing of the uranium oxide powder with the liquid metal and to serve as a vehicle for removal of the magnesium oxide product formed during the reduction.

a. Processing of Melt-refining Skulls

(1) Preliminary Treatment of Crucible Skulls

(T. R. Johnson, R. L. Christensen)

Oxidation has been proposed as a convenient and efficient method of removing melt-refining skulls from the zirconia crucibles. The oxidized product is a finely divided material which can be poured from the crucible and is amenable to further treatment in a liquid metal process for uranium recovery. Partial decontamination of the uranium in the skull may occur during oxidation through volatilization of those fission product elements which form volatile oxides (molybdenum, ruthenium, technetium and tellurium).

Melt-refining skulls were prepared by holding 300 to 600 grams of "fissium" alloy in zirconia crucibles for two hours at 1350 C. The nominal composition of the alloy was the following. cerium, 0.6; zirconium, 0.5; molybdenum, 2.5; ruthenium, 2.2; palladium, 0.6 weight per cent. The details of the method used for oxidation of the skulls was described in the previous quarterly report (ANL-6101, page 36). The oxidations were performed either with a static atmosphere or with a stream of diluted oxygen flowing through the furnace. Since the inlet gas was not directed into the crucible in either case, the oxygen reached the bottom of the crucible by diffusion.

The conditions of oxidation and the results of the completed experiments are summarized in Table 4. The weight of zirconium oxide crucible fragments included in the recovered product was calculated as the weight of the final product less the weights of the original skull and the oxygen added.

The rates of oxygen consumption are compared in Figure 5. The ordinate in Figure 5 was calculated from the estimated mol-equivalents of metal in the total skull and from the measured amount of oxygen absorbed. The reaction layer between the crucible and the melt oxidizes rapidly, forming the finely divided portions of the product. The metallic button oxidizes more slowly and tends to form larger particles. Screen analyses of the oxidized skulls are shown in Table 5. The percentage of the skull which was oxidized was calculated from the total amount of oxygen consumed and the theoretical amount estimated from the overall skull composition and weight.

Table 4

SUMMARY OF SKULL OXIDATIONS

Skulls prepared by melt refining 300 to 600 grams of "fissium" alloy in zirconia crucibles for two hours at 1350 C. Alloy composition: Ce, 0.6; Zr, 0.5; Mo, 2.5; Ru, 2.2; Pd, 0.6 weight per cent.

Estimated uranium recovery: 99 per cent

Skull Weight (g)	O_2 Conc in Argon (v/o)	Type of Atmosphere	Furnace Temperature (C)	Length of Oxidation (min)	Recovery in Oxide (per cent)		Crucible Fragments (g)	Comments
					Ru	Mo		
25.4	33[a]	static	500	180	(80)[b]	(80)[b]	1.2	Skull loosened from crucible.
17.6	33	static	700	45	-	-	0.0	Reduced with H_2 - 500 mm, 700 C.
32.8[c]	33[a]	static	700	270	81.6	73.8	1.3	
19.3	26	flow	700	280	-	-	-	
49.6	26	flow	700	325	92	-	8.1	Ru^{103} tracer
24.1	29	flow	800	340	95	-	5.8	Reduced and re-oxidized; Ru^{103} tracer
34.8[c]	20[a]	static	850	120	79.7	79.4	0.0	
26.5	25[a]	static	850	120	-	-	3.1	O_2 concentration 5 v/o for first 50 min.
30.8[c]	27[a]	static	850	170	83.4	79.5	2.1	
17.8	33	static	850	300	60.5	57.8	0.0	

---

[a] Oxygen content lower at beginning of run.

[b] Estimated values.

[c] Reported previously (ANL-6101, Table 2).

FIGURE 5
OXIDATION OF CRUCIBLE SKULLS

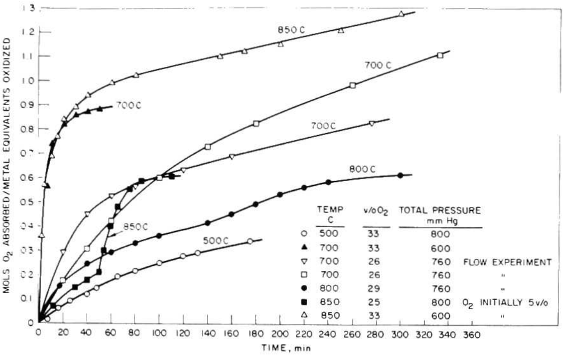

Table 5

SCREEN ANALYSES OF OXIDIZED SKULLS

Furnace Temperature (C)	Per Cent Oxidized[b]	Screen Fractions (wt %)		Size Distribution of Oxide Powder (wt %)		
		Metal Button	Oxide Powder	60 Mesh	60 to 325 Mesh	325 Mesh
500	20	42.3	57.7	38.9	41.0	20.1
700[a]	90	-	-	41.3	50.4	8.3
700	90	-	-	50.4	34.9	14.7
700	60	27.2	72.8	33.4	48.3	18.3
700	85	-	-	52.9	32.9	14.2
700	65	13.2	86.8	63.3	26.8	7.9
800[a]	90	-	-	47.5	43.2	9.3
800	80	-	-	57.0	35.1	7.9
850	55	41.5	58.5	43.1	42.9	14.0
850	60	34.8	65.2	44.7	44.8	10.5
850	30	44.5	55.5	64.9	26.0	9.1
850	100	-	-	55.7	37.1	7.2

[a] Oxidized in pure oxygen, 75 mm; reported previously in ANL-6101, Table 2.

[b] Oxidations were stopped when the oxygen consumption rate became too slow to follow.

The behavior of ruthenium and molybdenum has been investigated. The apparent recoveries of these elements in the product oxide indicated in Table 4 were calculated in the following manner: it was assumed that all the cerium in the melt-refining charge was transferred to the skull. Otherwise, the skull was assumed to have the same composition as the molten metal. These assumptions are not strictly correct, since the proportion of uranium appearing in the skull is larger than that of the combined noble metals. This results from the fact that uranium is more easily oxidized than are the noble metals and all the oxide formed during the melt refining remains in the crucible with the skull. Therefore, the estimated amounts of ruthenium and molybdenum present in the skull are higher than the actual amounts.

The product from the skull oxidation was screened and samples of each screen fraction were analyzed. Ruthenium analyses were performed by a standard wet chemical method or by a tracer technique. All molybdenum analyses were done by wet chemical methods. The coarser fractions contained a higher proportion of the ruthenium and molybdenum. The unreacted button was assumed to have the same composition as the melt.

Ruthenium tracer was prepared by irradiation of the metal. The 0.50-Mev gamma peak characteristic of ruthenium-103 was counted with a single-channel analyzer. Due to the large neutron-capture cross section of iridium, which was present in the ruthenium as a trace impurity, the specific activity of iridium-192 was comparable to that of the ruthenium. The analyzer, however, was capable of discriminating between the 0.31-Mev iridium peak and the 0.50-Mev ruthenium peak. The low-yield, 0.47-Mev gamma emission of iridium-192 contributed less than 10 per cent of the total activity. In those cases where ruthenium and iridium were separated during the experiment, a correction was made for the iridium interference in the counting standard.

Since the skull is known to be somewhat depleted in ruthenium and molybdenum, and since the recoveries of ruthenium and molybdenum agree in all the experiments, it is believed that the apparent recoveries shown in Table 4 indicate no significant volatilization of the oxides of these elements under the conditions employed, and that they probably correspond to actual recoveries close to 100 per cent. When active ruthenium was used in two of the runs, no activity was found in the furnace tube; the limit of detection was about 0.1 mg.

Several small-scale oxidations were performed in order to facilitate the investigation of a wide range of conditions. Two types of experiments were carried out. In the first, small pieces of "fissium" alloy (about 0.5 g total) were placed in the bottom of a 6-mm Vycor tube which was sealed at one end. The tube was evacuated, about 5 mm of argon was added to prevent ignition, the sample was brought to temperature, and one atmosphere of oxygen or hydrogen was admitted to the system. Tracer ruthenium in the samples was counted before and after each run. The temperatures were varied from 100 to 1200 C, and several samples were reduced and reoxidized after the initial oxidation.

No significant removals of ruthenium were observed. When samples were oxidized and evacuated to less than 1 mm above 900 C, significant quantities of molybdenum were volatilized and collected in the cooler portions of the tube as the trioxide and possible the pentoxide. Molybdenum removals exceeding 85 per cent were observed in three oxidations of the metal samples at 930 C.

In the second type of experiment, small pieces of the skull (about 0.5 g total) in combustion boats were placed in a resistance-heated 30-mm Vycor tube. Oxygen was passed over the samples at a flow rate of about 4 ft/min. Ninety per cent of the ruthenium was removed from a sample oxidized in pure oxygen for four hours at 930 C. This sample visibly ignited when oxygen was first added. Four-hour oxidations of samples in 20 per cent oxygen-80 per cent argon at 930 and 800 C gave ruthenium removals of 75 and 35 per cent, respectively. Because of the dilute oxygen, these samples did not visibly ignite. The tracer activity was spread uniformly over the cooler portions of the tube. Molybdenum removal was also noticed at 930 C, as evidenced by the collection of molybdenum trioxide in the cooler zones.

The following conclusions have been reached with regard to the oxidation of melt-refining skulls: (1) Oxidation appears to be an attractive method for separating the uranium-bearing material from the crucible. Complete oxidation can be achieved in 5 to 6 hours at temperatures above 700 C. The reaction rate does not increase greatly above 700 C, and it is easily controlled by dilution of the oxygen with an inert gas. (2) Over 50 per cent of the molybdenum is volatilized, probably as the trioxide, at temperatures above 850 C. (3) More than 50 per cent of the ruthenium can be volatilized, presumably as the tetroxide, at temperatures above 850 C, but only in a stream of flowing oxygen. (4) The volatilized molybdenum collects in the cooler portions of the apparatus as the trioxide and perhaps as the pentoxide, while the ruthenium appears to collect as the dioxide.

Revision of Previously Reported Results for Ruthenium Behavior during Skull Oxidation

(V. G. Trice, T. R. Johnson)

Recent refinements in sampling and analytical techniques show that data presented in ANL-5996, page 60, indicating essentially complete ruthenium removal by skull oxidation are in error. In the previously reported experiments, small pieces of "fissium" alloy containing 2.6 weight per cent ruthenium were subjected to several cycles of oxidation in pure oxygen and reduction in hydrogen. Samples of the final product which were submitted for analysis consisted largely of the more finely divided material.

It is now known that the composition of the oxidized skull material varies with the particle size and that the analytical techniques used previously are not reliable. The oxidation products of Run 10c, originally reported as free of 99 per cent of the original ruthenium, were re-analyzed. The results appearing in Table 6 cannot be used to determine the overall extent of ruthenium removal due to the difficulty in obtaining representative samples, but they do show that the amount of ruthenium is much greater in the coarse particles. The molybdenum content does not appear to vary significantly with the particle size.

Table 6

CORRECTED VALUES FOR RUTHENIUM AND MOLYBDENUM CONCENTRATIONS IN SKULL OXIDES[a,b]

Particle Size (mesh)	Size of Fraction (wt per cent)	Ruthenium Content (wt per cent)	Molybdenum Content (wt per cent)
> 60	56.3	10.0	2.1
60 to 325	34.9	0.5	1.8
<325	8.8	0.5	2.8

[a] Charge consisted of a button containing 89 per cent uranium, 3.9 per cent molybdenum and 2.6 per cent ruthenium.

[b] Results reported previously in ANL-5996 were based on incorrect analyses which showed 0.03 weight per cent ruthenium.

(2) Removal of skulls from Melt-refining Crucibles (R. D. Pierce, L. F. Dorsey)

Both complete and partial burning have been considered for removing crucible skulls for further processing. Direct mechanical removal has been abandoned as too difficult for remote operation.

Screened fractions of some oxidized "fissium" skulls from melt-refining runs have been analyzed to determine the inclusion of zirconia crucible fragments. Table 7 lists the results. The skulls in which cerium was present seem to contain more fine crucible fragments after burning. This is probably due to greater degradation of the crucible surface in the reaction zone.

Table 7

CRUCIBLE FRAGMENTS PRESENT IN OXIDIZED SKULLS

	Sample A[a] (w/o)			Sample B[a] (w/o)		
Screen Size	Screen Analysis	Uranium	Crucible Fragments	Screen Analysis	Uranium	Crucible Fragments
+ 25	6.1	77.1	6.2	10.3	71.2	9.4
- 25 + 45	23.2	74.8	6.3	13.8	71.1	7.9
- 45 + 80	22.3	71.7	7.9	22.9	72.6	6.3
- 80 +170	17.5	67.4	8.7	19.3	72.9	4.7
-170 +325	19.2	65.0	6.6	26.9	72.4	3.1
-325	11.7	65.0	12.2	6.8	75.6	2.3
Total	100	70.0	7.8	100	72.4	5.4

[a] Sample A was a blend of oxides for burning "fissium" skulls which contain cerium.

Sample B was a blend of oxides from burning "fissium" skulls, only 25 per cent of which contained cerium.

(3) Reduction of Oxides in Liquid Metal Solution
(R. D. Pierce, P. Nelson, J. C. Hesson, J. Lenc, L. F. Dorsey, J. Pavlik, K. Tobias, M. Bowden, J. Hepperly)

Following the oxidation of skull material to facilitate its removal from a crucible, the U_3O_8 formed must be reduced to metal. This is accomplished in a liquid metal solution in which the magnesium reducing agent may be dissolved in a cadmium or zinc solvent. Two general regions of magnesium concentration have been employed in the reduction studies: (1) high-magnesium concentrations, which result in solutions having very low solubility for uranium so that any uranium reduced separates out as a solid phase, and (2) low concentrations of magnesium, which allow the reduced uranium to appear in metal solution. A chloride flux was employed in most of the experiments.

In the case of low-magnesium concentrations, the course and extent of reduction can be determined by analyses of filtered samples of the metal solution. In the case of high-magnesium concentrations, several methods may be employed to ascertain the extent of reduction. The first involves the addition of sufficient cadmium or zinc to dissolve any reduced uranium and to enable sampling for analysis of the uranium in the final solution. This is a fairly attractive procedure because the precipitated uranium would be expected to go into solution quickly. However, this method can also be suspect because of the possible presence of elements which could precipitate uranium. Nickel, iron, silicon, and aluminum have already been found to do this in cadmium, and the effects of noble elements present in "fissium" (and therefore skull oxide) have not been established.

A second procedure consists of isolating the uranium product by distilling away the magnesium and the solvent metals, and analyzing the uranium residue for uranium, oxygen, and other elements, from which analyses the amount of uranium metal initially present may be calculated. Because of the high atomic weight of uranium, considerable accuracy must be achieved in these analyses to enable accurate determination of the metal content. The further reduction which may occur during a retorting step would tend to cloud the effects of reduction variables.

A third procedure now being investigated involves analysis for the magnesium oxide reaction product which appears in the flux phase. This method has promise and is being developed further.

Reductions in 6 Per Cent Magnesium-Cadmium Solutions

Several runs were made in which uranium oxide (U_3O_8) was reduced in 5.75 per cent magnesium-cadmium under Dow-230 flux in an argon atmosphere. The amount of uranium employed was such that sufficient solubility existed in the metal solution for dissolving all the uranium metal formed by reduction. Table 8 shows the conditions of these runs.

Table 8

REDUCTION OF URANIUM OXIDE IN 6 PER CENT MAGNESIUM-CADMIUM SOLUTION

Containers: High-purity aluminum oxide crucibles

Conditions						Results			
Charge, grams						Per Cent U in Melt		Per Cent of Original U in Solution	
Mg	Cd	Flux[a]	U_3O_8	Temp (C)	Time (hr)	Run SD-78	Run SD-79	Run SD-78	Run SD-79
115	1885	200	10	700	8	0.36	0.31	85	73

[a] Synthetic Dow-230 flux having the following composition (weight per cent): KCl, 55; $MgCl_2$, 34; $BaCl_2$, 9; CaF_2, 2.

In these runs the initial rate of reduction was high with an early leveling off. For example, in SD-78 the uranium concentration was 0.29 per cent (70 per cent reduction) at the end of $\frac{1}{4}$ hour of stirring and was 0.36 (85 per cent reduction) at the end of one hour, remaining at this value for the duration of the run.

As mentioned previously, uranium may be scavenged from cadmium by several materials, for example, iron, nickel, aluminum, carbon, and silicon. This sensitivity of cadmium-uranium solutions to the presence of contaminants is very acute in runs such as the above two, where very little uranium is present. This is illustrated by a blank run in which the same weight of uranium metal employed in the above runs was dissolved for thirteen hours in a 6 per cent magnesium-cadmium solution. Samples taken after six hours show a constant value of 91 per cent of the uranium dissolved. It is possible that some reduction of the alumina crucible might have occurred, producing aluminum in solution and precipitating uranium as a uranium-aluminum intermetallic. Therefore the percentage of uranium reduced in Table 8 should be regarded as minimum values.

Reduction in 20 Per Cent Magnesium-Cadmium Solution

Several large-scale (200 g of U_3O_8) reduction runs were made at 800 C in 20 per cent magnesium-cadmium solution under a synthetic Dow-230 flux in tantalum crucibles. During the reduction the uranium precipitated as metal, but the magnesium-cadmium solution employed was sufficiently low in magnesium (20 per cent) to make possible a subsequent dissolution of the reduced uranium within the available volume of the container by addition of more cadmium and zinc. Prior to the dissolution, the molten flux was removed by pressuring it through a tube into a receiver. The conditions and the results of the runs are given in Table 9.

In Run C-9a reduction of 85 per cent was shown by dissolution in cadmium. In this run the amount of uranium dissolved might have been hindered by close approach to the solubility limit of uranium in cadmium (1.55 per cent uranium in solution as compared to a solubility limit of 1.7 per cent uranium in a 0.9 per cent magnesium-cadmium solution at 460 C).

To avoid this difficulty in Run C-11, zinc was added with the cadmium to a concentration of 7 per cent, thus increasing the uranium solubility to around 4 per cent. A reduction value of 94 to 97 per cent was shown by analyses of filtered samples taken after six hours of agitation at 650 C.

Table 9

REDUCTION OF URANIUM OXIDE IN 20 PER CENT MAGNESIUM-CADMIUM SYSTEMS

Charge : 750 g of cadmium-2 per cent magnesium alloy
200 g of U_3O_8
800 and 600 g of Dow-230 flux[a] in C-9 and C-11, respectively

Containers: Tantalum Crucibles

Run Conditions				Per Cent Reduction by				
					MgO Content of Flux after (hr)			
Run	Temp (C)	Time (hr)	Additional Cd Solvent (g)	Metal Dissolution	$\frac{1}{2}$	1	6	$13\frac{1}{2}$
C-9	800	$15\frac{1}{3}$	480	85	Not Determined			
C-11	770	$13\frac{1}{2}$	585[b]	95	20	28	76	87

[a] Synthetic, made from "CP" grade materials to the following composition (w/o):

KCl	55	$BaCl_2$	9
$MgCl_2$	34	CaF_2	2

[b] Contained 7 per cent zinc.

The extent of reduction in this latter run was also obtained by determining the amount of magnesium oxide in the flux. A blank run with flux alone at 150 C indicated that the total concentration of magnesium, barium, and calcium (by EDTH method) was essentially constant over a five-hour period at 4.15 millimoles per gram of flux. During Run C-11 the total amount of these same constituents increased to 6.30 to 6.45 millimoles per gram of flux, which would account for the addition of 87 to 92 per cent of the magnesium oxide required for complete reduction of the uranium. Several intermediate values of the extent of reduction were obtained by this method. These results are plotted in Figure 6. Since magnesium oxide is not soluble in the flux, care was taken to sample the flux immediately after stopping the agitation. However, the success of this method in obtaining a representative sample was not determined. Concentrations of uranium in the flux are also shown on this plot. Uranium is removed from the flux more rapidly than can be accounted for by the appearance of magnesium oxide in the flux. Apparently some of the uranium enters the metal phase as an oxide, possibly coated with a uranium metal film, and continues to be reduced at a rather slow rate.

FIGURE 6
REDUCTION OF U_3O_8 BY CADMIUM-20 PER CENT MAGNESIUM WITH DOW-230 FLUX AT 770 C
(Run C-11)

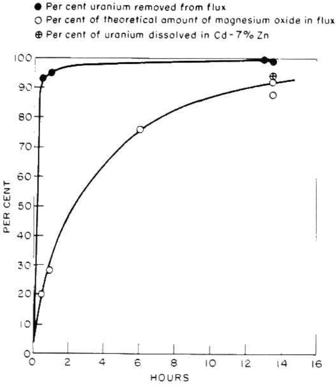

In these reduction runs, the tantalum crucibles were rather severely attacked. Four grams of material in the uranium residue obtained on evaporating the cadmium would not dissolve in aqua regia and were identified by X-ray diffraction to be mostly tantalum. Two other runs were lost because of failure of the tantalum crucible at a welded joint.

Some experience has also been obtained with molybdenum accessories in the reduction runs. By visual observation, these appear to be unattacked by flux-metal combinations at 800 C.

Conclusions

It is certain that high reductions (over 90 per cent) have been achieved. The reason for failure to achieve reproducibility has not been determined, but it is suspected that the instability of cadmium solutions of uranium to impurities is part of the explanation. The increasing list of elements which can affect the uranium solubility in cadmium is a disadvantage for cadmium. Since zinc solutions are more stable than are cadmium solutions, both systems are currently being studied. The corrosion advantage which cadmium possesses at low temperatures (ability to hold it in mild or 400 series stainless steels at 550 C and below) is largely nullified at high temperatures, where it is necessary to use tantalum or ceramic vessels.

Reduction of U_3O_8 by Liquid Magnesium

(A. Schneider, J. D. Schilb, J. W. Walsh,
C. R. Williams)

In this system, uranium oxide is agitated with molten magnesium. Since uranium metal is only slightly soluble in liquid magnesium, it is not possible to follow the progress of the reduction from the dissolved uranium content of samples periodically withdrawn from the liquid metal phase. Instead, the extent of oxide reduction was determined by dissolving the resulting ingot in liquid cadmium and obtaining samples for uranium analysis.

It was reported previously (ANL-6101, page 43) that the reduction of U_3O_8 by liquid magnesium was accomplished in the presence of magnesium chloride at temperatures above 870 C. It was believed that the magnesium chloride was essential for continuous dissolution of the magnesium oxide formed, which could have acted as a diffusion barrier. Two reduction runs performed in the absence of magnesium chloride gave the results indicated in Table 10. These results show that U_3O_8 is reduced readily by liquid magnesium at temperatures above 850 C, and that the presence of magnesium chloride is not essential. The low value of 35 per cent obtained at 714 C suggests that the reaction rate has a large temperature coefficient.

Table 10

REDUCTION OF U_3O_8 BY LIQUID MAGNESIUM

Experiment	12-29-9	1-11-0
Part I. Reaction with Magnesium		
Duration (hr)	5.5	2
Temperature (C)	850	714
Crucible	Alumina (Morganite)	
Stirring	Close-fitting tantalum paddle stirrer at 100 rpm; no baffles	
Total Metal Recovery (per cent)[a]	92.0	95.4
Part II. Dissolution in Cadmium		
Temperature (C)	654 to 662	676 to 688
Crucible	Tantalum	
Stirring	Tantalum paddle stirrer at 400 to 450 rpm	
(hr)	Uranium Content (weight per cent)	
0.5	-	0.29
1.0	1.21	-
1.5	1.25	0.33
2.5	1.27	0.38
3.0	1.29	-
Material Balances		
Magnesium accounted for (per cent)[b]	94.0	102.5
Uranium reduced (per cent)[b]	95.0	35.3

---

[a] Determined by weighing all metal recovered from the reaction crucible.

[b] Ingot dissolved in liquid cadmium, which was sampled and analyzed for uranium and magnesium.

Reduction of U_3O_8 by Molten Metals in Metaphosphate Fused Salt Systems

(M. D. Adams, M. L. Jones)

Molten sodium and potassium phosphates possess the ability to dissolve significant quantities of U_3O_8, but the viscosities of these salts are too great, even at 900 C, to consider their use in a process. The metaphosphates, however, are miscible with certain other molten salt systems, such as sodium chloride-potassium chloride. The viscosities of such mixtures containing 5 to 25 mole per cent sodium or potassium metaphosphate are low, and the solubility of U_3O_8 remains appreciable.

Several attempts were made to reduce U_3O_8 with cadmium-magnesium mixtures in these salts. Within a few hours all the uranium was removed from the salt phase. It was not, however, dissolved in the molten metal phase, but was found in the bottom of the crucible. The form of the uranium has not yet been identified; it yields a complex X-ray diffraction pattern which has not been interpreted.

Additional problems were encountered in using this system for the reduction of U_3O_8. The phosphate salt appears to react somewhat with the magnesium in the metal phase to form elemental phosphorus. The volatilized phosphorus collected on the walls of the furnace tube appears to react with cadmium volatilized from the same crucible. The system also has a tendency to disperse the molten metal in the salt phase. This effect is particularly evident in mixtures of salts which have a high percentage of phosphate. One mixture containing 15 mole per cent sodium metaphosphate produced complete dispersion of the metal in the form of small spheres and lumps. When the salt phase contained only 8 mole per cent metaphosphate, however, 85 per cent of the metal was recovered in one piece.

Mild steel, which was used as the crucible material in some cases, was attacked by the phosphate-containing salts. Molybdenum crucibles were unaffected.

Lithium chloride-potassium chloride mixtures containing about 25 mole per cent potassium metaphosphate dissolved as much as 5.8 weight per cent U_3O_8 at 775 C. The melting points of these systems were in the region of 650 C.

Although the metaphosphate-containing molten salt mixtures may be potentially useful for certain applications, they are not considered sufficiently promising for this specific reduction reaction to justify further investigation at the present time.

(4) Stability of Cadmium-Magnesium-Uranium Solutions

(R. D. Pierce, P. Nelson, J. Lenc, L. F. Dorsey, R. Zeman, J. Hepperly, M. Bowden)

Many of the unit operations required by the flowsheets that are presently being considered for recovery of melt-refining skulls and blanket processing require that uranium dissolve in cadmium-magnesium solutions and remain in solution for a period of several hours. Reduction of uranium oxide by cadmium-magnesium solutions (up to 6 per cent magnesium) requires stability of cadmium-magnesium-uranium solutions as high as 700 C. Distillation and liquid transfer of uranium-cadmium-magnesium solutions requires stability at 650 C and 500 C, respectively.

(a) Stability of Cadmium-Magnesium-Uranium Solutions for Reduction Equipment

(R. D. Pierce, L. F. Dorsey, J. T. Hepperly)

A dissolution run was made in tantalum to verify that metallic uranium can be dissolved quantitatively in cadmium-magnesium solution using the regular stock charge materials. Figure 7 presents the results, which show rapid dissolution of uranium in the first two hours and essentailly qualitative recovery in 9 hours at 700 C in cadmium-2 per cent magnesium.

FIGURE 7

SOLUTION OF URANIUM IN CADMIUM-2 PER CENT MAGNESIUM

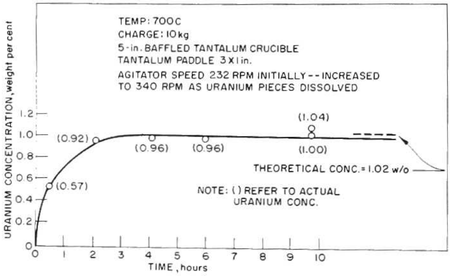

A four-step experiment (Figures 8 and 9) was performed to examine the stability of uranium solutions in tantalum and Type 410 stainless steel (SS) vessels. Uranium was dissolved in cadmium-3 per cent magnesium at 700 C in a tantalum crucible employing a tantalum agitator. The resultant solution was poured into a mold and frozen. The ingot was recharged to a cleaned tantalum vessel and agitated at 700 C for $10\frac{1}{2}$ hours, then poured and frozen. This ingot was subsequently charged to a 410 SS vessel equipped with a mild steel agitator. The solution was melted and stirred at 550 C for 21 hours and then at 700 C for 68 additional hours.

FIGURE 8

STABILITY OF URANIUM–CADMIUM–3 PER CENT MAGNESIUM IN TANTALUM

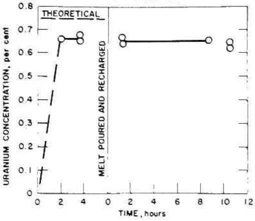

TEMPERATURE: 700 C
CHARGE: 8 kg
AGITATION:
TANTALUM PADDLE 2 1/2 inch by 3/4 inch
SPEED: 315 rpm
TANTALUM CRUCIBLES
5 inch Dia, 4 1/2 inch
BAFFLES

Only 88 per cent of the theoretical uranium concentration was achieved in the four-hour dissolution step (Figure 8). The concentration realized upon dissolution was also found when the ingot was remelted and held in a cleaned tantalum vessel for $10\frac{1}{2}$ hours, indicating that the missing 12 per cent remained behind in the original solution crucible. The holding run in steel shows the uranium solution to be stable at 550 C, but resulted in a marked uranium loss at 700 C (Figure 9). Since this entire loss was experienced early in the run, the iron surface may have become protected from further interaction with uranium, perhaps by the formation of a protective uranium-iron intermetallic layer. A uranium-rich deposit is formed on 410 steel equipment during contact at 700 C with uranium-cadmium solutions, as indicated by metallurgical and autoradiographic examination of the contact areas.

FIGURE 9

STABILITY OF URANIUM–CADMIUM–3 PER CENT MAGNESIUM IN 410 STAINLESS STEEL AT 550 C AND 700 C

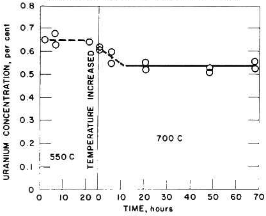

CHARGE 8 kg
AGITATION:
MILD STEEL PADDLE
2 1/2 inch by 7/16 inch
SPEED: 315 rpm
410 SS CRUCIBLE
5 inch Dia, 4 1/2 inch
BAFFLES

A second stability experiment (Figures 10 and 11) was performed under nearly the same conditions. The initial cadmium-magnesium charge material was pretreated with uranium and then filtered at 375 C. The ingot prepared in tantalum at 700 C (Figure 10) was split, one-half being used

FIGURE 10

DISSOLUTION OF URANIUM IN PRETREATED CADMIUM-3 PER CENT MAGNESIUM

(Run SD-60C)

TEMPERATURE: 700C
CHARGE: 8kg
TANTALUM CRUCIBLE:
5 in. Dia, 4 1/2 in. Baffles
AGITATION:
Ta PADDLE
2 1/2 in. by 3/4 in.
SPEED: 315 rpm

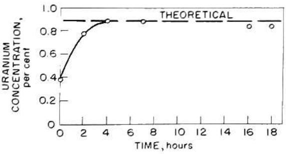

FIGURE 11

STABILITY OF URANIUM-CADMIUM-3 PER CENT MAGNESIUM IN 410 STAINLESS STEEL AT 550C AND 700C

o RUN SD-60D USING 1/2 INGOT FROM SD-60C
x RUN SD-60E USING BALANCE OF INGOT FROM SD-60C IN UNCLEANED CRUCIBLE AFTER POURING OUT SOLUTION FROM SD-60D

CHARGE: 4 kg (each)
AGITATION:
Mild Steel Paddle 2 1/2 in. by 7/16 in.
SPEED: 315 rpm
410 SS CRUCIBLE:
5 in. Dia, 4 1/2 in. Baffles

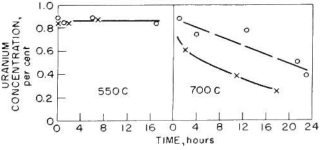

to make the holding run in the 410 SS crucible as before and the other half used to perform a second holding run in the same stainless steel crucible after the initial charge had been poured out. By dividing the 410 SS holding run into two parts, the possibility that the first use might condition the crucible for the second was explored.

The uranium added to the pretreated cadmium-magnesium solution was all present in solution after four hours agitation; however, some loss of uranium during the interval of 7 to 16 hours of run time was experienced (Figure 10).

The two holding runs in 410 SS again showed good solution stability at 550 C, but both runs showed extremely poor solution stability at 700 C. At 700 C the concentrations did not level off after an initial small drop, as was experienced previously.

The stability of uranium-cadmium in Type 405 stainless steel which is to be used in large-scale distillation equipment was also determined. Over a 92-hour period at 550 C, no detectable loss of uranium from solution occurred (see Figure 12). A temperature of 550 C appears to be the maximum safe temperature for containing uranium-cadmium solutions in mild steel or 400-series stainless steels. Uranium loss from solution occurs with increasing rapidity as temperatures are increased above this temperature.

Stability of Uranium-Cadmium Solutions in Graphite

One uranium dissolution in cadmium-2 per cent magnesium was performed in a graphite crucible at 700 C. This run was intended as a preliminary examination of the feasibility of occasional use of existing graphite equipment for handling solutions of uranium in cadmium. The uranium solution was not stable, as the results on Figure 13 illustrate.

FIGURE 12

STABILITY OF CADMIUM-MAGNESIUM-URANIUM SOLUTION CONTAINED IN TYPE 405 STAINLESS STEEL

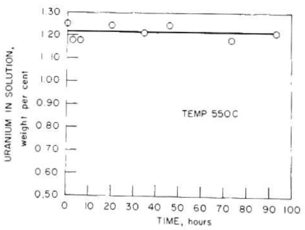

FIGURE 13

DISSOLUTION OF URANIUM IN CADMIUM-2 PER CENT MAGNESIUM IN A GRAPHITE CRUCIBLE

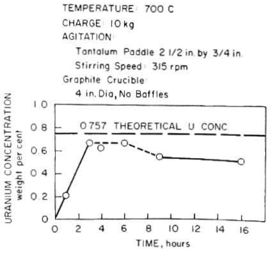

FIGURE 14
STABILITY OF URANIUM-MAGNESIUM-CADMIUM SOLUTION
IN 25 PER CENT NITROGEN-ARGON ATMOSPHERE

TEMP: 700 C
PRESSURE: 2 psig
CRUCIBLE: alumina
BAFFLES AND AGITATOR: tantalum

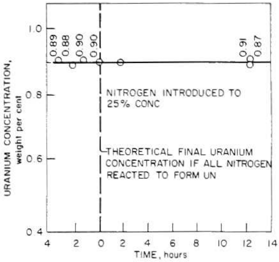

(b) Effect of Nitrogen on the Stability of Uranium-Cadmium Solutions

(R. D. Pierce, L. F. Dorsey, K. R. Tobias)

A master alloy of uranium in cadmium-2 per cent magnesium was melted in an alumina crucible incorporating tantalum baffles and agitator. After the solution had been stirred for four hours, the furnace atmosphere was changed from argon to argon containing 25 per cent nitrogen, and the melt was agitated in this atmosphere at 700 C for 12 hours. Interaction with nitrogen was found to be slow or negligible, as shown in Figure 14.

b. Development of Processes for Recovery of Plutonium from EBR-II Blanket Material

(I. O. Winsch, T. F. Cannon)

The separation of the plutonium product from magnesium by distillation is the final operation in processing blanket material. The bottom-loaded distillation unit described in ANL-5996 is being used to demonstrate this operation.

In order to demonstrate the plutonium-handling techniques which had been developed for this operation, a run involving about 1 gram of plutonium was made as preparation for runs of larger scale. In this run, an alloy composed of about 500 g of magnesium, 100 g of cerium, and 1.235 g of plutonium was charged to a tantalum still pot and loaded into the distillation unit. Tantalum baffles were provided in the vapor space above the still pot to restrict entrainment of the plutonium and cerium. The loading, distillation, and unloading operations were carried out smoothly without incident.

Table 11 indicates a plutonium material balance of 101.4 per cent, which is well within analytical error. The analytical results show that about 0.45 per cent of the plutonium charged was present in the distillate. This is equivalent to a decontamination factor of about 220.

Table 11

PLUTONIUM MATERIAL BALANCE IN SEPARATION OF MAGNESIUM FROM PLUTONIUM-CERIUM BY DISTILLATION

Charge: 500.5 g magnesium, 99.2 g cerium, 1.2346 g plutonium

Still Pot Charge Plutonium (g)	Plutonium Product Phase		Magnesium Distillate Plutonium		Plutonium Material Balance (%)
	(grams Pu)	(% of charge)	(g)	(% of charge)	
1.2346	1.234	99.99+	0.0055	0.45	101.4

3. Engineering Development for Liquid Metal Solvents

(L. Burris, Jr.)

Development of engineering techniques and equipment for liquid metal solvent processes is underway on distillation and retorting, liquid-liquid phase separations, and materials handling.

a. Distillation

Measurement of Temperature and Pressure for Distillation

(P. A. Nelson, J. Lenc, R. Zeman)

Several experiments were conducted to determine whether any difficulties would be encountered in controlling metal distillation processes carried on at high rates [5 grams of cadmium per (minute) (square centimeter)]. This study was initiated because it had been noted that the pressure above boiling cadmium and magnesium was lower than the vapor pressure data reported in the literature.[2]

The properties that must be known in order to calculate the vapor pressure of a boiling binary liquid are the temperature, the composition, and the activity coefficients at the surface of the liquid. If the evaporation rate is low enough so that the driving force necessary to maintain it is negligible, the pressure above the surface should agree with the pressure calculated from the liquid properties at the surface. Even at the contemplated evaporation rate it is not expected that a significant pressure difference will exist.

Figure 15 is a diagram of the equipment which was used to determine the temperature at various levels below the surface of boiling cadmium. The thermocouple used to measure the temperature near the boiling surface was a $\frac{1}{16}$-inch diameter stainless steel-clad thermocouple. It was shaped in such a way that it was parallel to the liquid surface for 1.5 inches from the junction in order to prevent conduction of heat from

---

[2] Ditchburn, R. W. and Gilmour, J. C., Revs. Modern Phys. 13, 310 (1941)

the junction. The location of the liquid surface was detected by determining the highest level at which an electrical circuit was completed between the body of the distillation unit and the thermocouple which was insulated from the head of the unit.

FIGURE 15
EQUIPMENT FOR MEASURING TEMPERATURE
DISTRIBUTION IN BOILING CADMIUM

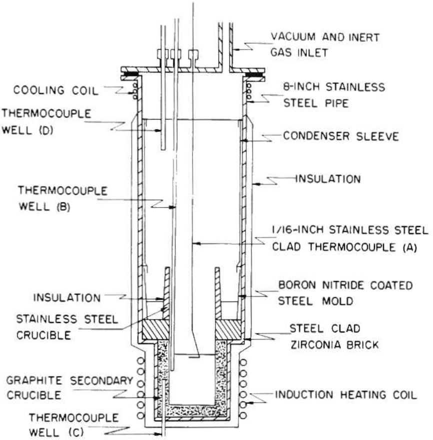

Table 12 illustrates the close agreement between the temperature measured at the surface and the temperature calculated from the pressure above the condenser as measured by an accurate (0.5 mm mercury) gauge.

The surface temperature was only 2 to 3 C lower than the bulk temperature.* Depending on the rate of evaporation, the temperature at the thermocouple in the well touching the side of the crucible through which heat was flowing was 2 to 10 C hotter than the surface temperature.

Two other runs were conducted, one with magnesium, and the other with cadmium but with only the thermocouple near the wall (A) for temperature measurement. The results indicated again that this thermocouple read about 2 to 13 C higher than the temperature calculated from

---

*This is contrary to results of H. W. St. Clair and M. J. Spendlove (U. S. Bureau of Mines R. I. 4710, 1950) which indicate a temperature difference of as much as 25 C under similar conditions with zinc.

Table 12

TEMPERATURE DISTRIBUTION IN BOILING CADMIUM

Evaporation Rate[a] [g/(hr)(sq cm)]	Pressure (mm Hg)	Distance of Thermocouple (A) below surface (in.)[b]	Temperature (C)		Calculated Temperature (C)[e]
			Thermocouple (A)[c]	Thermocouple (B)[d]	
0.1	180	0.06	647	652	651
	182	4.5	652	654	652
	160	0.06	643	648	643
	160	0.5	645	648	643
0.3	155	0.5	640	650	641
	155	1.0	641	650	641
	155	4.5	643	649	641
0.7	176	0.06	650	658	650
	178	0.06	650	653	651
	159	0.06	643	650	643
	161	0.06	643	651	643
	161	0.5	644	650	643
	176	2.0	652	658	650
	161	2.0	645	650	643
	161	4.5	646	652	643

---

[a] The evaporation rate was estimated from the temperature difference between the secondary crucible and the thermocouple near the crucible wall and comparison with data obtained in constant-rate runs.

[b] As measured from the surface of the liquid.

[c] Thermocouple (A) was located near the axis of the crucible (see Figure 15)

[d] Thermocouple (B) was touching the wall of the crucible at a depth of about 0.5 inch from the bottom (see Figure 15)

[e] The boiling point of cadmium at the measured pressure as calculated from the equation $\log P_{mm} = -5982/T - 1.8 \log T + 14.063$ (Ditchburn, R. W. and Gilmour, J. C., Revs. Modern Phys. 13, 310 (1941).

the pressure measurement at pressures above 10 mm mercury. At the highest evaporation rate [1.0 gram of cadmium per (minute)(square centimeter)] the thermocouple read 10 to 13 C higher than that calculated from the pressure. At pressures of 2 to 5 mm mercury the measured temperature was 10 to 21 C higher than the calculated temperature, indicating that the difference between the true vapor pressure at the surface and the pressure at the gauge was not negligible at low pressures.

At pressures above 20 mm mercury the pressure measurements of the inert gas above the condenser appear to agree with the correct vapor pressures within two per cent. This was indicated by comparing the pressure at which cadmium began to boil as the pressure was carefully lowered with the pressure measured during vigorous boiling at the same temperature.

In an experiment in which a magnesium-cadmium alloy was distilled, it was determined that the difference between the surface composition and the bulk composition during boiling was probably within the analytical error in determining the composition. The initiation of vigorous mechanical agitation of the molten solution caused no perceptible pressure change. Also, samples taken near the surface and deep within the melt showed no significant difference in composition.

After determining the accuracy of measuring the temperature, composition and vapor pressure of cadmium-magnesium alloys as described above, the accuracy of estimating the activity coefficients was considered. In an experiment with boiling cadmium-magnesium alloys, the vapor pressure and temperature were measured and then a sample was taken after rapidly raising the pressure to arrest the boiling. The vapor pressure was compared with that calculated from the temperature, the composition, and the activity coefficients obtained from cell measurements at 727 C.[3] After allowing for the inaccuracies in measuring the temperature, the composition, and the pressure as described above, the vapor pressure agreed with the calculated pressure reasonably well at 722 C. However, the pressure calculated by assuming that the activity coefficients did not vary with temperature was twice as high as the measured pressure at temperatures around 600 C.

From the results of the runs described above, the following conclusions have been drawn:

(1) No difficulty is foreseen in controlling high-rate distillation processes through measurement of the bulk liquid temperature and the pressure in the condensate receiver.

(2) The assumption that the activity coefficients obtained at 727 C in the cadmium-magnesium system do not vary appreciably with temperature is not sufficiently accurate to estimate the vapor pressure in the region of interest (600 to 650 C).

Full-scale Distillation Equipment

(P. A. Nelson, J. Hepperly)

A full-scale distillation station is being constructed to demonstrate metal distillation and retorting at expected plant rates and to

---

[3] Hultgren, Ralph, Selected Values for the Thermodynamic Properties of Metals and Alloys, Institute of Engineering Research, University of California, Berkeley, California (September 1956).

demonstrate other associated operations such as metal transfer, liquid-level detection, and freeze-valve operation. The major pieces of equipment have been received or are nearly completed and will be ready for delivery soon. The instrumentation drawings, the last part of the drafting effort, are proceeding. It is expected that the equipment will be complete and ready for the first tests by October 1, 1960.

Cadmium Distillation Test Unit

(I. O. Winsch, T. F. Cannon)

A distillation unit with a still pot capacity of about 50 kg of cadmium has been constructed to test several of the design concepts of the large-scale distillation unit. A sketch of the unit is shown in Figure 16.

FIGURE 16
CADMIUM DISTILLATION UNIT

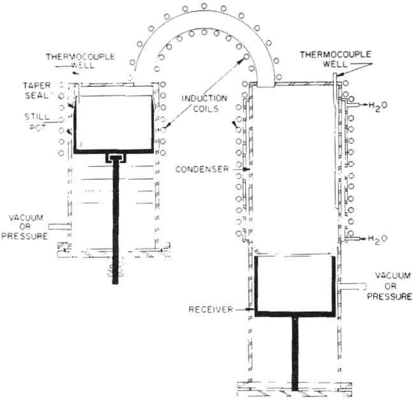

The still pot and receiver are bottom-loaded and unloaded. It is possible to raise and lower the still pot crucible within the distillation unit by means of a threaded shaft entering through the bottom flange of the still pot. A seal between the still pot crucible and the remainder of the distillation unit is effected by means of a taper on the top of the still pot fitting into a mating tapered section within the unit.

In this test unit, the still pot and vapor line are inductively heated. (In the plant unit, these components will be placed in a large resistance furnace and separate heating of component parts will not be required except for the still pot.) Metal vapors will condense as a solid on the water-cooled condenser wall. At the end of a distillation run, the condenser water will be drained. The condenser will then be inductively heated to melt the condensed metal into the receiver. If the unit operates satisfactorily, it will be used as a service facility for cadmium recovery.

The unit has undergone several shakedown tests. The induction coils have satisfactorily heated the distillation and condensing sections to expected operation temperatures.

The tapered joint on the still pot crucible was put through a series of tests to determine its sealing qualities. In two tests at room temperature and with an upward force of about 3000 pounds exerted on the crucible, leak rates of 0.28 and 0.02 cubic foot per hour at STP were measured at pressure differentials of 860 mm and 100 mm, respectively.

Three tests of the tapered joint were also made at high temperatures. An upward force of 2300 pounds was exerted on the crucible when the outside wall temperature of the still reached 600 C and the crucible reached 400 C. At a temperature of 730 C and a pressure differential of 960 mm, a leak rate of about 0.04 cubic foot per hour at STP was observed. With a pressure differential of 160 mm (160 to 0 mm), the leak rate was reduced to 0.001 cubic foot per hour at STP. At a temperature of 650 C and a pressure differential of 81 mm (81 to 0 mm), the leak rate was about 0.06 cubic foot per hour at STP.

All of these leak rates are low and well within the arbitrary maximum of 1 cubic foot per hour at STP. It is evident that the expansion of the inner crucible against the outer taper contributes substantially to producing a tight seal. This can be varied by the temperatures of the female and male tapers at the time the joint is made.

Once the seal had been made, disengaging was not possible by means of the screw mechanism alone. To effect disengagement, it was necessary to cool and then to expand the outer tapered section away from the inner tapered section by rapid heating of the outer section to 250 C.

Cadmium distillation runs are planned at frequent intervals in order to obtain long-term performance data on the above sealing method.

b. Retorting of Uranium Concentrates

(J. F. Lenc, P. A. Nelson, M. Bowden)

In liquid metals processing of melt-refining skulls, final recovery of uranium from the solvent metals after removal of the fission products will be accomplished by evaporating the solvent metals (magnesium, cadmium and/or zinc). The uranium product so obtained must be in a form suitable for removal from the crucible and subsequent handling by remotely contolled equipment. The major problem in achieving this objective is to find a satisfactory retorting crucible material. Experiments are being conducted, therefore, on evaluation of various crucible materials.

Since a definite flowsheet for skull processing has not yet been adopted, two alternative retorting procedures must be considered to accommodate flow sheets which are under consideration. In some processes the uranium is completely dissolved during or after reduction. The solution to be distilled would be free of flux, magnesium oxide, and uranium oxide. In other processes the uranium is not dissolved during reduction (which is carried out at high magnesium concentrations) and a clean separation of the flux, the magnesium oxide, and the residual uranium oxide from the uranium-liquid metal matrix is not possible. Liquid transfer of material from the reduction crucible to the distillation unit, as contemplated in the alternative processes in which the uranium is dissolved before distillation, would not be possible.

Retorting of Reduced U_3O_8

It is likely that the same container will be employed for reduction, phase separation, and retorting in those processes in which the uranium would not be dissolved during or after reduction. Tantalum crucibles were tested first for this service because ceramic coatings would not be likely to withstand the solidification and remelting of the ingot which would probably be necessary after the phase-separation step.

Several ingots resulting from the reduction of U_3O_8 were retorted in the same tantalum crucibles in which the reductions were conducted. The reductions were conducted with magnesium-cadmium alloys containing 20 to 50 per cent magnesium under an argon atmosphere and a synthetic Dow-230 flux cover. The ingots were prepared for retorting by removing the flux by siphoning it off while molten or by dissolving it in water after cooling. In every case the uranium product was found to adhere to the tantalum crucible after retorting and could not be completely removed except by dissolution in acid. Consequently, tantalum is not a suitable container material for reduction operations in which the uranium is not dissolved.

Retorting of Uranium-simulating Solution Distillation

Small-scale experiments on distillation of cadmium-magnesium-uranium alloys are hampered by insufficient amounts of uranium residue. This is because of the low solubility of uranium in cadmium solution (0.5 to 1.5 per cent depending on the magnesium concentration). In order to circumvent this disadvantage, the distillation process has been simulated by retorting alloys containing UCd_{11} formed by reacting uranium with cadmium.

The charge for one such run (A-9) consisted of a cadmium-magnesium-uranium ingot containing 453 g of uranium, prepared in an aluminum oxide crucible. The uranium was powdered by hydriding and dehydriding to facilitate its reaction with cadmium to form the intermetallic UCd_{11}. Retorting of the cadmium and magnesium was conducted in a tantalum crucible at initial conditions of 650 C and 175 millimeters pressure to final conditions of 880 C and 0.05 millimeter pressure.

A compacted uranium product, $\frac{1}{4}$- to $\frac{3}{8}$-inch thick and weighing about 300 g, was recovered from the bottom of the tantalum crucible. This product was easily removed and readily broken apart. An additional 100 to 125 g of material was removed from the crucible side wall. Apparently, this latter material was entrained in the cadmium-magnesium vapors during retorting and subsequently plated out on the side wall. Although the uranium product in this experiment was readily removed from the tantalum crucible, it should be pointed out that the crucible had been used in other experiments, so that surface impurities may well have been present. Such impurities could have prevented the uranium from adhering to the tantalum. This experiment is to be repeated with a new tantalum crucible in order to clarify this point.

Another retorting experiment was made at the same temperature and pressure conditions as above, using a graphite crucible flame-sprayed with a 30-mil-thick coating of aluminum oxide. This run, A-10, was similar to that described in ANL-6101, pages 80, 82, and 83, with the exception that twice the amount of uranium, 1000 g compared with 500 g, was used in preparing the charge ingot. After retorting, a compacted uranium product weighing 500 g was easily removed from the bottom of the aluminum oxide-coated graphite crucible. In addition to this compacted product, a thin film of material weighing 235 g was recovered from the crucible side wall.

Table 13 gives the analyses of the uranium products from the two retorting experiments described above, A-9 and A-10. Analyses of the two experiments reported in ANL-6101, pages 80, 81, 82, and 83, are also shown. On a larger scale, greater purity of the uranium product could be expected.

A general conclusion can be made that little difficulty is encountered in removing uranium from ceramic retorting crucibles or from ceramic-coated graphite or ceramic-coated metal retorting crucibles. Similar success has not been experienced using uncoated graphite or metal retorting crucibles. Consequently, emphasis in future experimentation will be placed on evaluating ceramic and ceramic-coated crucibles. The ceramic coatings are to be tested on graphite, stainless steel, tantalum, molybdenum, and tungsten-base materials.

Table 13

ANALYSES OF URANIUM PRODUCT AFTER RETORTING

Retorting was conducted at initial conditions of 650 C and 175 millimeters pressure to final conditions of 880 C (3 hr at 880 C) and 0.050 millimeter pressure.

Run No.	Crucible Material	Sample Location	Analyses (ppm)					
			B[a]	Al[a]	Ta[a]	O[b]	N[c]	C[d]
A-3	Boron Nitride	Bottom of Crucible	70	20	-	1350	1090	-
		Arc-melted Button	1000	<400[e]	-	1000	300	-
A-4	Al_2O_3-coated Graphite	Bottom of Crucible	-	1000	-	1810	916	749
		Arc-melted Button	-	<400[e]	-	6[f]	1459	273
A-9	Tantalum	Bottom of Crucible	-	<400[e]	2000	1100	1210	-
		Side of Crucible	-	<400[e]	2000	3000	1100	-
A-10	Al_2O_3-coated Graphite	Bottom of Crucible	-	3000	-	520	1240	580
		Side of Crucible	-	5000	-	510	1220	570

---

[a] Spectrographic analysis, accurate to within a factor of two

[b] Gas fusion

[c] Kjeldahl

[d] CO_2 evolution

[e] Limit of analysis

[f] Low value questionable

Melting of Compacted Uranium Recovered from Retorting

It is currently anticipated that the uranium product recovered from the final retorting step of the liquid metals process is to be fed back into the melt-refining furnace for consolidation. In Experiment M-1, 190 g of the uranium product recovered in the above Run A-9 was charged into a recrystallized aluminum oxide crucible together with 750 g of clean $\frac{1}{4}$-inch diameter uranium pins. This charge was vacuum melted by induction heating to 1438 C at a pressure of 3.4×10^{-4} millimeter. Visual examination of the resulting ingot indicated that better than 90 per cent of the retorted uranium product had coalesced with the molten uranium from the $\frac{1}{4}$-inch diameter pins. Complete coalescence was not achieved due to oxidation of the retorted product, as no special precautions were exercised to maintain the product under an inert atmosphere, save for storage in a sealed glass jar. In future experiments of this nature, the uranium recovered from final retorting will be maintained under an argon atmosphere to reduce this oxidation.

c. Development of Equipment for Molten Cadmium Service

Various equipment components are being tested and developed for incorporation into liquid metal equipment systems. These include freeze valves, check valves, mechanical valves, pipe joints, autoresistively-heated transfer piping, and liquid-level indication devices.

Fixed Liquid-level Probe

(J. C. Hesson, K. R. Tobias)

The liquid metal-level probe assembly shown in Figure 17 was tested with mercury at room temperature and with liquid cadmium at about 650 C. This probe assembly is designed for determining whether the liquid is above or below a fixed level by the change in resistance of the probe circuit. In testing with mercury, the probes were dipped into mercury in a beaker; in testing with liquid cadmium, the probes were dipped into liquid cadmium under flux in a crucible. When tested with mercury at room temperature or with liquid cadmium at about 650 C, the electrodes did not wet. The changes in resistance were about the same whether mercury or cadmium was used.

FIGURE 17

LIQUID-METAL-LEVEL TEST PROBE ASSEMBLY

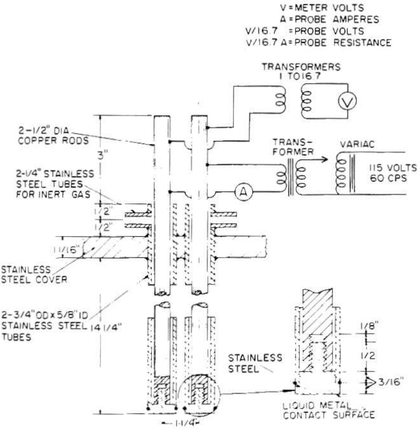

The computed probe resistances for copper, molten metal, and stainless steel resistivities of 1.7, 35 and 60 microhm-cm, respectively, were

probes not touching liquid	0.0050 ohm
probes touching liquid	0.00025 ohm.

The liquid metal-to-probe contact resistance apparently varies with probe current.

From the results it is seen that control and indicating devices based on either probe current or probe voltage changes could be used.

This type of probe has the advantage that there are no insulators which could be electrically shorted or through which gas could leak. A possible disadvantage is that a badly oxidized or corroded probe might make poor contact with the liquid metal.

Autoresistive Heating of Liquid Metal Transfer Lines

(I. O. Winsch, T. F. Cannon)

In the EBR-II drag-out and blanket process it will be necessary to transfer liquid metal phases from vessel to vessel. Investigations have been carried out to determine the feasibility of transferring liquid metals through autoresistively heated pipes. The design of this equipment was described in ANL-6101, page 56.

Several liquid metal transfer experiments have been completed. A Hobart welding unit was used to provide power for heating of the transfer lines instead of the transformer used in previous runs. In these experiments, the still pot charges were about 3.5 kg of cadmium-magnesium alloys which were heated to about 750 C. The transfer lines were heated from 550 to 700 C. Helium was introduced to the still at a pressure of about 25 psig to transfer the liquid metal to the receiver. Of the alloy charged to the still pot, 90 to 98 per cent was transferred to the receiver in these tests.

The results of these experiments indicated the importance of uniform insulation along the length of the transfer line to prevent hot and cold spots. It also was found necessary to blow the transfer line clear of residual metal to prevent plugging. If this procedure was not followed before reuse of the transfer line, the lowered resistance in these sections resulted in overheating the open sections. This appears to be the major difficulty in the use of autoresistively heated transfer lines.

Liquid Metal Sampling

(I. O. Winsch, T. F. Cannon)

Vycor and quartz tubing have been used almost exclusively for sampling of liquid metals. Difficulties have been encountered with the sampling tubes breaking off and reacting with the melts. The possiblities of overcoming this difficulty through the use of thin-wall metal tubing have been investigated.

Samples of molten magnesium at 750 C were taken using $\frac{1}{8}$-, $\frac{3}{16}$-, and $\frac{1}{4}$-inch diameter mild steel tubing with 5- and 10-mil wall thicknesses. Vacuum for raising the metal into the sampling tubes was provided by the vacuum bottle technique, bulb, and syringe.

It was concluded that the $\frac{3}{16}$- and $\frac{1}{4}$- inch diameter tubes with a 5-mil wall were the most suitable in taking the magnesium samples. It was very easy to peel off the thin wall and remove the sample. It was very difficult to remove the magnesium metal from the $\frac{1}{8}$- inch diameter tubing. The use of a syringe gave excellent control of the size of sample when compared with the bulb and vacuum bottle technique. An unfiltered thief sample of the melt gave an excellent sample 2 inches in length. In sampling liquid metal systems incompatible with mild steel, thin-walled tantalum or other metal tubing might be used.

d. Liquid Metal Corrosion Studies

(J. C. Hesson, H. Lavendel, J. Pavlik)

Dynamic Tests

The second forced corrosion loop (electromagnetically pumped) which was placed in operation at 550 C on November 17, 1959, has now been in trouble-free operation for over 3000 hours. An alloy of cadmium with a nominal 1.0 weight per cent uranium and 2.0 weight per cent magnesium and other fission product elements* is being circulated in the carbon steel loop. Periodic sampling indicates that the uranium concentration in solution has dropped from about 0.94 to 0.85 per cent since the startup.

C. Pyrometallurgical Research

(H. M. Feder)

1. Chemistry of Liquid Metal Solvents

(I. Johnson)

The chemistry of liquid metal systems is being investigated to permit the logical design of pyrometallurgical separations processes and to provide appropriate basic data. The separation process under consideration consists of the dissolution of the spent reactor fuel in an appropriate volatile liquid metal, separation of the fission products or other extraneous elements by recrystallizations and/or extractions into immiscible liquids (either fused salts or other liquid metals), and final recovery of the fissile metal(s) by evaporation of the solvent.

a. Solubilities in Liquid Metals

The solubilities of the elements whose separations are being attempted are of prime importance in the design of fuel-reprocessing

---

*Other elements: w/o

Strontium	0.007	Rhodium	0.003
Ruthenium	0.002	Palladium	0.002

schemes. The dependence of solubilities on temperature and solvent composition needs to be known. When the solubilities are determined for a new system, it is useful to characterize the solid phase in equilibrium with the saturated solutions.

Solubility of Thorium in Cadmium

(I. Johnson and K. D. Anderson)

The solubility of thorium in liquid cadmium was measured, using both the heating and cooling methods (see ANL-6068, page 66, for a discussion of the experimental method). The samples were obtained using magnesium oxide-coated Vycor sampling tubes and were analyzed for thorium by a colorimetric method. Four separate runs were made to cover the range in concentrations encountered. This was necessary to facilitate sampling of the liquid phase, since the thorium-cadmium intermetallic solid phase was less dense than the liquid phase. It was difficult to push the sampling tube through a thick layer of intermetallic into the liquid phase.

FIGURE 18
SOLUBILITY OF THORIUM IN CADMIUM

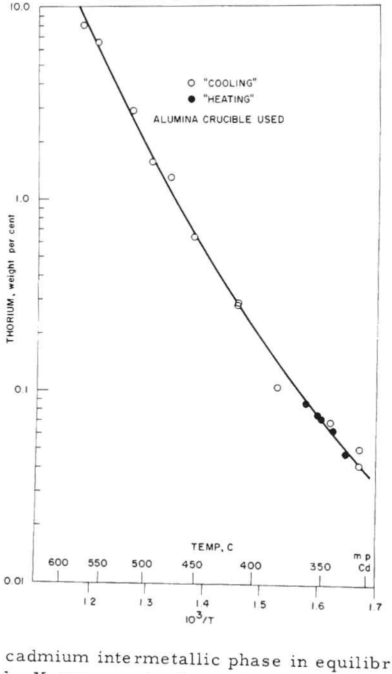

The solubility data shown in Figure 18 were fit to a quadratic equation in $1/T$ with the result

$$\log x = 11.620 - 15.358\frac{10^3}{T} + 3.175\frac{10^6}{T^2}$$

(where x is the atom fraction of thorium in the saturated liquid solution) with a standard deviation of 8.7 per cent.

The solid thorium-cadmium intermetallic phase in equilibrium with the solutions was found -ray examination to be a new species isomorphous with UCd_{11}. Prep- on of samples sufficiently pure for density determination and chemical sis is under way.

Cobalt-Cadmium

(M. G. Chasanov and P. D. Hunt)

The solubility of cobalt in liquid cadmium was determined by taking filtered samples of the saturated solution. The cobalt analyses were performed by a modification of the 2-nitroso-1-naphthol method reported by Sandell.[4] The values obtained for the solubility ranged from 1.9×10^{-3} weight per cent cobalt at 348 C to 1.8×10^{-2} weight per cent cobalt at 658 C. Figure 19 gives a plot of log solubility versus 1/T for this temperature range. These data are provisional and more detailed investigations may modify the values. In these projected studies, the lower solubility range will be investigated using radioisotope methods in addition to chemical techniques of analysis.

FIGURE 19

SOLUBILITY OF COBALT IN LIQUID CADMIUM

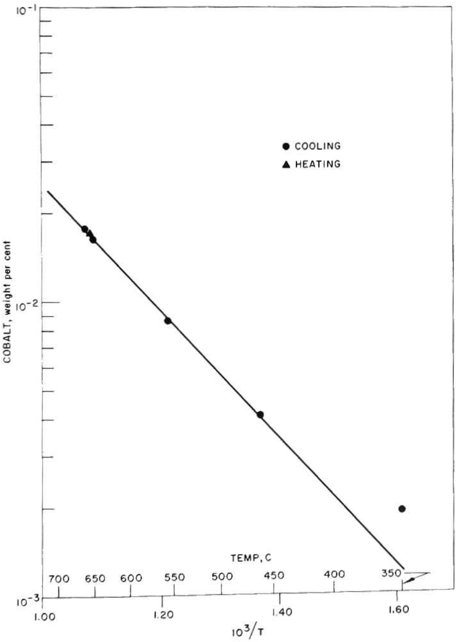

---

[4] Sandell, E. B., Calorimetric Determination of Traces of Metals, 3rd Ed., Interscience Publishing Inc., New York (1959), p. 422.

Microscopic examination of the ingot (1 weight per cent cobalt) from the above determination gave no indication of the presence of phases other than the original cobalt powder added. Early work on this system[5] reported the presence of an intermediate phase in a eutectic matrix for melts up to 10 weight per cent cobalt. Westgren and Ekman[6] reported an alloy of composition $Cd_{21}Co_5$, corresponding to 11.1 weight per cent cobalt; however, Lihl and Buhl[7] were unable to prepare alloys from amalgams or to prepare the above intermetallic by immersion of cobalt in cadmium at 700 C.

Manganese-Cadmium

(M. G. Chasanov, C. Wade, P. D. Hunt)

The solubility of manganese in liquid cadmium was determined by the usual method of filtered sampling of a saturated melt. The manganese analyses were performed using an ammonium persulfate method reported by Sandell.[8] The solubility values obtained ranged from 0.27 weight per cent manganese at 414 C to 1.43 weight per cent manganese at 661 C. Figure 20 is a plot of log solubility versus 1/T for the above range of temperatures. The scatter of the data at higher temperatures may be due to sampling errors. As noted in the case of the cobalt-cadmium system, the data reported here are preliminary and are subject to later revision when a more detailed investigation of this system is completed.

FIGURE 20
SOLUBILITY OF MANGANESE IN LIQUID CADMIUM
All data obtained by "cooling"

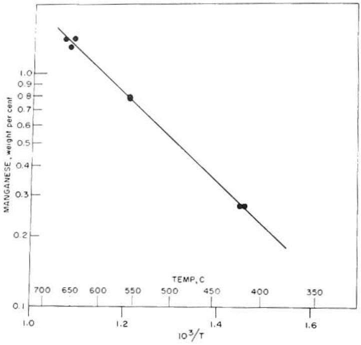

Examination of the ingot from this solubility determination (2 weight per cent manganese initial charge) revealed the presence of a different phase in the upper portion. Microhardness examination of the ingot indicated an average Vicker's Hardness Number (VHN) of 986 for this unknown phase. The manganese used in this study had an average VHN of 691. Cadmium, of course, is much softer than manganese. In addition, the unknown phase was quite brittle and cracked easily.

---

[5] Lewkonja, K., Z. Anorg. chem. <u>59,</u> 322 (1908).

[6] Westgren, A. and Ekman, W., Arkiv. Kemi, Mineral Geol, <u>B10,</u> No. 11, 1 (1930)

[7] Lihl, F. and Buhl, E., Z. Metallkunde <u>46,</u> 787 (1955).

[8] Sandell, C. B., <u>Colorimetric Metal Analyses,</u> 3rd Ed., Interscience Publishers Inc., New York, (1959), p. 611.

Zwicker[9] reported that cadmium and manganese form no alloys when heated up to 1200 C in a sealed silica bulb, and he suggested that there is a slight solubility of manganese in cadmium.

Future investigation of this system will include thermal analysis and X-ray analysis of powder compacts in order to prove the existence of and to characterize the intermetallic phase or phases indicated by the preliminary data presented above.

Nickel-Cadmium

(M. G. Chasanov and C. Wade)

The nickel-cadmium system has been studied by many investigators; however, Hansen's compilation[10] indicates there are little solubility data, especially above the peritectic decomposition temperature of the γ-brass phase (reported as 502 C by Voss[11] and 490 C by Swarz and Phillips[12]). The solubility of nickel in liquid cadmium was determined by filtered sampling of an approximately 18 weight per cent nickel melt in the usual manner; the data obtained are shown in Figure 21, along with the values of Swarz and Phillips.[12] The data indicate a peritectic transformation at about 496 C. These results are preliminary and may be revised when more detailed studies are completed.

FIGURE 21
SOLUBILITY OF NICKEL WITH LIQUID CADMIUM

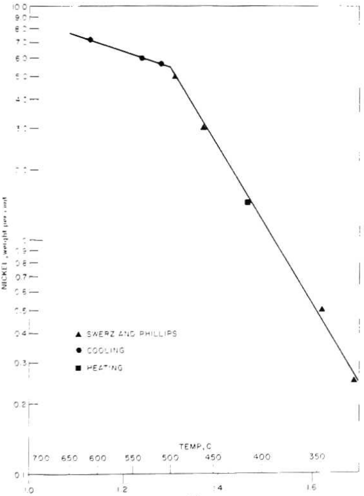

Future studies include a determination of the solid phase in equilibrium with the liquid at temperatures above the γ-brass peritectic.

---

[9] Zwicker, U., Z. Metallkunde 41, 399 (1950).

[10] Hansen, M. and Anderko, K., Constitution of Binary Alloys, 2nd Ed., McGraw-Hill Book Co., New York, (1958), p. 430

[11] Voss, G., Z. anorg. chem. 57, 69 (1908).

[12] Swarz, E. E. and Phillips, A. J., Trans. AIME 111, 333 (1934).

The Zinc-Niobium System

(A. E. Martin and C. Wach)

Additional work has been carried out on the zinc-niobium system beyond that reported in ANL-5959, pages 115 to 116. The combined solubility data are shown in Figure 22. It is apparent that two solubility lines are well defined by the data and that their intersection at 478 C marks a peritectic temperature in the system. The lines have been drawn dotted beyond their intersection, where they represent metastable solubilities. The fact that, in spite of holding times of two hours at the equilibration temperatures, two of the solubility points are much closer to the metastable lines than to the normal solubility lines suggested that the peritectic reaction is very sluggish. This was further indicated when it was found that the thermal arrest corresponding to this peritectic was unusually sensitive to the heating rate used in its measurement.

FIGURE 22

THE SOLUBILITY OF NIOBIUM IN LIQUID ZINC

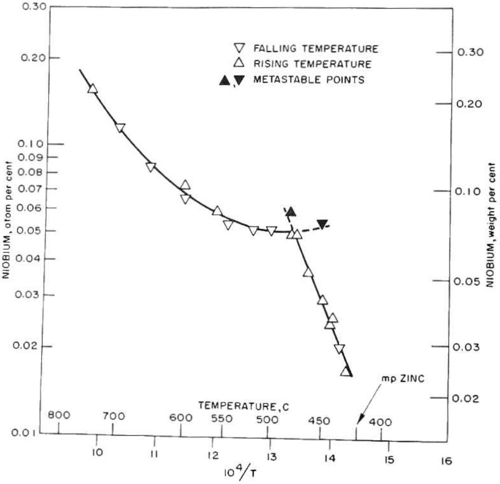

With the two metastable points omitted from consideration, the data above and below the peritectic were fitted by the least-squares method to the following equations:

(478 to 750 C)log(atom per cent niobium) = $5.924 - 10.938 \times 10^3\,T^{-1} + 4.142 \times 10^6\,T^{-2}$

(428 to 478 C)log(atom per cent niobium) = $5.029 - 4.749 \times 10^3\,T^{-1}$,

with standard deviations of 3.9 and 6.0 per cent, respectively.

Thermal analysis studies were made on charges containing 8 to 10 weight per cent niobium. As mentioned above, a confirmation of the 478 C peritectic was obtained. The arrest temperature, 485 C, is not considered as reliable a measurement of the peritectic temperature, however, as that from the solubility data, in view of the sluggishness of the peritectic reaction. Thermal arrests were also observed at approximately 425, 419 and 375 C. The 419 C arrest presumably marks the eutectic temperature; the low concentration of solute at the eutectic, indicated as less than 0.015 atom per cent niobium from the solubility data, requires that the eutectic temperature be not significantly lower than the freezing point of zinc. The nature of the 425 and 385 C arrests have not been indicated as yet; the former may be a peritectic and the latter a phase transformation.

The arrests obtained in the thermal analysis study suggest the presence of three and possibly of four intermediate phases in the zinc-niobium system, whereas the literature to date confirms no information on intermediate phases in this system.

X-ray diffraction studies are being made on crystals isolated from solubility ingots by selective leaching with hydrochloric acid, as well as on annealed compacts made from zinc and niobium powders at various mole ratios of zinc to niobium from 14:1 to 1:3. While these studies are not complete, Flikkema and Tani of this Laboratory have identified the intermediate phase richest in niobium, the one in equilibrium with the melt above 478 C, as being $NbZn_3$. It has an ordered cubic structure of the $AuCu_3$ type (LI_2) with $a_0 = 3.932$ Å and $\rho_X = 7.89_3$ g/cc. The measured pycnometric density was 7.8_3 g/cc.

b. Liquid-Liquid Distribution Studies

(F. Cafasso, R. Uhle)

Studies of liquid-liquid distribution may be used to serve a two-fold purpose: first, to provide information concerning the applicability of immiscible liquid-liquid systems to separation processes, and second, to either confirm existing thermodynamic data or to predict unknown thermodynamic quantities. The uranium-aluminum-cadmium system is the first being studied for this dual purpose.

Differential partition of uranium between liquid aluminum and cadmium was measured as a function of concentration in the range from 686 to 690 C. After bringing a charge to temperature, stirring for one hour, and allowing the melt to settle for one-half hour, the individual layers were simultaneously sampled and the samples analyzed. The aluminum layer was sampled by the conventional method, while the cadmium layer was sampled by the breakseal technique.

Results for these experiments are summarized in Table 14. These results indicate that the uranium concentrated in the liquid aluminum layer and that good agreement existed between duplicate samples in the individual experiments. The cadmium samples, however, showed some variation in uranium concentration in the 10^{-5} per cent range. It is felt that these variations reflect the analytical uncertainty for the low-level uranium analyses and show in two instances the existence of contamination picked up either in handling or during the analysis. Without the presence of aluminum the analytical uncertainty has been found to be ±12 per cent.

The values recorded in the summary are the averaged values for each phase. The two samples believed to be contaminated were not included in the average. Activity coefficients tabulated in Table 14 were calculated using values (from emf measurement) of the activity coefficient of uranium in pure cadmium. This procedure would be valid only if cadmium and aluminum formed two completely immiscible layers. Since they do not, a correction must be made for the effect of this mutual solubility on the activity coefficients. The equation of Alcock and Richardson[13] provides a convenient method for making an approximate correction. Corrected values of the activity coefficients of uranium in aluminum are also recorded in Table 14.

The atom fraction of uranium in the cadmium phase is shown in Figure 23 as a function of its atom fraction in the aluminum phase. In this type of plot, a straight line indicates a constant distribution coefficient, while a curved line represents a concentration-dependent system. Although a smooth curve does appear to fit the data, the line does not extrapolate through the origin. The small concentration dependence exhibited by this system is therefore questionable. When the experimental uncertainty is considered, it is apparent that three of the four points fall reasonably well upon the straight line passing through the origin which has been drawn in. Further experimentation is required in order to clarify this matter.

c. Solid-Liquid Reaction Study
(F. Cafasso, R. Uhle)

This study was initiated to explore the possible utility of a two-phase, solid-liquid system in separation processes. Such a system provides the advantage over liquid-liquid systems that final separation of

---

[13] Alcock, C. B. and Richardson, F. D., Acta Met. 6, 385 (1958).

Table 14

DISTRIBUTION OF URANIUM BETWEEN LIQUID ALUMINUM AND LIQUID CADMIUM

Experiment No.	Temperature (C)	Phase Distribution				Atom Fraction of Uranium (N_U)		$K_{avg} = \frac{N_{U\,(Cd)}}{N_{U\,(Al)}}$	γ_U (Al phase)	
		Aluminum Phase		Cadmium Phase		Aluminum Phase	Cadmium Phase		Uncorr	Corr[b]
		U (w/o)	Cd (w/o)	U (w/o)	Al (w/o)					
10AC[a]	686	4.8	8.0	3×10^{-5}	1.5	0.57	1.6×10^{-5}	2.8×10^{-5}	4.6×10^{-3}	1.27×10^{-3}
12AC	689	3.7	7.1	2.5×10^{-5}	1.5	0.43	1.1×10^{-5}	2.6×10^{-5}	4.3×10^{-3}	1.27×10^{-3}
13AC	687	2.3	7.9	1.9×10^{-5}	1.5	0.27	0.8×10^{-5}	3.0×10^{-5}	5.0×10^{-3}	1.29×10^{-3}
15AC	689	1.2	9.4	1.3×10^{-5}	1.5	0.13	0.6×10^{-5}	4.6×10^{-5}	7.6×10^{-3}	1.33×10^{-3}[c]

---

[a] Results for these experiments were reported in ANL-6101, page 72.

[b] Corrected for the effect of the mutual solubility of cadmium and aluminum.

[c] For the purpose of this calculation, the concentration of cadmium in the aluminum phase was assumed to be identical to that measured in Experiment 12AC.

the phases may be more readily effected. Solid aluminium and a liquid cadmium alloy were chosen as the model system for this experiment.

FIGURE 23
DISTRIBUTION OF URANIUM BETWEEN ALUMINUM AND CADMIUM

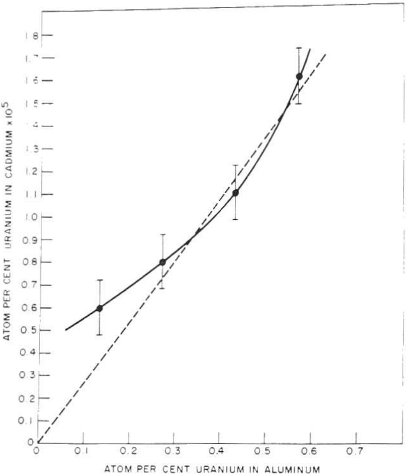

The experiment was conducted in two stages. Firstly, an alloy of cadmium containing, nominally, 1.0 weight per cent cerium, 1.6 weight per cent uranium and 0.18 weight per cent zirconium was fabricated and its composition established through analysis. Then, the ingot was remelted and maintained at 535 C for several hours before a solid piece of aluminum attached to the base of a tantalum stirring rod was lowered into the melt. The concentration changes which occurred in the melt were measured as a function of time by periodic sampling of the cadmium phase. The results are tabulated in Table 15 and are graphically represented in Figure 24.

Examination of this graph reveals that both zirconium and uranium were almost quantitatively removed from the solution (probably through the formation of intermetallic compounds of aluminum) after only four hours of stirring. In addition, it appears that zirconium was removed more readily than uranium. However, the cerium content of the melt decreased slightly (after standing in contact with solid aluminum overnight) to a value of 0.84 weight per cent, whereupon no further significant change in its concentration was measured. The small difference in composition between the alloy and the remelted alloy is probably due to the slowness with which the solid intermetallic phases present in the solid alloy redissolve. Apparently, all of the cerium did not dissolve until stirring was started. Removal of zirconium, however, occurred so rapidly that its concentration never returned to its initial value.

d. Thermodynamic Studies

Thermodynamic functions for key elements in liquid metal solvents and for the important solid intermetallic phases are being measured by two methods. Galvanic cells have proved to be especially useful for

Table 15

SUMMARY OF RESULTS OF SOLID-LIQUID (ALUMINUM-CADMIUM) REACTION EXPERIMENT

Nominal Composition of
Cadmium Melt: 1.0 w/o cerium
1.6 w/o uranium
0.18 w/o zirconium
Temperature: 535 C
Container Material: Alumina
Stirring Rod: Tantalum

Conditions	Uranium (w/o)	Zirconium (w/o)	Cerium (w/o)
Final sample obtained in the process of fabrication of the alloy	1.58	0.181	0.98
Final sample taken after remelting of the ingot but prior to lowering of aluminum into the melt	1.57	0.155	0.78
One hour of stirring with solid aluminum	1.60	0.102	1.00
Overnight standing - no stirring	1.15	<0.01	0.84
Two (total) hours of stirring	0.45	<0.01	0.88
Four (total) hours of stirring	No detectable U	<0.01	0.80
Six (total) hours of stirring	No detectable U	<0.01	0.84

FIGURE 24

SOLID-LIQUID (ALUMINUM-CADMIUM) REACTION EXPERIMENT

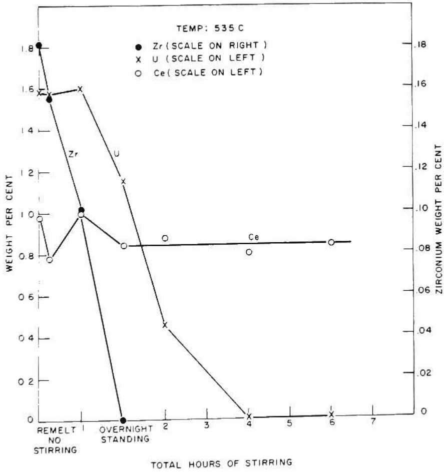

uranium-solvent systems. For those systems in which the galvanic cell method is not practical and in which only one of the components is volatile, measurement of the decomposition pressure by the effusion method is being used.

Thermodynamics of the Uranium-Lead System

(I. Johnson and R. M. Yonco)

A second uranium-lead galvanic cell has been set up to verify the results obtained with the first cell and to investigate more thoroughly the form of the emf-temperature relation in this system. The cell used is of the form

$$U \mid UCl_3 + KCl\text{-}LiCl \text{ (eutectic liquid)} \mid U \text{ (satd soln in liquid Pb)}.$$

The cell reaction is

$$U(s) + 3\ Pb \text{ (satd liquid soln)} \longrightarrow UPb_3(s).$$

Since the solubility of uranium in lead is very small (less than 0.2 atom per cent in the temperature range studied), no significant error is made by assuming that the above reaction is between uranium and pure liquid lead, and consequently the free energy of formation $\Delta F°$, of UPb_3, is obtained from the measured emf, E, using the equation

$$\Delta F° = -nFE.$$

The emf values obtained with the second uranium-lead cell agreed closely with values obtained from the first cell. For example, at 600 C the emf of the first cell was 0.1823 volt while the emf of the second cell was 0.1820 volt.

The dependence of the emf on temperature for both cells is characterized by a linear relation below about 600 C and a curved relation above 600 C. The data obtained using the second cell showed that the transition from the linear to curved relation occurred in a continuous manner. The values over the whole temperature range studied (374 to 846 C) may be represented by a cubic equation in temperature with a standard deviation of ± 0.5 mv. The free energy of formation of the uranium-lead intermetallic compound is given by the equation

$$\Delta F° = -23{,}460 + 21.61\ T - 1.899 \times 10^{-2}\ T^2 + 9.721 \times 10^{-6}\ T^3,$$

where $\Delta F°$ is in calories/gram mole and T is in °K. The corresponding equation for the heat of formation is

$$\Delta H° = -23{,}460 + 1.899 \times 10^{-2}\ T^2 - 1.944 \times 10^{-5}\ T^3.$$

e. Magnetic Studies

(F. Cafasso and C. McMillan*)

Magnetic studies have played a prominent role in the elucidation of the electronic structure of many alloy systems. Interest in this technique developed from the observation that the rare earth compounds $LaCd_{11}$, $CeCd_{11}$, $PrCd_{11}$ and $NdCd_{11}$ are isostructural with the intermetallic UCd_{11} which possesses simple cubic symmetry. These compounds constitute a magnetically dilute series which allows the magnetic effects of progressively changing element A in the AB_{11} binary alloys to be studied while interatomic distances and structures are held constant. In this manner, the susceptibility changes which develop as the number of 4f electrons increase from zero ($LaCd_{11}$) to three ($NdCd_{11}$) can be conveniently measured, correlated with electronic structure, and trends observed. At this point, it is of interest to see what can be learned about the ground state of the 5f electrons of uranium from a comparison of the magnetic properties of UCd_{11} and $NdCd_{11}$.

Four rare earth compounds ($LaCd_{11}$, $CeCd_{11}$, $PrCd_{11}$ and $NdCd_{11}$) were prepared in the following way. Stoichiometric amounts of the appropriate rare earth metal and cadmium were placed in a tantalum crucible, which was then sealed by welding a tantalum cover into place. Loading and welding operations were performed in an inert atmosphere. After enclosing the crucible in an outer stainless steel jacket, the unit was placed in a furnace assembly which was rocked to insure good mixing of the components when molten. All charges were heated to approximately 1000 C and maintained at this temperature for at least six hours before they were quenched in water. Subsequent treatment involved heating the alloys to a temperature just below the melting point of cadmium, holding at this point for two days, raising the temperature to a point just below the estimated peritectic temperature for each alloy, holding here for 48 hours and, finally, cooling slowly (10°/hour) to ambient temperature.

The crystal structure of each intermetallic compound was identified by X-ray examination. The composition of each alloy was established by chemical analysis.

Susceptibility measurements were made by the Faraday method. A sample of $CeCd_{11}$, the first alloy studied, was powdered by grinding a small ingot section with an agate motor and pestle. After filling a small quartz sphere with this powder, the sphere was enclosed in a copper capsule which was suspended from the arm of a microbalance by a cupronickel chain. This arrangement was contained in a cryostat cavity which was located between the pole pieces of an electromagnet. Weight-change measurements were made as a function of magnet current at three temperatures: 295.30 K, 77.33 K, and 4.19 K. Similar measurements made at

---

*Cooperating chemist, Chemistry Division room temperature with a substance whose susceptibility is accurately known (Mohr's salt; $Fe(NH_4)_2(SO_4)_2 \cdot 6\ H_2O$) permitted the conversion of the observed weight changes into susceptibilities. This was done by means of the following expression:

$$_M\chi_A = (M_A)\ \frac{F_A}{_{295}F_S}\ \frac{W_S}{W_A}\ (_{295}\chi_S) \quad .$$

In this expression, $_M\chi_A$ is the molar susceptibility of $CeCd_{11}$, M_A is the molecular weight of this compound, F_A is the measured force on the alloy sample, $_{295}F_S$ is the measured force on the Mohr's salt sample at room temperature, W_S and W_A are the weights of the salt and alloy samples, respectively, used in the measurements, and $_{295}\chi_S$ is the room temperature gram susceptibility of the salt sample calculated from the data of Jackson.[14] The forces on the empty quartz sphere and the copper container were also measured as a function of magnet current at room temperature. These values were subtracted from the forces measured on the $CeCd_{11}$ sample.

Low temperatures were obtained by using baths of liquified gases (helium and nitrogen) boiling under known pressures. Vapor pressure versus temperature curves for these gases were used to determine the temperature of the sample.

Preliminary values of the molar susceptibility for $CeCd_{11}$ are recorded in Table 16. No field dependence of the susceptibility was observed, indicating that the sample was free from ferromagnetic impurities. The contribution of the cerium atoms ($_M\chi_A$) was calculated for each temperature and these values are also tabulated in Table 16. In Figure 25, the reciprocal molar susceptibility of cerium is shown as a function of temperature. The effective number of Bohr magnetons (M_{eff}) calculated from the slope of this straight line, between room temperature and 77 K, is 2.53. This calculation was based upon the assumption that the simple Curie law is obeyed. The theoretical value for a Ce^{3+} ion in a $^2F_{5/2}$ state, that is, a tripositive cerium atom with one unpaired 4f electron in a spectroscopic state defined by the resultant quantum numbers $S = \frac{1}{2}$, $L = 3$, and $J = \frac{5}{2}$, is 2.56. For the Curie law to hold, the product of the molar susceptibility and temperature for a given system must equal a constant. Values of 0.77 and 0.79 were calculated at room temperature and 77.3 K, respectively, for the subject system. However, at 4.19 K, this product fell to a value of 0.54. The difference between the liquid helium values and higher temperature values is outside the limits of experimental error. Below 77.3 K, therefore, the system appears to follow a Curie-Weiss law [$\chi = (C/T) - \Delta$] with a very small $\Delta°$ value. Additional measurements, particularly in the low-temperature region, are needed, however, before the correct form of the susceptibility-temperature relationship can be determined.

[14] Jackson, L. C., Trans. Roy. Soc. (London) A224, 1 (1924).

Table 16

MOLAR SUSCEPTIBILITY OF CeCd_{11}

Temperature (K)	$M^{X}\mathrm{CeCd}_{11}(\mathrm{x}\ 10^{3})$	$M^{X}\mathrm{Ce}(\mathrm{x}\ 10^{3})$	$\left[M^{X}\mathrm{Ce}\right]^{-1} \mathrm{x}\ 10^{2}$	$M^{X}\mathrm{Ce}\ T$
295.30	2.368	2.591	3.861	0.77
77.33	10.045	10.268	0.971	0.79
4.19	127.73	127.961	0.079	0.54

FIGURE 25
EFFECT OF TEMPERATURE OF THE RECIPROCAL
MOLAR SUSCEPTIBILITY OF CERIUM

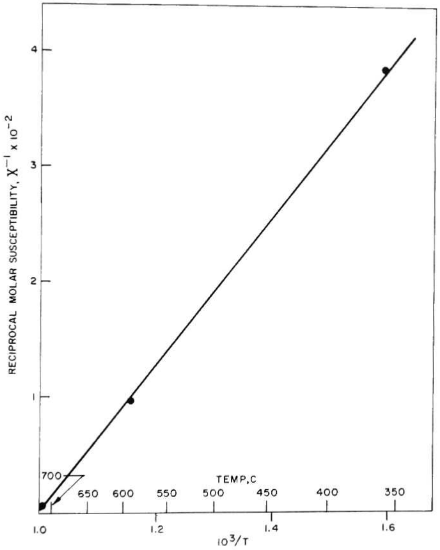

2. Calorimetry

(W. N. Hubbard)

The primary goal of this research program is the determination of thermodynamic properties of compounds of interest in high-temperature chemistry. Some of the compounds of interest are borides, aluminides, carbides, silicides, nitrides, sulfides and selenides of metals such as uranium, zirconium, molybdenum and tungsten. Some of the compounds of uranium are being prepared for the program by Stanford Research Institute. Two compounds (the disulfides of molybdenum and tungsten) have been prepared here.

Part of the program consists of the determination of heats of formation at 25 C by oxygen bomb calorimetry. Some of the compounds are difficult to burn in oxygen and the new technique of fluorine bomb calorimetry has been developed for their study. The accumulation of basic heat of formation data for fluorides is a necessary preliminary adjunct to fluorine bomb calorimetry and is a valuable program on its own merit.

The heats of formation at 25 C from oxygen or fluorine-combustion calorimetry will be combined with the changes in enthalpy measured by a high-temperature enthalpy calorimeter to determine thermodynamic properties at high temperatures. A calorimetric system for measurements up to 1500 C has been designed and is now being fabricated in the laboratory shops. Design concepts for an electron beam furnace to operate up to 2500 C are being tested in the laboratory.

a. Oxygen Bomb Calorimetry

(1) Calibration Experiments

(D. R. Fredrickson, S. S. Wise* and M. A. Frisch**)

Two series of calibration experiments have been carried out during this period. One series (six combustions with a platinum-lined bomb for oxygen-combustion studies) yielded a value for the energy equivalent with a standard deviation from the mean of 0.003 per cent. The other series (five combustions with a nickel bomb for fluorine-combustion studies) yielded a value with a standard deviation from the mean of 0.015 per cent. The precision of the series with the nickel bomb is typical, the precision of the other series being fortuitous.

(2) Combustions of Tungsten Disulfide in Oxygen

(R. L. Nuttall and D. R. Fredrickson)

Combustion techniques for completely burning tungsten disulfide to tungsten trioxide and oxides of sulfur have been developed. However, the products of the combustion contain a mixture of the oxides of sulfur, and combustion conditions have been varied in an effort to get most of the sulfur in a single state.

More than 99.5 per cent of a 2-gram sample of tungsten disulfide is burned in oxygen when the sample is in the form of a disc with a

---

*Resident Student Associate, University of Wisconsin

**University of Wisconsin

hole in the center. The disc is supported on a platinum ignition wire adjacent to a 25-mg bead of sulfur, which acts as a kindler. A gas composition of four atmospheres of oxygen and one atmosphere of either air or oxygen gives a good combustion of the pellet. With the argon-oxygen mixture, 50 to 80 per cent of the sulfur appears as sulfur dioxide. With the air-oxygen mixture which contains nitrogen to catalyze the oxidation of the sulfur, 20 to 50 per cent of the sulfur appears as sulfur dioxide. The use of higher pressures of oxygen results in a greater oxidation of the sulfur, but leads to fusion of the tungsten trioxide. This fused oxide may trap unburned tungsten disulfide and prevent it from burning.

Combustions have been carried out with various liquids in the bomb. Combustions with either pure water or an acid solution in the bomb left more than 50 per cent of the sulfur oxides in the gas phase. Combustions with 4 N sodium hydroxide in the bomb left none of the sulfur oxides in the gas phase after twenty minutes of rotation. An acid potassium dichromate solution added to the bomb absorbed all of the sulfur oxides and oxidized all the sulfur to sulfate.

(3) Analysis of Tungsten Disulfide

(E. Greenberg)

Analyses for tungsten and sulfur have been completed on the 50-gram calorimetric sample of tungsten disulfide. Sulfur was determined by combustion in oxygen, absorption of oxides of sulfur in 7 per cent hydrogen peroxide solution, further oxidation of sulfite to sulfate ion with bromine, and precipitation as barium sulfate. The apparatus was calibrated by combustion of pure sulfur. Tungsten was determined on the same samples used for sulfur by weighing the tungsten trioxide residue remaining after the combustion. The results of the analysis were tungsten, 74.13 ± 0.03 (74.14 theor) per cent, and sulfur, 25.95 ± 0.04 (25.86 theor) per cent. The sulfur to tungsten ratio was 2.007.

Spectrochemical analysis revealed no impurities above the lower limit of detection. X-ray diffraction examination indicated that the sample was composed of two related structures which are analogous to those described for molybdenum disulfide.[15]

b. Fluorine Bomb Calorimetry

(1) Fluorine Purification

(E. Rudzitis and J. Settle)

One problem that has plagued the fluorine bomb calorimetry program has been that of obtaining fluorine of consistently high purity. The commercially available fluorine that was used had a purity

---

[15] Bell, R. E. and Herfert, R. E., J. Am. Chem. Soc., 79, 3351 (1957).

range varying from 98.5 to 99.7 per cent. The substances that formed the impurities varied. In the most pure fluorine, oxygen and nitrogen comprised the bulk of the impurities, with only traces of saturated fluorocarbons (mainly carbon tetrafluoride). In one batch of gas analyzed, the impurities included oxygen, nitrogen, fluorocarbons, hydrogen fluoride, silicon tetrafluoride, sulfur hexafluoride, disulfur decafluoride, and probably carbonyl fluoride. In order to eliminate this chemical variable in the calorimetry, it was decided to try to purify the fluorine by fractional distillation. A trial still was constructed by L. Stein.* It was found that fluorine of 99.90 per cent purity, with oxygen and nitrogen as the only impurities, could be prepared by three successive distillations of the sample. With this still it took about 40 hours to purify a batch of fluorine, and the yield was only about 60 per cent of the starting material. Guided by the experience gained in the use of this still, a new still was designed, constructed and put into operation. The following conclusions have been drawn following the distillation of two batches of fluorine with the new still:

(a) In a single distillation the fluorine can be upgraded from 99.6 per cent to greater than 99.95 per cent purity.

(b) The distillation can be completed in 20 hours or less.

(c) Although the yield of the first two batches was about 60 per cent, the yield can be increased to about 75 per cent by starting with a larger charge. The holdup of the still was about 35 g out of a total charge of about 240 g.

It appears quite possible that fluorine approaching 99.99 per cent purity can be prepared with this still. Figure 26 is a schematic drawing of the still.

(2) Combustion of Zirconium in Fluorine

(E. Greenberg)

A series of four calorimetric combustions of zirconium in fluorine has been completed. The results are summarized in Table 17. The calculations include corrections for standard-state conditions and corrections for impurities in the zirconium sample. In terms of thermal effect, the most significant impurity is oxygen. The correction for this impurity amounts to about 0.3 per cent if the assumption is made that the oxygen is present as zirconia and this reacts to form zirconium tetrafluoride and oxygen.

The internal consistencey of α (the heat transfer coefficient) for the series and its agreement with the calibration experiments indicate that, calorimetrically, the combustions are satisfactory. The

---

*Cooperating chemist, Chemistry Division.

FIGURE 26
FLUORINE STILL

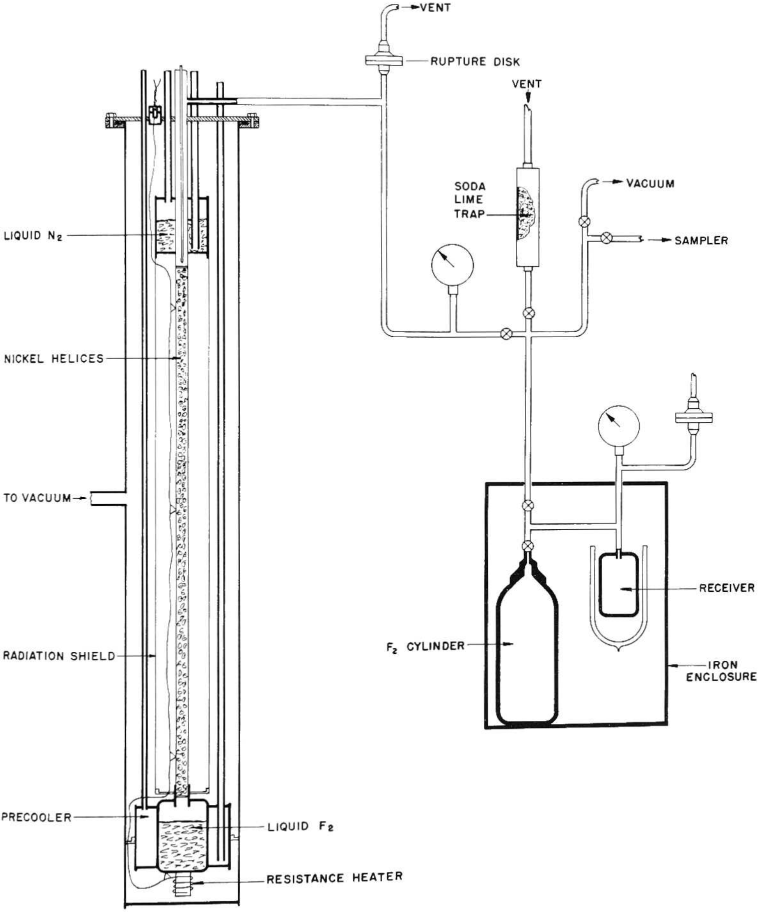

Table 17

CALORIMETRIC COMBUSTIONS OF ZIRCONIUM IN FLUORINE

Run No.	Mass Zr (gram)	$\alpha \times 10^4$ (sec^{-1})	$\Delta E_c^\circ/M$ (cal/gram of Zr)
4	0.94553	0.3372	4967
5	0.97777	0.3370	4968
6	0.96720	0.3430	4977
7	0.9867	0.3403	4986
			Avg = 4975

Std dev of mean = 4 or 0.08 per cent

amount of zirconium burned varied from 70 to 75 per cent of the sample introduced into the bomb. The mass of zirconium burned was determined by subtracting the mass of zirconium metal recovered after the combustion from the original mass of zirconium.

The standard deviation from the mean of 0.08 per cent for these runs is probably indicative of the precision which can be expected in the final results. Improvements in experimental technique may result in slightly better precision. A second series of combustions is currently in progress.

An X-ray diffraction analysis was made of the zirconium tetrafluoride combustion product. With the exception of a few very faint lines just above background level, all of the lines could be assigned to β-zirconium tetrafluoride. Infrared analysis of the product gases confirmed that the carbon and silicon impurities in the zirconium were burned to the respective tetrafluorides. Mass spectrometric analysis revealed the presence of 0.1 per cent and 0.2 per cent oxygen as the only other impurities in the product gases.

(3) Combustion of Boron in Fluorine

(S. S. Wise)*

Calorimetric measurements are presently being made to determine the heat of reaction between crystalline boron and fluorine. The sample of crystalline boron was obtained from the U. S. Borax and Chemical Co. in a 100-mesh crystal size. The sample was sifted again, however, and those crystals passing through a No. 325 screen were rejected, because they tend to burn spontaneously in fluorine. The larger crystals

---

*Resident Student Associate, University of Wisconsin are inert to fluorine at room temperature. The most satisfactory support for the boron in the bomb was found to be a circular plate, $1\frac{1}{2}$ inch OD x $\frac{3}{16}$ inch thick, of recrystallized alumina. The temperature of the reaction was reduced by diluting the fluorine half and half with argon; under these conditions no reaction of the alumina with fluorine during the combustion was detected.

A calcium fluoride-coated platinum dish had been considered as a support. However, the platinum, even though coated, reacted slightly with fluorine during boron combustions.

The combustion is initiated by electrically heating a short 4 mil titanium fuse wire (approximately 2 mg in weight) suspended above the boron crystals between two electrodes. The extent of reaction is determined by recovery of the unburned boron crystals remaining on the plate.

Work is continuing on the development of a capsule for containing samples that burn spontaneously in fluorine such as amorphorous boron and sulfur.

(4) Exploratory Combustions of Magnesium, Aluminum, Zinc and Cadmium in Fluorine

(E. Rudzitis)

This group of soft metals was chosen for exploratory combustion experiments at the same time because of the possibility of applying similar combustion techniques to them. Ignition experiments have shown that massive samples of these metals may be ignited by using a wire-to-foil-to-sample technique in much the same manner as was used for zirconium. However, the fluorine pressure required to burn one metal completely may differ widely. For example, 5 to 10-mil wires and foils of cadmium and magnesium ignited and burned in fluorine at approximately 75 psi pressure. A 50-mil zinc wire required 150 psi for a partial ignition. At lower fluorine pressures the wire would melt without burning.

Combustion experiments with 2- to 5-gram cadmium samples indicated that once the sample has ignited the burning proceeds vigorously, melting the sample and, if the fluorine pressure is sufficiently high, fluorinating the liquid metal. Because of the comparable low melting points of zinc, magnesium, aluminum and cadmium, it is reasonable to expect that most or all of them will be liquid during fluorination. Therefore, for satisfactory studies with these metals, a suitable arrangement must be found for supporting liquid samples as they burn.

The similarity of this group of metals extends also to the chemistry of the fluorinated end products. A single oxidation state of the metal is obtained as a result of the reaction. This fluoride is soluble in water. The latter statement suggests a convenient method for separation of unburned metal from the product fluoride.

II. FUEL CYCLE APPLICATIONS OF VOLATILITY AND FLUIDIZATION TECHNIQUES

The volatilities of uranium and plutonium hexafluorides are the bases for various volatility schemes proposed for processing irradiated fuels. These schemes include a Direct Fluorination Process, the Aqueous Dissolution Fluorination (ADF) Process and the Fused Fluoride Volatility Process. A firm knowledge of the chemistry of fluorine and fluorine compounds, fluidization and volatility separations techniques are important in the development of the separation processes. Application of fluidization techniques is also being made to preparation of uranium compounds.

The Direct Fluorination Process is currently aimed toward the processing of the Zircaloy-clad uranium dioxide fuel typical of the Dresden Reactor. Equipment has been constructed from which information can be obtained to substantiate a process flowsheet in regards to plutonium hexafluoride transfer, fluorination of uranium and plutonium oxide mixtures, and separation of uranium and plutonium hexafluorides. The use of sulfur tetrafluoride as a fluorinating agent is being investigated in reactions with uranium tetrafluoride, uranium dioxide, U_3O_8, uranium trioxide, uranyl fluoride, plutonium dioxide, and plutonium tetrafluoride.

One approach pursued in the study of the chemistry involved in the separation of plutonium hexafluoride from uranium hexafluoride utilizes the preferential reduction of the more chemically reactive plutonium hexafluoride by sulfur tetrafluoride.

The direct fluorination of dense uranium dioxide pellets submerged in an inert fluidized medium was carried out in a three-inch reactor at 500 C at fluorine concentrations up to 30 per cent. Negligible fines were produced with a three-inch pellet bed under the conditions used, although substantial amounts of fines were found in deeper beds. Uranyl fluoride was identified as the major species in the fines. The reaction rate was found to be directly proportional to fluorine concentration. The concentration of unreacted fluorine in the off-gas decreased approximately exponentially with bed height, with corresponding increase in overall fluorine efficiency. The formation of solid intermediate uranium compounds was observed in the case of pellet beds deeper than three inches.

Experimental work has continued to determine the mechanism of the nickel-fluorine reaction. As a means of checking the validity of the experimental method, both oxidation and fluorination reactions have been used. The results indicate that the mechanism for the nickel-fluorine reaction is one in which fluorine migrates through the nickel fluoride film. Work has been started to obtain rate data on the reaction of fluorine with zirconium in a conventional tube reactor and in a thermobalance. The film formed on the zirconium is appreciable and not protective in nature, but controlled reactions have been obtained between 300 and 500 C. Controlled fluorination reactions of uranium (in the form of thin coupons) have been made in the temperature range from 300 to 500 C.

Work continued on the development of the ADF process, with current emphasis being directed toward recovery of uranium from low-uranium-Zircaloy-2 fuel alloys. Major process steps are aqueous dissolution of the fuel, fluid-bed drying of the solution to a dry powder, and fluorination of the powder to remove and recover the uranium as the hexafluoride. The use of additional anhydrous hydrogen fluoride as part of the fluidizing gas during drying did not lower the residual oxygen and water contents of the dryer products, whereas a separate hydrofluorination step carried out at slightly higher temperatures (450 C) eliminated about two-thirds of these components. A jet-target grinder capable of higher attrition rates than the ordinary attrition jets was successful in stabilizing the particle size distribution during the recent dryer studies.

A new 2-inch diameter, six-foot tall, static-bed fluorination reactor was installed and operated to gain additional information on the effects of powder (cake) depth on fluorine efficiency and pressure drop. This information will help set criteria for the design of a disposable fluorination vessel now being considered. Collection of the relatively small amounts of evolved uranium from a flowing gas stream was demonstrated using cold traps made of coiled $\frac{3}{4}$-inch copper tubing.

Other experiments explored alternate "dry" fluorination processes, such as direct contact of the metal with gaseous reactants to eliminate the aqueous dissolution step. A mixture of hydrogen fluoride and hydrogen chloride appears promising for gas-phase conversion of zirconium-base fuels to fluoride compounds.

A series of four dissolutions was carried out semicontinuously in the graphite pilot-plant dissolver, in accordance with the Fused Salt Fluoride Volatility Process flowsheet. In this process, uranium-zirconium matrix fuel is dissolved in molten fluoride salts at 600 to 700 C with a hydrogen fluoride sparge, and the uranium is then volatilized as the hexafluoride in a fluorine sparge. The use of graphite as a material of construction for the dissolver-hydrofluorinator avoids corrosion incurred by metal systems. Partial salt transfers and salt makeup are carried out between dissolutions. Dissolution rates up to 2.3 mg/(min)(sq cm), or about 9 mils/hr, were obtained. Synthetic fuel elements were carried to 90 per cent dissolution in as little as six hours. Graphite heaters and other components functioned satisfactorily. Accumulation of salt in the off-gas system was handled with a regular procedure. Effects of continued operation on processing rates and conditions are being studied.

Additional studies of the one-step fluid-bed process for the conversion of uranium hexafluoride to uranium dioxide with steam and hydrogen confirmed the facts that this gas-gas reaction is very rapid and that it results in the formation of intermediate fluoride solids. Current uranium hexafluoride rates are up to 60 g/min [equivalent to 105 lb uranium/(hr)(sq ft reactor cross section)]. Material of lower residual fluoride content is produced when greater excesses of reactants, higher temperatures and longer residence times are used. A 20-lb batch of dioxide containing only 130 ppm residual fluoride was prepared for sintering studies (application toward ceramic nuclear fuels) using a second cleanup step with additional steam and hydrogen. Consideration is being given to alternative two-step processes using only one of the reactants at a time. A correlation showing particle size effects (particle growth or fines production) as a function of starting average particle size of the bed and fluidizing velocity is presented.

A method for achieving controlled downward transport of solids in multistage fluidized-bed reactors using external vibrators without the use of internal downcomers is being investigated. A six-inch diameter, 3-stage Pyrex and metal unit was installed. The effects of induced vibrational frequency, type of frequency transmitter, vibrator on-time, feed particle size and particle size distribution on throughput using an air-glass bead system were determined.

A. Direct Fluorination Process for Oxide Fuels

The Direct Fluorination Process is being directed toward the processing of the Zircaloy-clad uranium dioxide fuel similar to that used in the Dresden reactor. Prior to any chemical processing, the fuel bundle can be cut to release the fuel elements. This permits the discarding of unwanted metal, such as the bail and centering pin. The released tubes can then be cut into small pieces to expose the uranium and plutonium oxides to the fluorinating agent. Alternatively, the cladding can be removed by reacting the zirconium with hydrogen chloride to form the volatile tetrachloride or fluorinated to form zirconium tetrafluoride. To afford a separation between uranium and plutonium, the oxide mixture may be selectively fluorinated, the separation depending on the relatively rapid formation of uranium hexafluoride as compared to plutonium hexafluoride upon reaction with fluorine. Partial fluorination would yield a plutonium-rich solid phase and a uranium hexafluoride vapor phase containing little or no plutonium hexafluoride. Alternatively, a selective fluorination of uranium trioxide (obtained by oxidizing the uranium dioxide) to uranium hexafluoride can be made with sulfur tetrafluoride, after which plutonium hexafluoride can be made by reaction with fluorine. Complete fluorination of uranium and plutonium oxides would necessitate a separation of the hexafluoride to the nonvolatile tetrafluoride by either thermal decomposition or chemical reduction with sulfur tetrafluoride.

1. Fluorine Chemistry and Fluoride Separations Studies
(J. Fischer)

a. Sulfur Tetrafluoride Reaction with Uranium Oxides
(C. Johnson, M. J. Steindler, J. Stockbar, G. Redding)

In a direct fluorination reprocessing scheme for power reactor fuels, the selective fluorination of uranium from plutonium, thereby effecting a separation, is attractive. Studies have been made which indicate that sulfur tetrafluoride can be used as a selective fluorinating agent to convert uranium (VI) oxides to uranium hexafluoride. The plutonium can be fluorinated in a subsequent step to produce plutonium hexafluoride.

A study of the reaction of sulfur tetrafluoride with uranium oxides was made using a recording thermobalance. All experiments were run at constant temperature. The flow of gaseous sulfur tetrafluoride past the sample varied slightly for different experiments but did not fluctuate once an experiment was in progress. It is quite difficult to trap the gaseous products quantitatively when using the thermobalance; therefore, the stoichiometry of the reaction will be studied in another system designed specifically for this purpose.

Plutonium dioxide and plutonium tetrafluoride were contacted with sulfur tetrafluoride according to the procedure and in the equipment described previously (ANL-5875, page 5), with the exception that sulfur tetrafluoride replaced fluorine.

Materials that have been fluorinated with sulfur tetrafluoride are uranium tetrafluoride, uranium dioxide, U_3O_8, uranium trioxide, uranyl fluoride, plutonium dioxide and plutonium tetrafluoride. The uranium tetrafluoride was Mallinckrodt Chemical production grade material. The uranium dioxide and uranium trioxide are Chemical Engineering Division pilot plant-produced materials. The U_3O_8 was purchased from The National Bureau of Standards. The uranyl fluoride was obtained from General Chemical Co. The plutonium dioxide was obtained from Los Alamos and the plutonium tetrafluoride from Rocky Flats.

No reaction was observed when uranium tetrafluoride, plutonium dioxide and plutonium tetrafluoride were exposed to sulfur tetrafluoride with the experimental conditions employed. These data, as well as those obtained from experiments in which sulfur tetrafluoride reacted with U_3O_8, are given in Table 18. The data for U_3O_8 are plotted in Figure 27 as weight change versus time. Initially the materials undergo a weight increase prior to removal of uranium, presumably as uranium hexafluoride. When uranium dioxide was treated with sulfur tetrafluoride there occurred a reaction which requires further study.

Table 18

REACTION OF SULFUR TETRAFLUORIDE WITH URANIUM AND PLUTONIUM COMPOUNDS

Time of experiment: 30 minutes

Material	Sample Weight (g) Initial	Sample Weight (g) Final	SF_4 Flow (cc/min)	Temp (C)	Products (w/o) UF_4 [a]	Products (w/o) UF_6 [b]
UF_4	0.4001	0.3992	100	350		
U_3O_8	0.3998	0.2390	100	350	50.6	49.4
PuO_2	0.5045	0.5089	25	375		
PuO_2	0.5182	0.5081	25	375		
PuO_2	0.5081	0.5065	25	375		
PuF_4	0.3053	0.3037	25	375		
PuF_4	0.3037	0.3033	25	450		

[a] Product residue analysed as UF_4

[b] w/o UF_6 calculated from weight loss assuming volatile product is UF_6

FIGURE 27

REACTION OF SULFUR TETRAFLUORIDE WITH U_3O_8 AT 350 C

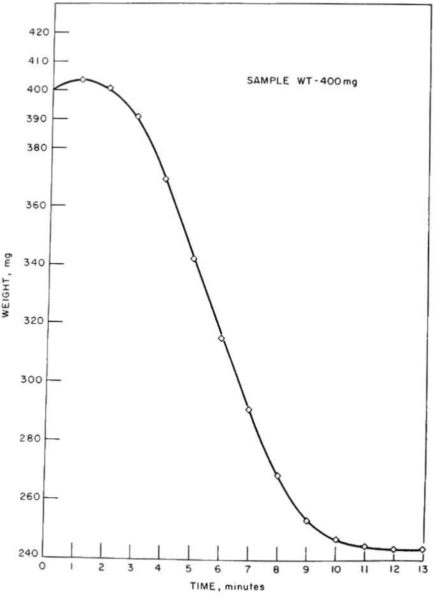

When sulfur tetrafluoride is allowed to act upon uranium trioxide or uranyl fluoride at temperatures of 300 to 400 C, gaseous products, which are assumed to be uranium hexafluoride and thionyl fluoride, are formed. Both solids react smoothly and generally the reaction goes to completion. In one or two cases as much as ten per cent of the solid remained unreacted. Neither solid reacted to any appreciable extent below 300 C. Reactions with uranium trioxide have not been run at temperatures much above 420 C because of the thermal decomposition of uranium trioxide into U_3O_8 and oxygen, which begins at about 450 C.

Figure 28, a plot of weight change versus time, best typifies what occurs with uranium trioxide. The gaseous sulfur tetrafluoride initially adsorbs on the solid prior to reaction. This phenomenon is not observed with uranyl fluoride. Other data from experiments on the reaction of sulfur tetrafluoride with uranium trioxide are given in Table 19.

FIGURE 28
REACTION OF SULFUR TETRAFLUORIDE
WITH URANIUM TRIOXIDE AT 379 C

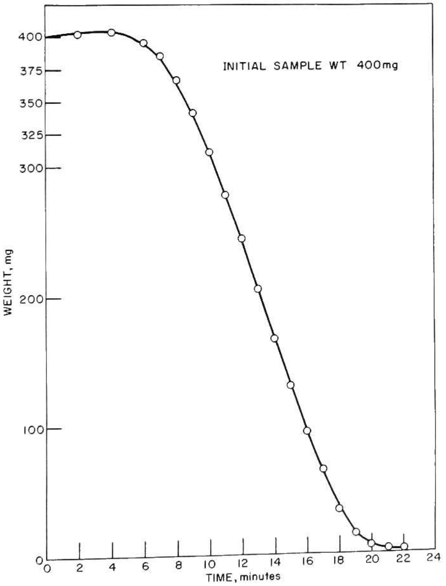

Table 19

CONVERSION OF URANIUM TRIOXIDE TO URANIUM HEXAFLUORIDE BY SULFUR TETRAFLUORIDE

SF_4 Flow Rate: ~110 cc/min
Reaction Time: 15 to 30 min

Initial Weight (g)	Final Weight (g)[a]	Temperature (C)	Rate [mg/(min)(sq cm)][b]
0.4001	0.0051	383	11.7
0.4000	0.0120	379	10.8
0.4519	0.0121	324	9.53
0.4412	0.0161	425	12.3
0.4442	0.0125	337	11.1

[a] The actual chemical composition of the residue is unknown. Possible constituents are nickel fluoride, from corrosion of nickel sample support, and possibly some unreacted uranium.

[b] Exposed area of the sample - not the true surface area of the solid.

b. Plutonium Hexafluoride Studies - Separation Chemistry
(M. Steindler, D. Steidl)

The chemistry of plutonium hexafluoride is important in fluoride separations processes applied to irradiated reactor fuels. A program has been started to determine the chemistry of plutonium hexafluoride in the process steps involving its separation from uranium hexafluoride. Two approaches have been pursued. One is the thermal decomposition of plutonium hexafluoride at temperatures at which uranium hexafluoride remains unaffected. The other approach is the selective reduction of the more chemically reactive plutonium hexafluoride. Either approach may possibly be used as the basis for a separations process.

(1) Thermal Decomposition of Plutonium Hexafluoride

Exploratory experiments have been carried out on the thermal decomposition of plutonium hexafluoride. As reported previously (ANL-6101, page 83), plutonium hexafluoride is passed through a heated nickel wool plug (1000 sq cm estimated surface area) and the amount of hexafluoride recovered after passage through the heated zone is determined. Results obtained at several temperatures are shown in Table 20. The decomposition product remained on the packing from one experiment to the next. The experiments were carried out in a reproducible manner; however, it was not possible to estimate residence times in the heated zone.

Table 20

DECOMPOSITION OF PLUTONIUM HEXAFLUORIDE IN THE VAPOR PHASE ON HEATED NICKEL WOOL

Area of nickel: ~1000 sq cm
Vacuum transfer at P $\leq$ 125 mm Hg
Nickel wool prefluorinated by F_2 and PuF_6
Average experiment time: 6 minutes

T (C)	PuF_6 Transferred (g)	PuF_6 Decomposed (%) [a]
300	0.7518	73.2
300	0.8106	66.9
300	0.7187	61.5
300	0.6548	74.1
300	0.4148	64.7
400	0.8317	75.0
400	0.6752	77.4
400	0.6485	78.2
500	0.6617	84.4
500	0.5019	85.7

[a] Per cent of amount of plutonium hexafluoride transferred.

Owing to the fact that at least one stream in the proposed fluoride separation process involves both fluorine and plutonium hexafluoride, a number of experiments were carried out to determine the effect of a fluorine carrier on the extent of decomposition of plutonium hexafluoride on heated nickel wool. The experiments were carried out in the same manner as those involving the vacuum transfer of plutonium hexafluoride. The results are shown in Table 21 together with comparable data from vacuum* transfer experiments.

---

* Pressures less than the vapor pressure of plutonium hexafluoride at the experimental temperature.

Table 21

DECOMPOSITION OF PLUTONIUM HEXAFLUORIDE IN THE VAPOR PHASE ON HEATED NICKEL WOOL USING FLUORINE AS A CARRIER GAS

Area of nickel: ~1000 sq cm
Transfer at P: 1 atm
Carrier gas: F_2
Nickel wool prefluorinated by F_2 and PuF_6

Temp (C)	Time (min)[a]	F_2 Flow (cc/min)	PuF_6 Transferred (g)	PuF_6 Decomposed (%)	Comparable Vacuum Decomposition (%)
30	95	43	0.3129	16.7	6[b]
300	120	45	0.5259	44.5	68[c]
400	110	54	0.5061	34.8	77[c]
400	60	48	0.5338	39.6	77[c]

[a] Time required to transfer the hexafluoride from the fluorination tube through the heated packing.

[b] Weight of sample ~1 g.

[c] Average weight of samples, ~0.7 g .

Two experiments using mixtures of uranium hexafluoride and plutonium hexafluoride were carried out. The hexafluoride mixture was transferred through the nickel wool under vacuum. The mixtures were formed in a mixing tube and the total contents of the mixing tube were used for an experiment. Aqueous chemical analyses were carried out on the hydrolyzed product of the reaction. The results of the experiments are shown in Table 22.

The thermal decomposition of plutonium hexafluoride appears to be a relatively complicated process, particularly in view of the extreme chemical reactivity of the hexafluoride and the equilibrium between the hexafluoride, plutonium tetrafluoride and elemental fluorine. Experiments carried out both in vacuum and in the presence of a fluorine carrier indicate that although a separation based on the thermal decomposition may be possible, considerable additional work is required to establish the method. In addition, engineering problems associated with the recovery of the product, plutonium tetrafluoride, must be solved before application in the process is assured.

Table 22

DECOMPOSITION OF MIXTURES OF URANIUM HEXAFLUORIDE AND PLUTONIUM HEXAFLUORIDE IN THE VAPOR PHASE ON HEATED NICKEL WOOL

Area of Nickel: ~1000 sq cm
Vacuum transfer at $P \leq 5 \times 10^{-3}$ mm Hg

Temp (C)	Sample Weight (g)[a]	Composition (w/o)		Mixing Tube Loss[b] (%)		PuF_6 Decomposed[c] (%)
		UF_6	PuF_6	UF_6	PuF_6	
30	2.3288	91.8	8.2	93	42	80.3
300	1.9891	91.7	8.3	64	29	98.7

---

[a] Initial sample charged to mixing tube.

[b] Per cent of initial sample.

[c] Per cent of sample transferred from mixing tube.

(2) Reduction of Plutonium Hexafluoride with Sulfur Tetrafluoride

Possibly a more desirable approach to the separation of uranium and plutonium than thermal decomposition is based on the chemistry of the two hexafluorides. Plutonium hexafluoride has been shown to react with compounds which do not react with uranium hexafluoride. A separation of the hexafluorides based on the differences in their chemical reactivity therefore appears feasible.

Sulfur tetrafluoride has been shown to react with uranium (VI) compounds to form uranium hexafluoride. Estimates of the free energy for the reaction

$$PuF_6 + SF_4 \longrightarrow PuF_4 + SF_6$$

indicated the reaction to proceed as written. Measured samples of plutonium hexafluoride and sulfur tetrafluoride were condensed into a reaction vessel and allowed to warm to the desired temperature. The reactions appeared to take place in the vapor phase. The results of exploratory experiments are shown in Table 23.

On the basis of these data, the reaction of plutonium hexafluoride and sulfur tetrafluoride proceeds smoothly at modest temperatures. Experiments on the reaction of plutonium hexafluoride in mixtures with uranium hexafluoride are in progress.

Table 23

REACTION OF SULFUR TETRAFLUORIDE AND PLUTONIUM HEXAFLUORIDE

(Reaction carried out in a 50 cc nickel vessel)

				Extent of Reaction (%)	
T (C)	Time(hr)	PuF_6(g)	SF_4(g)	Pressure Measured	Weight of Residue
30	1	0.753	0.0841	70[a]	83[b]
30	17	0.1181	0.1305	102	98
70	1.5	0.1154	0.1367	-	99
70	0.2	0.1166	0.1274	100	

[a] Probably low

[b] Chemical Analysis

c. Bench-scale Experimental Equipment

(G. J. Vogel, L. Anastasia, G. Redding, H. Griffin, T. Baker)

The Direct Fluorination Process has been developed to the point where it is now necessary to employ larger amounts of plutonium than the gram quantities or less used before. Equipment has been constructed from which information can be obtained to substantiate a process flowsheet. This equipment has been installed in two glove boxes. In one box multigram quantities of plutonium hexafluoride will be prepared to demonstrate the transfer of plutonium hexafluoride as required in the process. Equipment suitable for fluorinating mixtures of plutonium and uranium oxides and for separating the product hexafluorides has been installed in the other box. The two boxes containing the experimental equipment are totally enclosed and contain glove ports for manipulation of the equipment and "bag-out" ports to facilitate material additions and withdrawals.

The plutonium hexafluoride preparation and transfer experiments will be employed to demonstrate the transfer of multigram quantities of plutonium hexafluoride under process conditions. The hexafluoride will be prepared by reacting plutonium tetrafluoride with fluorine, purified by sublimation, and transferred through a suitable system so that effects of some or all of the following variables may be studied: (1) temperature, (2) materials of construction - nickel, Monel, brass, Teflon, (3) pretreatment of materials of construction, (4) rate of transfer, (5) amount transferred, (6) area of transfer path, and (7) transfer medium - vacuum, inert gas, or fluorine.

The equipment flow diagram for the system is shown in Figure 29. Plutonium tetrafluoride will be placed in the boat reactor and heated to the reaction temperature of 600 C while fluorine is circulated through the system. The plutonium hexafluoride will be condensed in two cold traps in series. The purification step involves transferring the product plus any impurities to one cold trap, warming the trap contents to room temperature, vacuum transferring the warmed gas through a second cold trap held at -70 C, where the plutonium hexafluoride will desublime and impurities more volatile than the plutonium hexafluoride will be removed by vacuum pumping. A vapor pressure measurement will be made to check the purity. The plutonium hexafluoride will be volatilized into the transfer loop in which the variables outlined can be studied by transferring plutonium hexafluoride from one cold trap through the component to be tested to the other cold trap.

FIGURE 29

SCHEMATIC EQUIPMENT FLOWSHEET OF THE PLUTONIUM HEXAFLUORIDE PREPARATION AND TRANSFER SYSTEMS

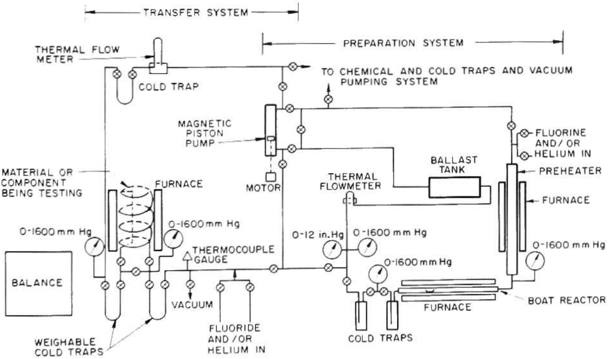

The equipment to study plutonium uranium hexafluoride separation procedures is shown in Figure 30. Effects of such process variables as temperature, flow rate and gas diluents may be studied for all or part of the following:

1. the fluorination of uranium dioxide-plutonium dioxide mixtures representing declad fuel elements, with and without a solid diluent such as calcium fluoride;

2. the fluorination of uranium dioxide-plutonium dioxide-zirconium mixtures representing chopped but otherwise untreated fuel, again with and without a solid diluent such as calcium fluoride;

3. the selective fluorination of oxidized uranium-plutonium dioxide mixtures with sulfur tetrafluoride; and

4. thermal or chemical reduction of plutonium hexafluoride in uranium-plutonium mixtures.

FIGURE 30

SCHEMATIC EQUIPMENT DIAGRAM FOR URANIUM-PLUTONIUM SEPARATION EXPERIMENTS

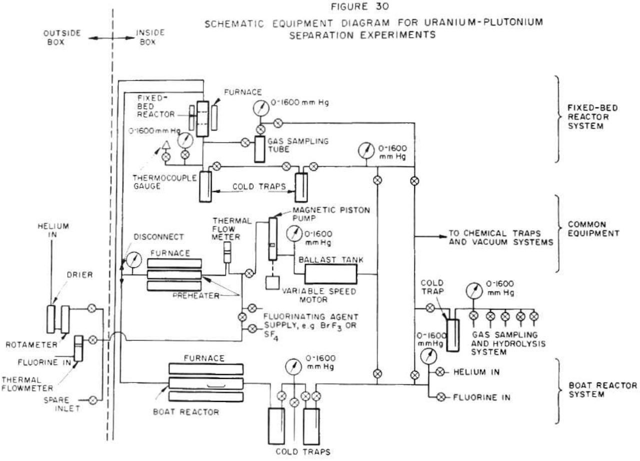

The equipment shown in Figure 30 is divided into two parts - a vertical, fixed-bed reactor system and a boat reactor system, The circulation pump, preheater, chemical traps, vacuum pumps and reactant gas supply manifold are common to both systems. The boat-reactor system will be used primarily to prepare plutonium hexafluoride for experiments. The fixed-bed reactor will be used for fluorination studies. The separation of uranium from plutonium can be studied, for example, by passing fluorine through a mixture of the uranium-plutonium oxides, periodically sampling the exhaust gas from the reactor and analyzing the gas for uranium and plutonium contents. A material balance can be made at the completion of each run by sampling the product and the reactor residue.

2. Engineering-scale Studies

(W. J. Mecham, A. A. Jonke)

a. Direct Fluorination of Uranium Dioxide Fuels

(J. D. Gabor, J. Wehrle)

Since uranium dioxide will be used as fuel in many power reactors, a process based on direct fluorination of uranium dioxide to uranium hexafluoride is of interest. Laboratory work (ANL-6029, page 73) and preliminary pilot plant-scale work (ANL-6101, page 118) has shown that dense pelleted material can be fluorinated at practical rates. When uranium dioxide is converted directly to the hexafluoride in an atmosphere of fluorine, the heat released is about 1100 kcal/kg uranium. A means of controlling the reaction and removing the large amount of heat is required. Although dense pellets of the kind proposed for several nuclear reactors are too large to be fluidized directly, the use of an inert granular fluidizable material to cover and to fill the void spaces of a packed bed of pellets has been studied to achieve some of the advantages of fluidization for solid-gas reactions, particularly the removal of heat.

In the previous report (ANL-6101, page 118) results of preliminary experiments were presented, in which the reaction of uranium dioxide pellets with fluorine in a fluidized bed of magnesium fluoride appeared promising, although production of substantial quantities of fines occurred during the reaction. The process variables for the reaction are: temperature, fluorine concentration, bed height, and particle size. The effects of most concern are fluorine efficiency, reaction rate, and process control. In this report, results of runs are presented showing conditions under which fines production was negligible, and showing the effect of fluorine concentration and bed height on reaction rate and fluorine efficiency. The major uranium compounds in the fines were identified.

In these tests high-density uranium dioxide pellets, approximately 1 cm in height and diameter, of the same type previously tested, were used. A preheated mixture of fluorine and nitrogen was passed through the reactor and uranium hexafluoride product was collected in cold traps which were removed and weighed. Off-gas samples were taken and the solid residues were removed and weighed after each run.

(1) Effect of Fluorine Concentration

A series of three runs, UOF-6, 7, and 9, was made to determine the effect of fluorine concentration on reaction rate and fluorine utilization. All three runs were made at 500 C with a superficial gas velocity of 0.5 ft/sec, and with a uranium dioxide pellet bed height of 3 inches submerged by 6 inches in a bed of 60- to 80-mesh magnesium fluoride. The range of inlet fluorine concentration was 10 to 30 per cent. A schematic diagram of the equipment is shown in Figure 31. Results of the runs are given in Table 24.

FIGURE 31
REACTOR CONFIGURATION IN STUDIES OF DIRECT FLUORINATION OF URANIUM DIOXIDE

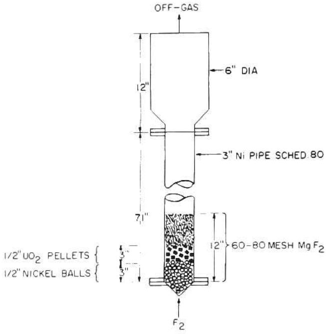

(BED HEIGHTS ARE THOSE FOR RUNS UOF-5 THROUGH 9)

The durations of these runs were varied to give equal amounts of uranium hexafluoride production, since it was expected that the rate of uranium hexafluoride formation would be proportional to the fluorine concentration. This turned out to be so, as can be seen from the data in Table 24. These data also show that the weight of material lost from the bed agreed closely with that collected in the cold trap as uranium hexafluoride, when calculated as uranium dioxide equivalents. In each batch run, about 30 per cent of the uranium dioxide was reacted. The amount of fines entrained by the gas and collected in the filter chamber in these runs was less than 7 grams or about one per cent of the material reacted.

Values of the specific reaction rate of uranium hexafluoride formation and of fluorine utilization are given in Table 25. For the same bed height in Runs UOF-6, 7, and 9, the uranium hexafluoride production rates were proportional to inlet fluorine concentration. Fluorine utilization efficiencies based on fluorine introduced and uranium hexafluoride product collected showed nearly the same value of about 70 per cent

Table 24

REACTION RATE AND EFFICIENCY FOR DIRECT FLUORINATION RUNS

Pressure:	1 atm
Temp:	500 C
Superficial Gas Velocity:[a]	0.5 ft/sec

Run Number, UOF-	6	7	9	11	12
Run Time, hr	3.0	1.5	1.0	1.5	1.5
Inlet F_2					
Conc,[b] %	10	20	30	20	20
Total charged, g	348	313	352	377	372
Starting Bed					
UO_2, g	1762	1760	1770	5262	3491
MgF_2, g	1163	1146	1075	2026	1916
UO_2 bed height, in.	3	3	3	9	6
MgF_2 bed height, in.	12	12	12	18	15
UO_2 initial pellet surface, sq cm	737	736	740	2200	1459
Solid Residues, bed					
UO_2,[f] g	1106	1058	1076	3696	2440
MgF_2,[g] g	1264	1274	1210	2898	2310
Filter Fines	6.5	4.0	6.5	210	74.5
Product Collected, UF_6, g	719.5	744.5	693	637	716
UO_2 Equivalent of UF_6, g	552	571	531	489	550
Uranium Removed[h] from bed (as UO_2)	548	570.5	572.5	484	583
Overall F_2 Utilization					
Based on UF_6 produced					
Inlet F_2, cu ft[e]	7.26	6.54	7.55	7.87	7.76
Equivalent UF_6, g	1077	970	1118	1168	1153
Avg F_2 efficiency,[c] %	66.8	76.8	62.0	54.6	62.1
Inlet F_2 conc, %	-	-	-	21.0[d]	21.3[d] 19.8[d]
Exit F_2 conc, %	-	-	-	1.04[d] 1.73[d]	3.52[d] 2.10[d] 1.84[d]
Avg F_2 efficiency, %	-	-	-	93.5	87.9

---

[a] Total initial gas flow at process conditions based on open tube area

[b] Determined by calibrated orifices, nitrogen diluent

[c] Based on UF_6 collected

[d] Analyzed by mercury method

[e] At standard conditions

[f] Includes all material collected on 1/4-inch screen

[g] Includes all material passing through 1/4-inch screen

[h] Calculated as weight difference between "starting bed" and "solid residue"

for three concentrations. The manner in which efficiency is related to bed depth is discussed below.

Table 25

EFFECT OF BED HEIGHT ON FLUORINE EFFICIENCIES

(Approximately equal amounts of fluorine; conditions given in Table 24)

Run	UO_2 Bed Height (inches)	Total F_2 Efficiency (%)	F_2 Utilized to Form UF_6 (%)	F_2 Utilized to Form Intermediates (%)
UOF-7	3	77	77	~ 0
UOF-12	6	88	62	26
UOF-11	9	94	55	41

Analyses of fluorine concentration in the process gas were also made and reported in Table 24.

Fluorine utilization efficiency data give an indication of the formation of intermediate fluoride compounds of uranium, since the difference between the total fluorine consumed and the fluorine consumed to form uranium hexafluoride represents the fluorine content of intermediates. If no intermediates were formed, the two fluorine efficiencies, one based on uranium hexafluoride collected and the other on exit fluorine concentration, would be equal. From the material balances and fluorine efficiency data for these runs, and also from the indications of negligible fines and residue bed caking, it is concluded that little intermediate formation occurred in Runs 6, 7, and 9. The fluorine utilization values based on uranium hexafluoride collections, which are quite accurate, are believed to approximate closely true total fluorine utilization values in these runs. The values based on gas analysis by the potassium iodide method are questionable for the reasons mentioned above.

(2) Effect of Bed Height

The effect of bed height is shown by the results of Runs UOF-7, 11, and 12, given in Table 24. These runs were made under the same process conditions except for pellet bed heights of 3, 9, and 6 inches, respectively. The pellets were submerged by the same depth, six inches, in the magnesium fluoride bed. The effect of fluorine efficiencies are summarized in Table 25.

Additional indication of the relative amount of formation of intermediate uranium fluorides was given by operational data. These indications were caking of residue bed due to solid deposits between pellets, and the formation of fines which resulted mainly from the reaction of uranium dioxide with fluorine to produce uranyl fluoride. These points are covered more fully in the following discussion.

The decreasing rate of uranium hexafluoride product formation with increasing bed height is explained by the competing reaction to form intermediate fluorides. In each run the amount of fluorine added was nearly the same, and therefore smaller fractions of the stoichiometric amount of fluorine were added in deeper beds.

(3) Production of Fines

In the reactor used, fines passing from the disengaging section to the filter were not returned to the reactor. In runs previously reported, a substantial amount of filter fines were collected in runs with three-inch deep pellet beds fluorinated at 400 C with 10 per cent fluorine at 0.55 ft/sec. In current runs at 500 C and 0.35 ft/sec, the amount of fines was very small with the three-inch deep bed, but again substantial fines were found for deeper beds.

The size analysis for typical fines is given in Table 26, which shows that about 54 per cent of the fines collected in the filter have a particle size smaller than 325 mesh. The fines remaining with the 60- to 80-mesh magnesium fluoride bed have a similar size distribution.

To identify the compounds making up the fines, X-ray diffraction analysis was carried out on typical samples.* These showed uranyl fluoride to be the predominant species, with U_3O_8 present as a minor species. No magnesium fluoride, uranium dioxide or uranium tetrafluoride was detected in the filter fines by this method. Uranium fines retained in the magnesium fluoride bed also showed uranyl fluoride as the major uranium compound. These results show that production of fines is brought about by a chemical reaction rather than by attrition, and that the reaction to form uranium hexafluoride goes through a preliminary uranyl fluoride step.

One run was made in which the residue fines from a pellet run were fluorinated to obtain a rough indication of their reaction rate. The following conditions were used: 20 per cent fluorine, 500 C, and 0.35-ft/sec gas velocity. The fluorine was passed through the bed for 10 minutes. However, the fines had completely reacted in less than this time, thereby making it impossible to calculate a reaction rate. The fact that the fines had completely reacted in less than 10 minutes was indicated by a very low fluorine efficiency of 37.6 per cent and by the observation that no more uranium hexafluoride

---

* Courtesy of R. Schablaske

was collected when the bed was further fluorinated after the run. It can be concluded that the fines react at a much higher rate than the uranium dioxide pellets and therefore enter quite significantly into the reaction mechanisms. This point will be covered in future experiments.

Table 26

SIZE ANALYSIS OF FINES PRODUCED DURING FLUORINATION OF URANIUM DIOXIDE

(Run UOF-11)

Filter Fines

Mesh	wt (g)	%	Comment
+200	7.5	4.5	mostly green flake material
-200 +325	103.8	62.8	black powder [a]
-325	54.0	32.7	
	165.3	100.0	

Bed Residue

Mesh	wt (g)	%	Comment
-60 +100	143.0	69.7	mostly 60 to 80 mesh MgF_2
-100 +200	10.8	5.3	
-100 +325	34.6	16.8	black powder [a]
-325	16.9	8.2	
	205.3	100.0	

---

[a] Chiefly UO_2F_2 (as determined by X-ray diffraction)

(4) Kinetics of the Reaction

The kinetic mechanism of the direct fluorination reaction is important to the design of engineering-scale equipment. The facts that reaction rate was shown above to be proportional to fluorine concentration and that overall fluorine efficiency was independent of fluorine concentration indicate that the reaction has a first-order dependence on fluorine partial pressure and that deeper beds are capable of very high fluorine efficiencies.

(5) Operational Experience

The same bed of 60- to 80-mesh magnesium fluoride has been used for all runs. It has been used in over 20 fluorinations at elevated temperatures and shows no sign of decrepitation or deterioration. It is a sintered material obtained as by-product slag from uranium metal reductions operation.

The direct fluorination of uranium dioxide is highly exothermic, but no temperature control problems have been encountered at conditions used in these runs. Temperature profiles for Runs UOF-6, 7, and 9 showed variations of less than ±25 C throughout the run. In Run UOF-11, a chromel-alumel thermocouple junction was inserted within a hole in a uranium dioxide pellet, and the temperature was compared with that measured in a thermowell in the bed. The pellet was located midway between the top and bottom of the pellet bed and about halfway between the vertical thermowell (at the center axis) and the wall. The temperature at the pellet interior was not very different from that measured by the center thermowell. The temperature difference ranged from about 50 degrees lower at the pellet interior near the start of the run to about 20 degrees higher at the end.

In removal of the bed residues in the 6- and 9-inch bed runs, it was noted that a substantial part of the remaining pellets did not fall freely from the reactor but were agglomerated and attached to the wall by solid deposit. This occurred at the upper part of the pellet bed and was undoubtedly due to reaction of uranium hexafluoride with uranium dioxide to form uranyl fluoride, uranium tetrafluoride or other fluoride intermediates. Near the end of Run UOF-11, it was noted that additional pressure drop developed, which was probably due to these deposits. In Run UOF-12, the remaining pellets were caked upon the wall with an open center of about one-half the reactor diameter extending through the caked zone. While the bed could no doubt be completely fluorinated, this effect may limit practical bed depth and influence rates and efficiencies when batch reactions are carried toward completion.

Further study will be directed toward (1) a wider range of process variables and (2) fluorination process conditions required by specific flowsheets for complete processing from decladding to uranium-plutonium separation. Runs at higher fluorine concentrations are planned in a forced air-cooled reactor now being installed. This unit should permit greater heat dissipation than is possible in the existing natural convection-cooled reactor.

B. Metal Fluorination Studies

(R. L. Jarry, W. H. Gunther, J. Fischer)

Experimental work has continued on the mechanism of the nickel-fluorine reaction. As a means of checking the validity of the experimental method, both oxidation and fluorination reactions have been used. The oxidation experiments in addition allow a verification of the stated mechanism for the oxidation process.

Preliminary study of the zirconium-fluorine reaction is reported.

1. Nickel-Fluorine Reaction

Both fluorination and oxidation reactions have been studied in order to elucidate the mechanism of the nickel-fluorine reaction. Results reported previously (ANL-6101, page 88) had shown that the mechanism for the nickel-fluorine reaction was that of fluorine migration through the nickel fluoride film.

As a further check on the mechanism the "wedge" experiment, as previously used and described by the Metal Oxidation Group of this Division (ANL-5974, page 74), was used. For this experiment two coupons, each 1 x 2 x 0.165 cm, were welded together along the one-cm edge forming a very small angle "wedge." These were then fluorinated or oxidized at 700 and 980 C, respectively, to produce films of suitable thickness. By this method the character of the interface, produced as the separately growing films meet, would indicate the mechanism of the reaction. For example, a definite line of demarcation at the interface would indicate migration of the gas phase, while a continuum of reaction product across the interface would be indicative of metal migration.

The "wedges" that had undergone reaction were mounted in Bakelite, polished through 1-μ diamond paste and microscopically examined. This examination showed that the mechanisms for the fluorination and oxidation were in fact different. A definite interface was present between the films in the fluorinated sample, but not in those oxidized. Therefore, the mechanism for the nickel-fluorine reaction is one in which gas migration occurs, while the mechanism for the oxidation reaction is one in which nickel migration occurs. The mechanism for the fluorination reaction was substantiated by the spreading of the "wedge" due to the pressure of the outward growing films. These results are shown in the photomicrographs: Figure 32 for the fluorination and Figure 33 for the oxidation.

2. Zirconium-Fluorine Reaction

Experimental work has been started to obtain rate data for the reaction of fluorine with zirconium. Fluorinations have been carried out in a conventional tube reactor. The reaction progress was sensed by measurement

FIGURE 32

PHOTOMICROGRAPH (100 X), FLUORIDE FILM GROWTH FROM OPPOSING SURFACES
(Static Fluorination, A-nickel, 650 C, 54 hours)

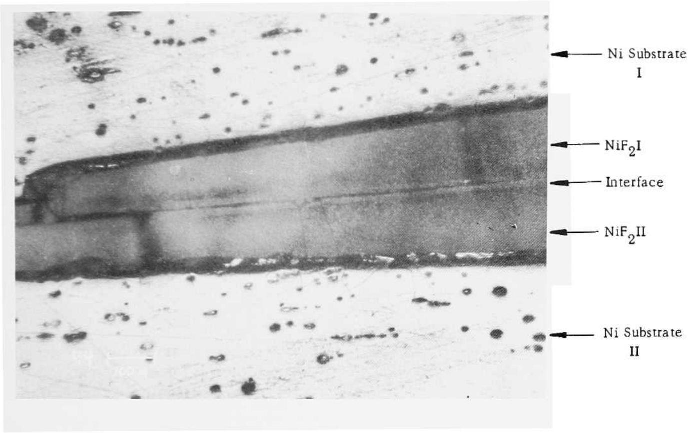

FIGURE 33

PHOTOMICROGRAPH (285 X), OXIDE FILM GROWTH FROM OPPOSING SURFACES
(Static Oxidation, A-nickel, 980 C, 40 hours)

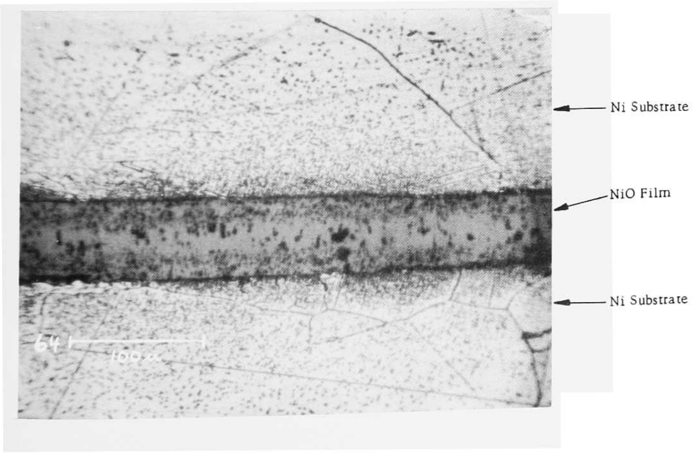

of pressure change. The conversion calculations based on pressure change were checked against the initial and final weights of the coupons on an analytical balance. The agreement was good, being about ±2 per cent at high conversion and ±15 per cent at low conversion.

The tube reactor system consisted of a one-inch nickel reactor, a Booth-Cromer null-point gage for sensing the pressure, and a metal gas-handling manifold, and a gas-circulating pump of the Rosen type (ANL-6003, page 32).

The zirconium metal was obtained from sheet, approximately 0.065 inch thick. Coupons, 1 by 5 cm, for the tube reactor were cut from this sheet and used as such after degreasing. Chemical and spectrographic analyses indicated a maximum purity of 99.7 per cent. Principal contaminants were as follows (in ppm): oxygen, 1580; nitrogen, 157; carbon, 430; and iron, 600.

FIGURE 34

FLUORINATION OF ZIRCONIUM IN THE TEMPERATURE RANGE 300 TO 500 C

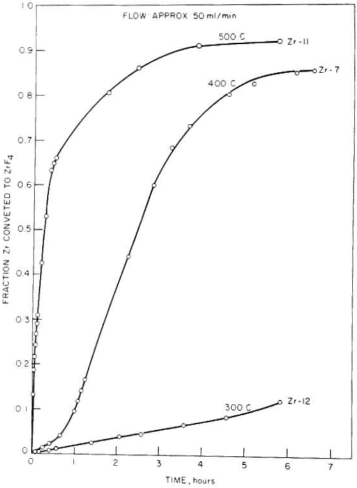

Fluorinations were accomplished at 300, 400, and 500 C. Figure 34 shows the results obtained as plots of the fraction zirconium converted versus time in hours.

The film formed on the zirconium as a result of the reaction with fluorine was not protective in nature. The white zirconium tetrafluoride retained the shape of the coupon but was not adherent. In the higher conversion runs, most of the film scaled off during the course of the run.

X-ray crystal analysis of the product showed that it was beta zirconium tetrafluoride. In the immediate surface layer a definite pattern for the alpha tetrafluoride was obtained and further down in this layer a pattern for zirconyl fluoride ($ZrOF_2$). It appears that these were the results of the fluorination of the thin oxide coating on the zirconium.

3. Uranium-Fluorine Reaction

Some preliminary work has been done on the reaction between uranium and fluorine in the temperature range from 300 to 500 C. Both static and flow experiments have been made with the tube reactor described in the previous section on zirconium.

The uranium metal, in the form of sheet 0.065 inch thick, was of a maximum purity of 99.9 per cent. The results of chemical and spectrographic analyses showed (in ppm) carbon 530, nitrogen 75, oxygen 74, potassium 70, magnesium 50, and all other elements less than 50 ppm. Coupons, 1 by 2.5 cm. were cut from this sheet. Treatment of the coupons prior to reaction consisted of polishing through 1-μ diamond paste followed by a degreasing step. The coupon was then placed in a vacuum at a pressure of less than 1 micron. Fluorine was then added to about one atmosphere pressure and the heating period started. (This last part of the procedure was found necessary due to the very rapid, uncontrolled initial reaction which occurred when fluorine was admitted after the uranium was brought to the operating temperature.) In the flow runs the pump was started after the operating temperature was reached.

Reaction between uranium and fluorine became noticeable (by pressure-drop measurement) at about 150 C but was not appreciable before 300 C. Under flow conditions (50 ml/min) at 300 to 500 C the product formed was uranium hexafluoride. In the static runs at 300 and 400 C the product was uranium tetrafluoride. Conversion rate, expressed as the fraction of uranium converted for unit time (hr), varied from 0.72 to 1.03 for 300 C and 500 C, respectively, for the size of coupon used in the flow runs above. Results are shown in Figure 35. At 400 C under static conditions, the same function dropped to a value of 0.12. The pressure-drop calculations were checked against weight gain for the formation of the tetrafluoride and against uranium analyses in the case of the hexafluoride; the agreement was good.

The tetrafluoride formed in the static runs was not protective. It was loosely layered and easily removed. A small quantity of a fluffy, white, hygroscopic material was usually present on the surface of partially reacted coupons. It was not possible to identify this material by X-ray analysis, as the pattern obtained was too diffuse. The presence of this white material, probably an intermediate fluoride (UF_5), had previously been reported, but not identified by workers at Brookhaven.[16]

---

[16] BNL Memo to C. Williams, from L. P. Hatch et al., Fuel Element Dissolution Studies, August 21, 1958.

FIGURE 35

FLUORINATION OF MASSIVE URANIUM IN THE TEMPERATURE RANGE 300 TO 500 C

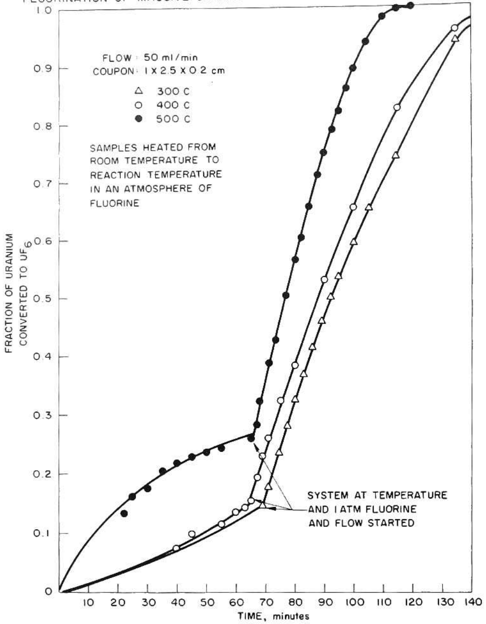

C. ADF Process Development for Enriched Uranium-Zirconium Fuel

(N. Levitz, A. A. Jonke)

The ADF process for recovery of uranium from spent fuel is comprised of three principal steps: aqueous dissolution of the fuel, conversion of the solution to dry granular solids, and fluorination of the solid to volatilize and separate the uranium as the hexafluoride. Current process development is directed toward recovery of uranium from zirconium-base fuels of the type containing low concentrations of fully enriched uranium alloyed and clad with Zircaloy. Fluidization techniques are being used in the drying step, while static (nonfluidized) beds are used in the fluorination step. A disposable vessel to serve as both the fluorinator and the waste container is being considered. Exploratory work on alternate nonaqueous gas-solid reactions on the base metal has started.

1. Fluid-bed Drying

(J. Barghusen, D. Raue)

The fluid-bed drying step of the ADF process consists of spraying the fuel solution into a heated fluidized bed where water is flash evaporated and the metal fluoride salts are deposited on the bed particles. During the past quarter, two runs (ZCP-75 and 76) were made to prepare material for fluorination studies, using the conditions indicated in Table 27. A jet-target grinder was substituted for the attrition jet in the bed to provide a high attrition rate to counteract particle growth.

Table 27

CHEMICAL ANALYSES OF ZIRCONIUM FLUORIDE MATERIAL PREPARED IN ADF PROCESS STUDIES

	Feed			Chemical Composition of Drier Products (w/o)			
						Oxygen	
Run No.	Zr (M)	F/Zr	Temp (C)	Zirconium	Fluoride	Before Hydrofluorination	After Hydrofluorination
ZCP-73	3.6	7	300	51.0	42.4	2.05	0.76[c]
ZCP-74	1.4	5.5	240	50.0	41.2	3.63	1.19
ZCP-75[a]	2.3	7	355	46.3	43.0	-	-
ZCP-76[a]	2.8	7	385	49.2[b]	41.3[b]	-	-

[a] HF added to the fluidizing gas - 4 moles HF per mole Zr in feed.

[b] Heating in air for 3 hr at 480 C changed the composition to 49.8 per cent Zr, 40.6 per cent F.

[c] Fluorination of this material at 700 C produced a residue containing 0.31 per cent oxygen.

Dryer Operation

The jet-target grinder which has been shown to produce much more attrition than an attrition air jet (see ANL-6068, page 103) was installed for Run 76. It produced an attrition rate high enough to maintain fairly uniform particle size distribution. The device consisted of a 0.60-inch diameter target plate affixed one inch in front of a Spraying System Co. spray nozzle and was mounted in the same position as the feed liquid spray nozzle but displaced 90 degrees. Approximately 5 scfm of air was supplied through the liquid side of the nozzle (0.040 inch diameter) to provide the desired attrition. Other operating conditions were similar to those used previously (ANL-6068, page 95).

Particle size distribution remained essentially constant throughout Run ZCP-76, in which the jet-target grinder was used. The +40 mesh fraction oscillated between 50 and 60 per cent and contained less than 5 per cent +20 mesh particles, while the -60 mesh fraction varied between 5 and 15 per cent. Evidently satisfactory particle size control can be exercised if sufficient attrition is provided. About 200 hours of satisfactory running time have now been accumulated on the new spray nozzles (see Figure 24, ANL-6068, page 94).

Chemical analyses of products from Runs 75 and 76 and several previous runs are presented in Table 27. Residual oxygen is undesirable since it consumes fluorine during the subsequent process step. Additional anhydrous hydrogen fluoride introduced as part of the fluidizing gas stream in Runs 75 and 76 at a rate of 4 moles per mole of zirconium in the feed solution had negligible effect on reducing formation of oxygenated compounds. On the other hand, a separate hydrofluorination of fluid-bed dryer products at 450 C resulted in a significant decrease in oxygen content. The duration of hydrofluorination did not prove to be important, since 2.5 and 3.6-hour periods gave similar results.

A 3-hour heating test made at 480 C on the dryer product from Run XCP-76 indicated that only a very slight loss of water or hydrogen fluoride occurred. This test simulated the conditions during the heat-up period of the fluorination experiments, and it was of interest to know if any material was being evolved which might require separate handling.

Dryer products from feeds of high zirconium (up to 3.6 M) concentration did not produce materials of markedly different compositions from that produced at 1.4 molar concentration.

2. Separation of Uranium from Uranium-Zirconium Fluoride Mixtures by Fluorination

(E. Carls, J. Barghusen, L. Marek, D. Raue)

Additional fixed-bed fluorination experiments were carried out at 700 C in bench-scale and pilot-scale equipment described previously (ANL-6101, pages 96 and 101). Runs were also made in a newly installed deep-bed (2-inch diameter by 6-foot tall) reactor designed to test the effect of bed (cake) height on fluorine efficiency, uranium removal and pressure drop. The fluorine recycle pump was used in order to reduce overall fluorine consumption. Of prime interest in this work is the determination of the minimum fluorine requirements for the desired uranium removal (taken as 99 per cent). Bench-scale experiments are being undertaken to investigate the effects of various combinations of hydrofluorination, pyrohydrolysis and fluorination of dryer products on uranium removal.

Recent laboratory results (ANL-6101, page 103) indicated that a partial pyrohydrolysis of fluorinated zirconium fluoride materials "activates" the material, permitting further uranium removal upon refluorination. A series of eight runs was made in the two-inch diameter vertical bench-scale reactor to investigate this effect further. The sequence of operations included one or more of the following teatments of the fluid-bed dryer product, but not necessarily in this order: hydrofluorination at 450 C, pyrohydrolysis with steam at 350 C, and fluorination at 700 C. The hydrofluorinations were carried out in fluid-bed reactors. The pyrohydrolyses were made on either the powder in a fluid-bed reactor or the caked residue (after fluorination) directly in the static-bed unit. The fluorination procedure was described previously (ANL-6101, page 96). The charge was 250 grams of material in each case.

The experiments were conducted so as to use insufficient amounts of fluorine for complete uranium removal, thereby permitting better comparisons. The various treatments were given letter designations for ease of analyzing the data (see Table 28) and results show that the B-D sequence (pyrohydrolysis-fluorination) gave the best uranium removal.

Table 28

RESULTS OF BENCH-SCALE STATIC-BED FLUORINATION EXPERIMENTS

Equipment: 2-inch diameter x 12-inch vertical nickel tube
Charge weight: 250 grams
Dryer product from Run ZCP-74[a]
Initial uranium concentration: 1.1 per cent[a]

Treatment	Code Letter
Dryer product (no treatment)	A
Pyrohydrolysis-steam: 350 C[b]	B
Hydrofluorination: 450 C	C
Fluorination: 700 C	D

Run No.	Treatment Schedule	Fluorine Used (g)	Moles F_2 / Mole O_2	Final Uranium Concentration Top Half (w/o)	Final Uranium Concentration Bottom Half (w/o)
1	A + D	51.9	2.4	0.19	0.06
2	A + B + D	67.0	2.0	0.07	0.06
3	A + C + B + D	64.4	1.0	0.44	0.15
4	A + C + D	33.5	5.0	0.19	0.10
5	A + C + D	50.6	7.5	0.12	0.07
6	A + B + C + D	51.2	7.6	0.21	0.12
7	A + D + B + D	67.7[c]	1.64 and 1.0	0.11	<0.008
8	A + C + D + B + C + D	51.2[c]	5.0 and 2.6	0.12	0.02

---

[a] Exception is Run 3, in which material was from ZCP-71 and contained only 0.29 per cent uranium.

[b] Pyrohydrolyzed materials contained about 5 per cent oxygen in all cases except Run 3 in which 10 per cent oxygen remained.

[c] Total fluorine used in both fluorination steps. First contact was 35.5 grams.

The best example is Run 7, for which ratios of fluorine to oxygen were only 1.64 and 1.0 for the two fluorinations and analysis of the bottom half of the cake (residue) showed the residual uranium concentration to be below the detectable limit ($<$0.008 per cent*). The initial uranium concentration in this case was 1.1 per cent. The fluorine-to-oxygen ratio is of importance, since oxygen consumes fluorine and was present in concentrations 50 to 100 times that of uranium on a mole basis. The fairly large differences in uranium concentration noted for upper and lower ends of the cake were found to be more pronounced when low fluorine excesses were used (see ANL-6101, page 97).

Results of the B-C-D sequence (pyrohydrolysis, hydrofluorination, fluorination) also showed a beneficial effect of the pyrohydrolysis in the case where a double hydrofluorination-fluorination was performed with an intermediate steam treatment (Run 8); however, this lengthy treatment is undesirable from a process standpoint. In this instance the major fraction (85 to 90 per cent) of the uranium was probably removed in the first half of the run (compare with Runs 4 and 5). The last half of the run used a ratio of fluorine to oxygen of 2.6 and the lower half of the cake contained only 0.02 per cent uranium. In comparison the best value for the single B-C-D- sequence (Run 6) was 0.12 per cent residual uranium. The hydrofluorination treatment alone preceding the fluorination showed no improvement over the direct fluorination of the dryer product (compare Runs 4 and 5 with Run 1). This was experienced in some of the earlier work.

Exploratory experiments on alternative schemes for processing low uranium-zirconium alloy fuels were made. Very encouraging results were obtained upon fluorination of a hydrided and hydrofluorinated specimen of 1.4 per cent uranium-zirconium alloy. Hydriding of the 3.3-g specimen was carried out at 825 C in a 5-psig hydrogen atmosphere for an overnight period (14 hours). The hydride was degraded to a fine powder (-200 mesh) in only one minute in a mechanical mortar, and a portion of this material was then hydrofluorinated at temperatures up to 450 C and fluorinated at 600 C on a thermobalance. The uranium content of the residue after this treatment was only 0.01 per cent.

Another experiment involved dissolution of a somewhat larger section of the above alloy plate in anhydrous ammonium bifluoride[17] at about 200 C. The specimen weighed 28.4 g and its dimensions were 0.1 by 1 by 2.13 in. The dissolution, which was completed in several minutes, was followed by volatilization of the excess bifluoride by heating at 300 C, and subsequent fluorination of the caked residue at temperatures of 525 and 600 C. Uranium removal was low, with residual values of 0.33 and 0.25 per cent, respectively. This approach does not appear promising as a means for recovery of uranium from fuel of this type by a volatility process.

---

*Limit for X-ray spectrochemical analysis.

[17] Long, J. R., ISC-97 (1948).

3. Direct Hydrofluorination of Zircaloy

(J. Barghusen, N. Levitz, D. Raue)

Experimental work has started on the direct hydrofluorination of Zircaloy coupons, using anhydrous hydrogen fluoride and mixtures of hydrogen fluoride-hydrogen chloride gas with an inert fluidized bed as heat transfer medium. This work has application to both Zircaloy-clad and uranium-Zircaloy alloy fuels, cases in which the uranium (and plutonium) would be made available for processing via fluoride volatility schemes.

Initial experiments have been carried out in a $1\frac{1}{2}$-inch diameter reactor using calcium fluoride as the inert fluidized medium. The data are summarized in Table 29. Temperatures between 450 to 500 C were used with gas streams of the following compositions: 0 to 100, 5 to 95, and 11 to 89 volume per cent for the hydrogen chloride-hydrogen fluoride concentrations, respectively. The Zircaloy specimens were prepared with an oxide coating by autoclaving in steam for 4 days at 350 C to simulate the film formed on the fuel plates in a nuclear reactor. A single coupon suspended in the bed by a nichrome wire was used for each run. The coupons were of two sizes, 0.12 x 0.5 x 0.75 inch or 0.07 x 0.5 x 1.25 inches, and weighed approximately 4 g each. The unit was brought to temperature with nitrogen and then the reacting gases were admitted.

Table 29

CONDITIONS AND RESULTS OF DIRECT HYDROFLUORINATION OF ZIRCALOY

(Zircaloy coupon autoclaved 4 days at 350 C to provide oxide coating)

Coupon size - 0.12 x 0.5 x 0.75 inch for Runs 1 and 2
- 0.07 x 0.5 x 1.25 inches for Run 3

Run No.	Temp (C)	Run Duration (hr)	Nominal Inlet Gas Composition HF (v/o)	Nominal Inlet Gas Composition HCl (v/o)	Weight Loss of Coupon (%)	Average Penetration Rate (mils/hr)
1A	510	3	100	0	18.8	~1.6
1B	525	4	100	0	52.2[a]	~1.6
2	540	4	89	11[b]	100[b]	>15
3	450	4	95	5	84	~5[c]

---

[a] Cumulative for the total seven-hour run period.

[b] It is believed that the 1.9 g of coarse (+40 mesh) material found at end of run were the remains of the coupon, since the bed was entirely of -60 mesh CaF_2 initially.

[c] Remaining material broke while being measured, indicating somewhat higher penetration had occurred.

The most severe conditions tried, 11 volume per cent hydrogen chloride at 540 C, resulted in complete disintegration of the sample in 4 hours, giving a penetration rate in excess of 15 mils/hour. About 2 g of coarse (+40 mesh) material found in the bed at the end of this run was probably part of the reacted coupon, since the starting bed was all minus 60 mesh calcium fluoride. The anhydrous hydrogen fluoride at temperatures between 510 and 525 C produced a modest penetration rate of about 1.6 mils/hr, while the addition of only 5 volume per cent hydrogen chloride at 450 C resulted in at least a 5-mil/hr rate. The rate of intergranular attack was probably higher in the latter case, since the specimen was found broken into three sections at the end of the run.

Chemical analyses of the bed, filter fines, and off-gas scrub solution, to indicate whether there is a loss of zirconium as the volatile tetrachloride (sublimation point: 331 C) from the system, are pending. These preliminary experiments will be followed by hydrofluorination of samples of uranium-Zircaloy alloy and fluorination of the final bed to demonstrate uranium removal. Direct fluorination of other (stainless steel) cladding materials is also being considered.

D. Fused Salt Processing of Zirconium Matrix Fuels

(W. J. Mecham, A. A. Jonke)

In the fused salt process for recovery of uranium from zirconium-matrix fuel, the alloy is dissolved in the fused salt at 600 to 700 C with a hydrogen fluoride sparge, and the uranium is then volatilized as the hexafluoride in a fluorine sparge. The use of graphite as a material of construction for the dissolver-hydrofluorinator avoids corrosion incurred by metal systems. Results are reported on the semicontinuous operation of the graphite pilot-plant dissolver in which four synthetic fuel assemblies were dissolved in succession. Specific dissolution rates up to 2.3 mg/(min)(sq cm), or about 9 mils/hr, were obtained. Synthetic fuel elements were carried to 90 per cent dissolution in as little as six hours. Graphite heaters and other components functioned satisfactorily. Accumulation of salt in the off-gas system was handled with a regular procedure. Effects of continued operation on processing rates and conditions are being studied.

Graphite Dissolver Tests

(R. W. Kessie, W. Mecham, J. Gates, R. Kinzler, W. Murphy, A. Rashinskas)

In the present period four dissolution runs at flowsheet conditions under semicontinuous operation were completed, with the objective of determining reproducible processing rates and equipment performance.

Before the present operations were carried out, some changes in equipment, other than those previously reported, were made. These consisted of replacement of a graphite heater and salt transfer downline. In both cases, graphite components had cracked, not during process operations but during shut-down (in the case of the heater) and during idleness (in the case of the salt line). The cause of the heater failure is attributed to salt entrapment in the annulus, and was discussed in detail in the previous report (ANL-6101, page 107).

The salt line consisted of a six-foot length of impregnated graphite pipe, 1 inch OD and $\frac{1}{2}$ inch ID. This pipe had male threads (#8 NC) on the top end, which was screwed into an Inconel coupling to the Inconel salt transfer line. Because the autoresistively heated Inconel transfer line has a rather long unsupported length, mechanical shock or strain can be transmitted back to the graphite pipe. Since the last process salt transfer was made without difficulty, the damage must have occurred after processing, during the period of maintenance in the area. The graphite pipe was replaced with a spare one.

A new heater, design Mark III, was fabricated and installed to replace the damaged heater. The Mark III unit has a shell-to-head shrink fit supplemented with a Viton "O" ring seal. The leakage rate of argon gas used to purge the heater was determined at room temperature as 0.25 scfh at 20 psig. This degree of leak tightness allows purge gas to exclude salt from the heater annulus completely. The other heater was the Mark II unit used previously. The Mark II heater, which was apparently unaffected by a previous 900 hr of operation, had been provided with drain holes to prevent salt holdup. Its leak rate was found to be ~4 scfh at 10 psig.

The synthetic fuel elements used in these tests were made by welding together ten individually fabricated fuel plates consisting of a low uranium-zirconium alloy clad in zirconium. The overall uranium content was about one weight per cent. The plate thickness and the channel spacing were both approximately 0.09 inch. Some assemblies were made of unoxidized plates, and one was made of plates with black oxide resulting from previous autoclaving. The plate widths were $2\frac{1}{2}$ inches and the assembly length was three feet. The edge welds were continuous. The side plates were approximately $\frac{3}{16}$ inch thick.

The following operating procedure was used in all runs:

1. The fuel element was charged through the air lock and rested vertically over the gas distributor at the bottom of the dissolver. A six-inch, remotely operated gate valve provided the air lock seal. This valve used Viton "O" ring gate seals and was vacuum tight in these operations. The salt depth was sufficient to just cover the fuel element and to allow a 30-inch freeboard in the dissolver.

2. Hydrogen fluoride was vaporized through the dissolver, sparging the salt and passing through the off-gas system, in which excess hydrogen

fluoride was condensed. Batch boiler and condensate receivers were weighed continuously and contained enough material for a complete run without interruption. (This system was described in detail in ANL-6101, page 107.)

3. At the conclusion of the run, salt samples were taken through an air lock.

4. Sodium fluoride pellets ($\frac{1}{8}$ inch) were added through a screw feeder system between runs in order to maintain salt composition about equimolar in sodium fluoride and zirconium tetrafluoride. Pellets were added at a rate of 15 lb sodium fluoride per hour. The dissolution rate of these pellets was reported previously (ANL-5896, page 35). Salt composition was adjusted between 40 and 50 mole per cent zirconium tetrafluoride.

5. Partial transfers of salt were made at the end of each dissolution to maintain a predetermined salt level. Electrodes and a telegage system indicated the salt level. A freeze valve provided the seal on the salt discharge piping, which was autoresistively heated. The transfer operation required about 30 min from heating to refreezing of the freeze valve.

The operation was carried out on a daily schedule in which 15 hours (2 shifts) were allowed for processing and 9 hours were unattended, with the equipment in standby condition. Time consumed in startup and shutdown to the standby condition would largely be eliminated in full 24-hr operation. For routine operation it is estimated that approximately three dissolutions could be carried out in a twenty-four-hour period, if 5 to 10 per cent metal "heels" remain from each dissolution. A substantial saving in process time could be achieved by using a continuous, rather than a batch, hydrogen fluoride system.

Earlier, some difficulty was encountered with entrained or sublimed salt plugging the slug-charging chute and off-gas lines. No plugging of the slug chute was encountered in these runs, although small hard deposits were noted in the chute at the connection to the dissolver head. These were prevented from accumulating by using the fuel-charging claw to remove some of the deposit.

Fine dust was carried from the salt by the exit sparge gas. The first section of the off-gas line was a 2-inch pipe, which extended from the slug chute to the desublimer vessel. After Runs A6 and A7, this line was found to contain 38.9 g of loose powder, which presented no obstruction to flow. An additional 38.8 g of this material had entered the absorber. After Runs A8 and A9, however, a partial plug developed in this line. The amount of powder was 151 g, which had compacted into a plug at the gate valve in the middle of the line. Some portions of this plug were fairly hard. This line was straight, with a flange at the downstream side to facilitate cleaning without disassembly of equipment other than the flange. If frequent or remote cleaning is required, a cleanout rod with a sliding seal could readily be installed. The effect of solids in the off-gas system is under investigation.

The resistances of the graphite heaters remained at between 0.037 and 0.042 ohm, with no detectable trend during the present two-week period of operation.

The course of the dissolution was indicated directly by hydrogen evolution, which was measured by a wet test meter. These data are given in Figure 36, in which the total off-gas (including an argon purge of approximately 2 cfh) is plotted against run time. Dissolution rates and other data are given in Table 30.

FIGURE 36
OFF-GAS EVOLUTION RATE IN FUSED SALT DISSOLUTION

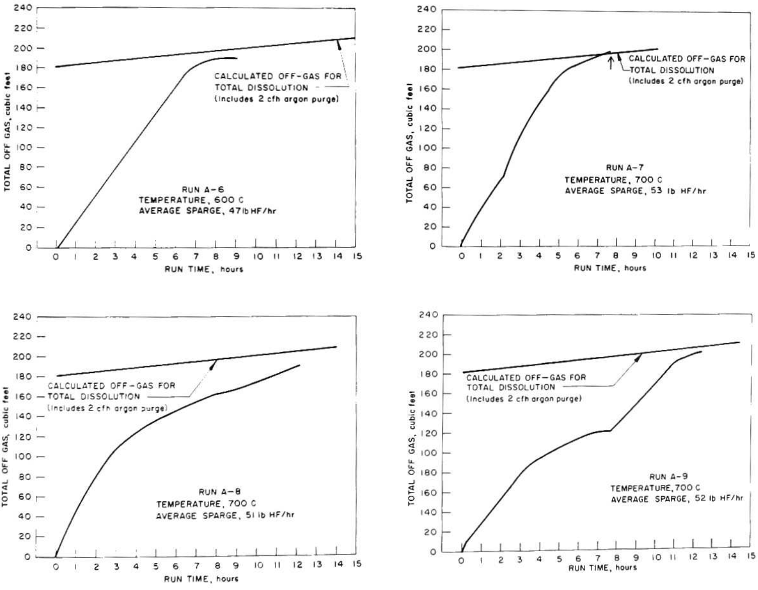

From Figure 36 it can be seen that the dissolutions showed an initial high-rate period, in which up to about 90 per cent of the metal reacted, followed by a decreasing rate period up to complete dissolution. Dissolution rates in this first period were usually constant and close to the maximum rate reported in Table 30. Specific rates were calculated on the basis of the total initial surface area of the metal.

Table 30

DISSOLUTION OF ZIRCONIUM-URANIUM FUEL ELEMENTS BY THE FUSED-SALT PROCESS

(Graphite Dissolver)

Temperature: 700 C, except 600 C for Run A6
Average Sparge Rate: 50 lb HF/hr

Run No.	Fuel Element Weight (lb)	Maximum Dissolution Rate[a]			Time for 90% Dissolution[a] (hr)	Avg HF Utilization[c] (%)
		(lb Zr/hr)	[mg Zr/(min)(sq cm)][b]	(mils/hr)[b]		
A6	21.4	2.9	1.8	6.6	7.8	4.7
A7	21.2	3.7	2.3	8.6	4.8	4.8
A8	21.2	3.7	2.3	8.6	11.3	4.5
A9	21.2	2.5	1.6	5.8	10.5	4.9

[a] Calculated from hydrogen evolution

[b] Based on initial surface area of 12,000 sq cm

[c] HF consumed per throughput (average for dissolution up to 90 per cent of metal).

In Runs A8 and A9 the duration of the high-rate period was progressively shortened, so that the initial high rate fell off considerably before 90 per cent dissolution. Such effects might be expected from poorer gas-metal contacting or, less likely, from poor salt circulation. It is possible that undissolved portions of plates from a previous dissolution might obstruct channels in a subsequent dissolution. In Run A9 it was found that shutting off the hydrofluoric acid flow and then restarting it resulted in reestablishing a high-rate period. Further tests are in progress to determine the causes of successive run variations. In all of these runs, however, the time required for 90 per cent dissolution was less than 12 hours.

E. Conversion of Uranium Hexafluoride to Uranium Dioxide

(I. Knudsen, N. Levitz, M. Jones, J. Kincinas)

Further studies of the fluid-bed process for the conversion of uranium hexafluoride to uranium dioxide were made in the 3-inch diameter Monel reactor (see ANL-6101, page 125). Simultaneous pyrohydrolysis-reduction reactions were carried out on uranium hexafluoride using steam and hydrogen; the newly formed material was deposited as a dense coating on the particles in the bed, or formed new seed particles. Application of the process to production of uranium dioxide for nuclear fuel is the principal purpose of this work. The process may also be applied to the recovery of fluoride (as hydrogen fluoride) from the stores of depleted uranium hexafluoride.

Previous work has demonstrated that the gas-gas reaction of uranium hexafluoride with steam and hydrogen to produce solid intermediate fluorides is very rapid, and that any loss of uranium as hexafluoride is negligible even at high throughput. The extent of conversion of the solid compound to uranium dioxide is incomplete except at low feed rates. This may necessitate a second stage in which the intermediate solid compound is reacted with additional steam and hydrogen to complete the conversion. In a few instances some of the solid product appeared to form in the gas phase, thereby causing production of very fine particles.

The major objectives this quarter were to establish more accurately effects of temperature and other process variables on product composition and particle size in the bed and to determine the effects both chemical and mechanical of operating the unit at higher feed rates.

Evaluation of these runs were made on two bases: 1) factors which affected conversion, determined primarily by residual fluoride content of the product; 2) factors which affected particle size distribution of the bed, e.g., growth or fines formation or both. Condition and results of the runs are given in Table 31.

1. Conversion

The fluoride content of the product was lower when higher temperatures, longer residence times, and higher reactant excesses were used, as might be expected. A comparison of Runs 33 and 34 shows the temperature effect. The residual fluoride content was 5.0 per cent at 550 C and 1.1 per cent at 650 C. The effect of residence time and reactant excess are shown in Figure 37. Some of the points shown are from previous work.

FIGURE 37

EFFECT OF SOLIDS RESIDENCE TIME AND REACTANT EXCESS ON RESIDUAL FLUORIDE CONTENT

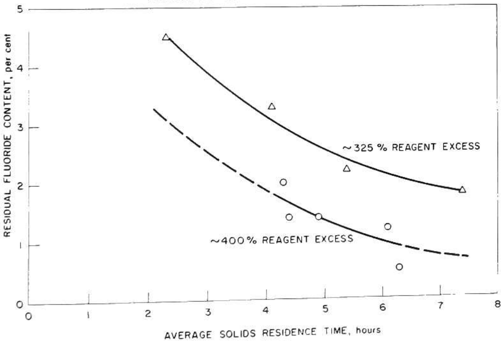

Table 31

SUMMARY OF RUNS ON FLUID-BED CONVERSION OF URANIUM HEXAFLUORIDE TO URANIUM DIOXIDE

Equipment: 3-inch diameter Monel column
Bed Heights: 12 and 18 inches

Run No.	Temp. (C)	Superficial Gas Velocity (ft/sec)	Average UF_6 Rate (g/min)	Reactant Excess		Run Duration (hr)	Average Bed Weight (kg)	Average Residence Time (hr)	Analytical Results		
				Steam (%)	Hydrogen (%)				Residual Fluoride (w/o)	U^{+4} [a] (w/o)	Total U (w/o)
32	600	1.5	60	310	340	4.75	6.6	2.3	5.3	31.7	81.8
33	550	1.1	38	420	430	5.0	6.0	3.4	5.0	35.5	81.6
34	650	1.1	39	430	410	7.5	5.8	3.2	1.1	59.7	85.8
36	600	1.1	37	440	430	7.0	8.7	4.9	2.1	59.0	85.4
37	600	1.1	45	360	340	3.0	8.8	4.1	2.2	64.9	85.2
38	600	1.1	40	380	400	5.0	8.4	4.4	1.7	45.6	84.4

---

[a] Per cent of compounds which is U^{+4}

These results point out that high excesses and long residence time are required for the single-stage process. For example, a 6-hr residence time with 400 per cent reagent excess leaves about 1 per cent fluoride in the product while a 325 per cent excess left about 2 per cent fluoride. The product of the high-temperature run (650 C) was found to contain only 40 ppm nickel, which indicates that the corrosion occurring in this Monel system may not be excessive at this temperature.

Negligible amounts (less than 0.01 per cent) of uranium were carried out of the reactor into the off-gas scrubber even at the highest feed rate of 60 g/min (105 lb uranium per hour per cubic foot of bed volume).

In order to investigate the removal of fluoride from the solid intermediate compound, about 20 lb of products from Runs 35 and 37 was batch contacted with additional steam and hydrogen at 600 C. Results showed 0.035 and 0.026 per cent fluoride remaining after 4 hours, and 0.013 per cent remaining after an additional 4 hours. This material will be tested and evaluated for the production of nuclear ceramic uranium dioxide pellet fuel by an industrial uranium fuel producer.

2. Particle Size Effects

Optimum operation of a fluid-bed system would be one which sustained the starting particle size distribution over extended run periods by having the growth and attrition rates offset each other. An attempt has been made to correlate the data accumulated to date so as to determine significant factors (operating conditions) which have contributed to particle size changes. Both excessive fines or growth are undesirable, but the latter may be overcome by several means: attrition, grinding, recycling, etc., while there is no immediate solution for the former.

The formation of fines is believed to be due to the reaction taking place in gas bubbles within the bed as opposed to the reaction occurring on the surface of the particles in the bed. Therefore, fines formation should be proportional to the gas-solid ratio in the bed. Since higher fluidizing velocities increase this ratio, they lead to greater fines formation under normal fluidization operations. This effect is noted in Figure 38, a plot of average particle size (diameter calculated from average ratio of volume to surface) of the starting bed versus the superficial gas velocity. The data may be divided into two zones, one of particle growth, the other of fines formation. Operation at the borderline might give a balanced situation, although this is only conjecture at this point. Self-attrition is discounted as a major factor since it was found to be small. Particle size effects may be directly related to the ratio of the superficial velocity to the minimum fluidizing velocity with growth occurring when operating near the minimum where gas-bubble size is small and gas-solid contact is improved. Analysis of additional data also indicates lower steam partial pressures favor fines formation, such as in the case where a high hydrogen excess was used (see point for Run 27 in Figure 38).

FIGURE 38
PARTICLE SIZE EFFECTS NOTED AS A FUNCTION OF VELOCITY AND STARTING BED PARTICLE SIZE

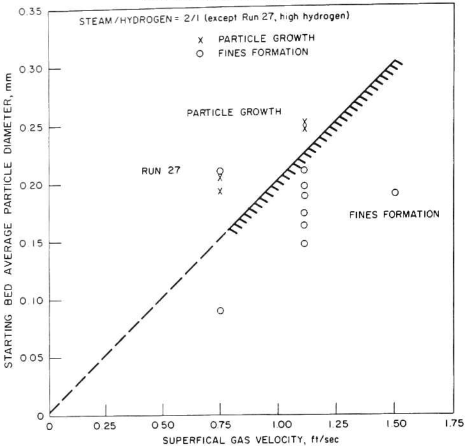

Discussion

The principal problems requiring additional study in this process are (1) control of the particle size of the fluidized bed, (2) selection of design and operating conditions for high capacity with complete conversion to uranium dioxide, and (3) preparation of a product with sintering properties suitable for fabrication of high-density uranium dioxide forms.

Since complete conversion is difficult to achieve in the single-step process, the following alternatives may be considered: (1) a two-step process in which hexafluoride is reacted with steam to produce uranyl fluoride which is then reduced with hydrogen to produce dioxide, (2) a two-step process in which hexafluoride is reacted with hydrogen to produce uranium tetrafluoride which is then pyrohydrolyzed with steam to dioxide, (3) a single-step process at low feed rates. Alternative (2) may also be considered as a means of producing metal-grade uranium tetrafluoride.

The use of the alternative two-step processes may yield products of different sintering characteristics for production of high-density ceramic forms. It is planned to explore these several alternative methods before concentrating the development work on any specific process route.

F. Fundamental Fluidization Studies

Multistage Fluidization*

(K. Williamson, Jr.)

Multistage fluidization reactors equipped with downcomers have been found to be somewhat troublesome in operation due to a variety of causes related to the gas distribution plate and the downcomers. To eliminate this problem and thus make multistage fluidization reactors more reliable, a method is being investigated that achieves controlled downward transport of solids in a fluidized-bed system without downcomers. Two findings[18] made this study appear feasible: 1) good fluidization is achieved above a simple supporting screen if a layer of particles that the screen will not pass is incorporated as part of the bed support, and 2) vibration applied to the bed support "shakes down" the fluidized particles through the "fixed bed" of large particles and screen, thus providing a method for solids level control. Throughput in a one-stage experiment was found to be a function of bed depth, superficial gas velocity, depth of large, nonfluidized particles, and particle size.

1. Description of Equipment

For this investigation a 6-inch diameter, 3-stage column (see Figure 39a) has been constructed. The plates are 24 inches apart and the column is built of alternate Pyrex glass pipe and metal sections. The glass sections permit visual observation while the metal sections permit external connections to be made. Fluidizing gas enters near the bottom of the column and leaves at the top through porous metal filters. Humidified air was used to avoid static electricity effects. Solids are fed to the top of the column by a screw feeder and the product is removed at the bottom.

A bed support consists of a lower plate, a layer of large, nonfluidized spherical material and an upper plate (Figure 39b). Each plate consists of a wire screen and a punched-metal plate. Vibrational energy is transmitted to the screen-plate cover by a pointed steel rod to which a vibrator is attached. An important characteristic of this column is the fact that material is passed through a bed support only when the vibrator to that bed support is energized.

---

* Work being done to fulfill doctoral thesis requirements for Pennsylvania State University under participating institution plan.

[18] Williamson, K., Work done on Master's degree thesis at Pennsylvania State University.

FIGURE 39

a. SCHEMATIC DRAWING OF THE 6–INCH MULTISTAGE FLUIDIZATION COLUMN

b. DETAIL OF A BED SUPPORT

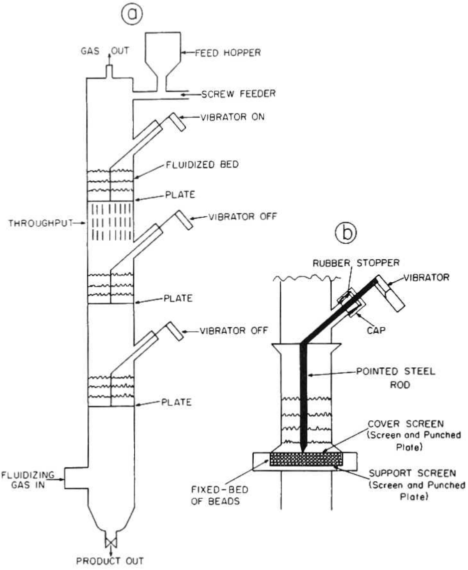

2. Experimental Program

The experimental program is divided into two sections. The first (approximately half completed) is an investigation of the factors affecting the column operation. Using the glass bead-air system, a study was made of vibrational frequency, vibrator-to-plate vibration transmitters, feed particle size and particle size distribution, throughput rates, and the percentage of time that the vibrators are in operation. Variables yet to be studied are superficial gas velocity, bed depth of fluidized particles, plate resistance and uncontrolled throughput.

The second section of the experimental program will investigate the adsorption of water vapor by silica gel and/or activated alumina. In this work mass transfer coefficients will be determined and the effects of various moisture contents of the fluidizing gas, bed depths, superficial vapor velocities and feed rates will be investigated.

3. Experimental Results

The following is a discussion of the experimental results from the investigation of vibrational frequency, types of vibration transmitters, feed particle size and particle size distribution, and the percentage of vibrator on-time.

a. Vibrational Frequency

For runs to test the effects of vibrational frequency, two sizes of Martin Engineering Company air vibrators were used: Model-BD, Nos. 10 and 13. Vibration is produced by a revolving steel ball which generates centrifugal force. The experimental data for both vibrations was correlated as shown in Figure 40. This is a plot of centrifugal force produced by the revolving steel ball, "corrected" for vibrator lever arm length and vibrator weight, versus the throughput rate. The lever arm length is the distance from the axis of ball rotation to the point where the vibrator is attached to the steel rod. The ordinate of Figure 40 can also be thought of as energy per unit vibrator weight. The parameter is the percentage of the total run time that the vibrators were in operation. From these runs it was concluded that the throughput rate was a function of the generated centrifugal force and that a threshold centrifugal force was necessary to initiate solids flow.

FIGURE 40

ENERGY PER UNIT VIBRATOR WEIGHT VERSUS THROUGHPUT RATE

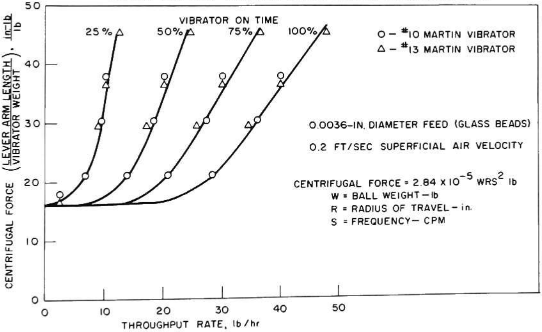

b. Type of Vibration Transmitters

Runs were made using five different types of vibration transmitters. It was found that a simple steel rod with a pointed end (Figure 39b) which fits into a hole in the cover plate gave the most efficient use of the generated centrifugal force. This transmitter will be used for all future runs. A rubber stopper is used to seal the opening where the steel rod enters the column. A Teflon gasket seal, which did not diminish the effectiveness of the vibrational energy, has also been used.

c. Feed Particle Size and Particle Size Distribution

The results of work on the effects of feed particle size and particle size distribution are shown in Figures 41, 42, and 43. Figure 41 is a plot of percentage vibrator "on" time versus the throughput rate. A maximum throughput rate of 72 lb/hr was achieved with the feed material of smallest diameter. For these runs the large "fixed bed" was composed of beads of 0.0357-inch diameter in the bed support. From this work it was deduced that the size of the openings in the top plate and bottom plate is unimportant as regards the throughput rate, since all of the tested materials easily passed through the support and cover screens.

The important factor appears to be the "critical diameter," shown in Figure 42. This "diameter" is that of the largest sphere that will fit between the tightly packed "fixed bed" of beads. Figure 43 shows the dependence of this factor. It is a plot of the ratio of "critical" diameter/feed bead diameter versus maximum throughput (vibrator on 100 per cent of the time). From this figure it can be concluded that, to get appreciable throughput, the feed material must have a diameter slightly smaller than the "critical diameter."

d. Percentage of Vibrator On-Time

It was found that a linear relationship exists between the percentage vibrator on-time and the throughput rate. When operating half the time, 50 per cent of the maximum throughput rate was achieved.

FIGURE 41
PERCENTAGE VIBRATOR ON-TIME VERSUS THROUGHPUT RATE FOR VARIOUS SIZES OF FEED MATERIAL

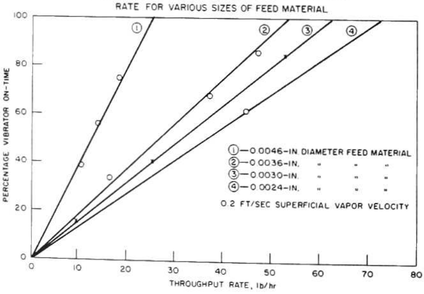

FIGURE 42
RELATIONSHIP BETWEEN "CRITICAL DIAMETER" AND "FIXED-BED" BEAD DIAMETER

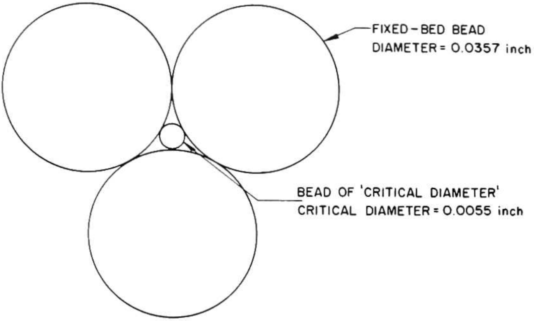

FIGURE 43
"CRITICAL" RATIO VERSUS THE MAXIMUM THROUGHPUT RATE

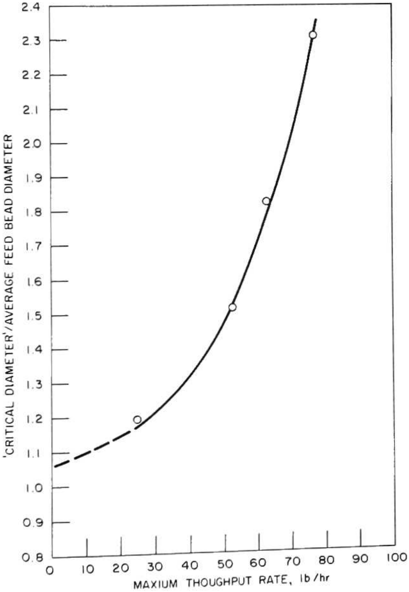

III. REACTOR SAFETY

The oxidation, ignition, and combustion processes of uranium, zirconium, thorium, and plutonium are being studied in order to provide information leading to an understanding of the reactions. This knowledge should make it possible to minimize the hazards associated with handling these nuclear reactor materials.

Since one of the most common hazards involves the ignition and burning of chips and turnings from machining operations, considerable effort has been directed toward understanding the combustion processes. Although chips and turnings have irregular cross sections and are not uniform along their lengths, it has been demonstrated that comparable results are obtained with either turnings or foil strips. Studies of the propagation of burning along foil strips have provided a method for more carefully appraising the effects of many variables on the combustion process. Previous studies on uranium (ANL-5959, page 71; ANL-5996, pages 196 and 204; ANL-6068, pages 129 and 135, and ANL-6101, page 135) and on zirconium (ANL-6029, page 119, ANL-6068, pages 137 and 140 and ANL-6101, page 136) have included (1) the effects of varied thickness, width and shape in both oxygen and air, (2) the effects of surface and gas contaminants, and of alloy additives, (3) the effects of varied oxygen content of the gas, (4) the completeness of combustion, and (5) burning temperature profiles.

Although gas contaminants of moisture, carbon dioxide, and ozone have very limited effects, the character of burning propagation of both uranium and zirconium in air is considerably altered by the presence of 5 per cent chlorobromomethane or chlorodifluoromethane (Freon 22). For 0.13-mm thick uranium, the propagation rate, the extent of reaction, and the burning temperature are all markedly reduced. Pure zirconium foil, 0.13-mm thick, would not sustain burning in air contaminated with these agents. Even the 14.9 atom per cent titanium-zirconium alloy foil, which normally burned rapidly in air, would not sustain burning in air contaminated with 5 per cent Freon 22 and showed considerably reduced propagation rate, burning temperature, and burning zone length in air contaminated with 5 per cent chlorobromomethane. The effects on uranium combustion were shown to be uniformly dependent on the concentration of the agent present in the range up to 9 per cent. In an effort to identify more precisely the mechanism by which these halogenated compounds lower the burning propagation rate of uranium, several other agents, such as carbon tetrachloride, dibromomethane, ethyl bromide, and difluorodibromomethane, were also studied.

Because of the common use of aluminum and silicon in conjunction with uranium in nuclear reactors, the study of the effects of small quantities of these elements in uranium was extended beyond that reported in

ANL-5974, pages 15 to 23. The ignition temperatures in oxygen of 8.5-mm uranium cubes containing greater than 75 parts per million of either aluminum or silicon or as a combined total were markedly decreased.

Preliminary ignition experiments with plutonium demonstrated that useful ignition data for plutonium and its alloys can be obtained by burning-curve or shielded ignition experiments. Information to assist in establishing specifications for the pure metal and alloy specimens is being gathered. Burning-curve experiments in air and in oxygen on samples with varied impurity content indicate a gradual increase of ignition temperature with increasing purity below approximately 1000 ppm. The ignition temperature of plutonium appears not to be strongly influenced by iron content but is strongly influenced by carbon content.

Because of the importance of uranium powders and the need for extension of the specific area relationship, an investigation of the ignition of metal powders is being carried out. Ignition temperatures of specially prepared uranium powder which has essentially spherical particles confirmed the strong dependence on specific area or particle size and to a lesser extent on sample weight. The agreement of the data for samples greater than 0.5 gram with ignition temperatures calculated on the basis of equations derived from bulk oxidation data, heats of formation, and particle size indicates the possibility of defining a fundamental relationship.

Ignition temperatures of a variety of metal foils have been determined by shielded ignition experiments. The relationships between the logarithm of the specific area and the reciprocal ignition temperature for titanium, iron, and molybdenum, in addition to uranium and zirconium, appear to follow the equation

$$\log S = \log I + (E/2.3\,RT) \quad ,$$

where

E is the activation energy of the oxidation process (cal/mole),

T is the ignition temperature (K),

R is the gas constant (cal/mole-degree),

S is the specific area (sq cm/g), and

I is an empirical constant for each metal.

Further consideration of how values of I are related to oxidation kinetic data and thermal and physical properties of the metals should result in a more general understanding of metal-ignition behavior.

The experimental program to determine rates of reaction of molten reactor fuel and cladding metals with water is continuing. The principal laboratory-scale method involves the rapid melting and dispersion of metal wires in a water or steam environment by a surge current from a bank of condensers. A series of runs with 30-mil uranium wires was completed. Runs up to initial temperatures of 2200 C showed relatively slow rates of pressure rise and up to 20 per cent reaction. Runs with initial temperatures above 2500 C showed an explosive pressure rise and up to 30 per cent reaction. The change in character of the reaction rate of uranium was not as abrupt as for zirconium. The data for extent of reaction as a function of initial temperature for 30-mil wires were nearly identical to those reported previously for 60-mil wires. This suggests that a linear rate law may be applicable.

A second laboratory-scale method involves the rapid contact of steam with heated metal. In this method, the metal receives a "pressure pulse" of water vapor. A series of preliminary runs with liquid zirconium in the range from 1850 to 2100 C and water vapor at 20 mm was completed. The zirconium was found to be contaminated with thorium through contact with the thoria crucibles used to contain the zirconium. Tentative results indicated that the oxidation of the liquid metal followed the parabolic rate law.

A series of twelve experiments has been conducted in the TREAT reactor. In these experiments, a stainless steel autoclave containing a fuel pin, gold foils, helium and water was subjected to a short burst of neutrons. The pins were 20 per cent enriched uranium completely clad in Zircaloy-2 cans. Small defects in the form of 3- and 15-mil holes were introduced into the clad before the runs. Reactor transients up to 60 megawatt-seconds caused partial melting of uranium and bursting or bulging of the Zircaloy can. More energetic transients caused up to 20 per cent of the uranium to be dispersed into fragments and fine particles. Very energetic transients in the range from 90 Mw-sec to 175 Mw-sec caused complete melting of the core and cladding, and extensive spraying of metal and fine particle production. Up to 10 per cent of the uranium reacted with water under these conditions.

A relation between the total energy of the reactor transient and the energy absorbed by the pin was derived from the data. A preliminary correlation of all the TREAT runs to date is presented. This correlation will be the basis for a more extensive analysis on the analog computer.

A. Metal Oxidation-Ignition Studies

(J. G. Schnizlein)

1. Uranium Ignition Studies

(L. Leibowitz, J. D. Bingle)

a. Burning Propagation of Uranium Turnings

A variety of incidents involving combustion of uranium powders, chips, and turnings have prompted this study of their burning properties. Burning-propagation rate measurements have proven to be valuable and reproducible quantities in comparing the effect of various factors on the combustion process.

Since such data could be obtained only by the use of quite uniform samples, most of our work has involved the use of metal foils. To compare the results obtained on the foil strips with those more closely related to the turnings, which are of greater practical interest, a quantity of uranium turnings was obtained. These were of varied sizes and shapes, and in general were not straight. It was possible to measure average burning-propagation rates for these samples by marking the turnings near each end, measuring the length of the metal strip between the two marks, and determining photographically the burning time over that distance. Measurements were made of the thicknesses and widths of the various turnings and typical cross sections were photographed. In Figure 44 the rate data for turnings are compared with those previously reported (ANL-6068, page 129) for various uranium foils and wires. The propagation rates of the turnings agree with the relationships that have been established for foils in both air and oxygen.

b. The Effect of Halogenated Hydrocarbons on the Burning Properties of Uranium in Air

Because of the danger of fires which exists when working with uranium, considerable study has been given to various factors which influence metal pyrophoricity. Burning-propagation rate and ignition temperature have proven to be reliable, reproducible quantities which can be used to explore the variables of interest. A number of measurements of burning-propagation rate have been carried out in air to which various substances have been added. The results of these measurements are shown in Table 32 and Figure 45. It is noteworthy that the various halogenated hydrocarbons tested markedly diminished the burning-propagation velocity.

FIGURE 44

RELATIONSHIP BETWEEN CROSS-SECTIONAL AREA AND BURNING PROPAGATION RATES IN AIR AND OXYGEN FOR URANIUM

(Data for lines previously reported ANL 6068 page 129)

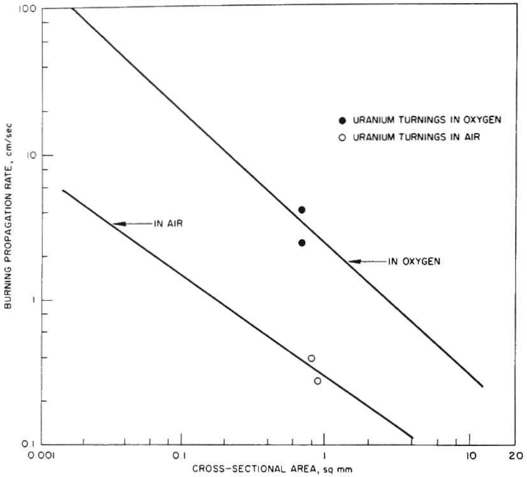

THE EFFECT OF VARIOUS GAS CONTAMINANTS ON THE BURNING-PROPAGATION RATE OF URANIUM FOILS IN AIR

(SMF-5 uranium foil strips: 0.13 x 3.0 x 70. mm)

Contaminant	Concentration (volume %)	Heat Capacity of Contaminant, (0 C, 1 atm)	Burning-propagation Rate (cm/sec)
None	-	-	0.555
CO_2	5.0	8.75	0.514
O_3	1.0	~9.	0.575
H_2O	3.1	8.	0.546
He	5.0	5.	0.505
CH_2BrCl	5.21	12.67	0.398
CH_2BrCl	8.77	12.67	0.304
CHF_2Cl	5.0	13.35	0.403
CCl_4	4.27	19.92	0.425
C_2H_5Br	5.48	17.55	0.371
CH_2Br_2	2.18	13.09	0.419
CH_2Br_2	3.16	13.09	0.365
CF_2Br_2	4.42	18.45	0.349
CF_2Br_2	9.31	18.45	0.285

FIGURE 45
EFFECT OF VARIOUS GAS CONTAMINANTS ON THE BURNING PROPAGATION RATE OF URANIUM FOILS IN AIR

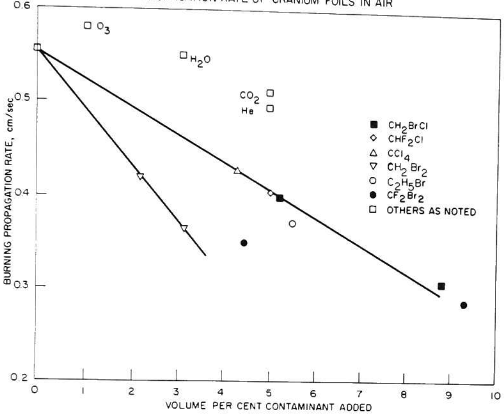

Since the inorganic agents tested did not change the propagation rate, it is clear that the effect of the organic vapors is not simply one of dilution. Moreover, inspection of column three of Table 32 shows no clear correlation of inhibiting effect with heat capacity of the contaminant. It thus appears that a chemical effect is involved. Measurements of the amount of metal consumed showed that the reaction was much less complete in the presence of the organics. Observation of the brightness of the combustion zone indicated that the burning temperature was much lower than in pure air. Several oxide residues were analyzed for halogen and small quantities were detected. Attempts to identify the halogen-containing phases in the oxide are now being made.

It is interesting that these organic compounds are well-established[19] inhibitors of gas-phase hydrocarbon combustions and presumably operate through a chain-breaking step by halide atoms. More precise identification of the mechanism by which these halogenated compounds lower the burning-propagation rate of uranium is currently being attempted.

In view of these results, some measurements were made of ignition temperatures of 0.13 x 3-mm uranium foils in air with 4 per cent CH_2Br_2 and ~6 per cent CF_2Br_2. Values of 285-290 C were

---

[19] Belles, F. E., Chemical Action of Halogenated Agents in Fire Extinguishing, NACA-TN-3565 (September 1955).

found, which are markedly lower than the value of 385 C found in pure air. The contrasting effects of the contaminant on burning-propagation rate and ignition temperature indicate a probable lack of interdependence.

The possibility seems to exist now, of finding an atmosphere in which the propagation rate will be lowered to its limiting value; that is, if the propagation rate is lowered so much that insufficient heat is generated to sustain the reaction, the fire will be extinguished. We seem to be not too far from this point with these uranium foils and have actually achieved it with zirconium (see below).

c. The Effect of Aluminum and Silicon on the Ignition Temperature of Uranium

As part of our continuing study of the ignition behavior of uranium, we have been examining the effect of a number of alloying agents. Much of this work has already been reported (ANL-5974, page 15). It has been noted that additions of relatively small quantities of aluminum or silicon had a marked effect on the ignition temperatures of 8.5-mm uranium cubes in oxygen. Because of the common use of both of these metals in conjunction with uranium in nuclear reactors, the study of the effect of small quantities of them in uranium was extended beyond that reported in ANL-5974. A number of alloys containing low levels of either or both of these two elements have now been examined. The ignition temperatures obtained are presented in Table 33 and shown graphically in Figure 46. The sudden fall in ignition temperature in the region of 70 to 80 ppm indicates the wisdom of maintaining a total aluminum and silicon level below that concentration. This must not be construed as necessarily the most important cause of incidents involving uranium. The effect of aluminum diminishes as the specific area is increased, so that it causes no decrease of ignition temperature for samples with a specific area greater than 10 sq cm/gram. In addition, in air the effect of 1 atom per cent aluminum on the basis of experiments conducted to date has been difficult to demonstrate clearly. Burning-curve experiments in air show no effect of aluminum, whereas modified shielded experiments at 500 C show that aluminum causes a more drastic initial self-heating and an approximate doubling of the oxidation rate, but burning was not sustained (ANL-6101, page 133). Additional experiments should be designed to determine whether or not the aluminum or silicon content increases the danger of ignition in an array of reactor fuel assemblies.

Table 33

IGNITION TEMPERATURES OF ALUMINUM AND SILICON ALLOYS OF URANIUM IN OXYGEN

(8.5-mm cubes in 1200 cc/min flowing oxygen)

Metal	Ignition Temperature[a] (C)	Metal	Ignition Temperature[a] (C)
Previous BMI-base Metal	575	Previous Si Alloys	
New BMI-base Metal	590	2890 ppm	420
ANL-base Metal	595	1080	465
High-purity Uranium	595	530	385
Previous Al Alloys		New Si Alloys	
2260 ppm	370	185 ppm	380
1130	350	80	400
580	360	60	555
550[b]	365		
380[b]	365	New Al-Si Alloys	
95[b]	405	210 ppm Al; 230 ppm Si	360
70[b]	570	105 ppm Al; 105 ppm Si	360
New Al Alloys			
235 ppm	385		
75	420		
55	575		

---

[a] Determined by burning-curve technique.

[b] Prepared by Pyrometallurgical Group, Chemical Engineering Division, ANL: all other alloys prepared by Battelle Memorial Institute.

FIGURE 46

THE INFLUENCE OF ALUMINUM AND SILICON ON THE IGNITION TEMPERATURE OF 8.5-mm URANIUM CUBES IN OXYGEN

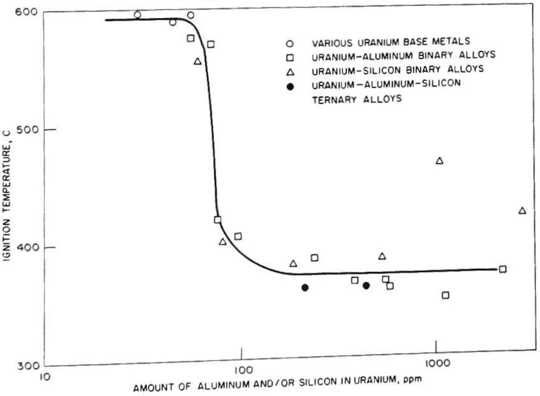

2. Zirconium Ignition Studies

(L. Leibowitz, J. D. Bingle)

a. Burning-propagation Rate of Zirconium Turnings

As was explained above for uranium, measurements of burning-propagation rates of zirconium turnings were also carried out. Similar good agreement with information obtained from foils was obtained and the applicability of work done with foils to practical ignition problems was illustrated.

b. The Effect of Halogenated Hydrocarbons on the Burning-propagation Rate of Zirconium in Air

Experiments similar to those outlined above for uranium have been carried out on zirconium foil strips. A number of measurements of burning-propagation rates in air have been made with chlorobromomethane and chlorodifluoromethane (Freon 22) as contaminants. The inhibiting effect observed for zirconium was even more pronounced than that found for uranium. Pure zirconium foil, 0.13-mm thick, would not sustain burning in air contaminated with either of these two halogenated hydrocarbons, thus illustrating that, for this foil at least, one can lower the propagation rate to its limiting value. Even the 14.9 atom per cent titanium-zirconium alloy foil, which normally burned rapidly in air, would not sustain burning in air contaminated with 5 per cent Freon 22, and showed considerably reduced propagation rate, burning temperature, and burning zone length in air contaminated with 5 per cent chlorobromomethane. All of the values obtained for the various zirconium foils are summarized in Table 34, along with data using several inorganic contaminants previously reported.

3. Plutonium-ignition Studies

(J. G. Schnizlein, D. F. Fischer)

The increasing importance of plutonium to the nuclear energy program and concomitant handling of the metal in various forms makes knowledge of its ignition and combustion behavior essential to safety. Relatively little information on the oxidation or ignition characteristics has been previously published.

A glove box facility for handling metallic plutonium is being constructed and arrangements have been completed with Hanford* to prepare special plutonium and plutonium alloy samples for this study.

---

* Fabrication of Samples under the supervision of O. J. Wick, R. W. Stewart, and P. G. Pallmer, General Electric Company, Hanford Atomic Products Operation, Richland, Washington.

Table 34

EFFECT OF VARIOUS GAS CONTAMINANTS ON THE BURNING-PROPAGATION RATES OF ZIRCONIUM FOILS IN AIR

Contaminant	Concentration (volume %)	Burning-zone Length (cm)	Burning-propagation Rate (cm/sec)
Zr foil, 0.13 x 0.60 x 70 mm			
None	-	1.3	0.463
H_2O	3.1	1.4	0.542
CO_2	5.0	1.1	0.432
O_3	1.0	1.7	0.569
He	5.0	1.2	0.475
CH_2BrCl	5.2	Did not propagate	
CHF_2Cl	5.0	Did not propagate	
2.12 a/o Ti-Zr alloy foil, 0.13 x 0.60 x 70 mm			
None	-	2.6	0.835
H_2O	3.1	2.6	0.805
He	5.0	2.2	0.851
CH_2BrCl	5.2	Did not propagate	
CHF_2Cl	5.0	Did not propagate	
14.9 a/o Ti-Zr alloy foil, 0.12 x 0.60 x 70 mm			
None	-	3.7	1.06
CH_2BrCl	5.2	1.7	0.708
CHF_2Cl	5.0	Did not propagate	
Zr foil, 0.020 x 0.90 x 70 mm			
None	-	~2	3.23
CHF_2Cl	5.0	1.4	1.98

Prior to the completion of the new glove box facility, exploratory experiments are being performed in a glove box in the plutonium analytical facility. A few samples of metal were obtained from the Metallurgy Division,* ANL, in addition to preliminary preparations from Hanford.

---

*The cooperation of L. R. Kelman and R. J. Dunworth is greatly appreciated.

The objectives of these current exploratory ignition experiments are: (1) to gain experience in handling metallic plutonium and in glove box manipulations; (2) to develop suitable apparatus and techniques for carrying out the measurements within the limitations imposed by glove box operation; (3) to determine whether useful ignition data for plutonium and its alloys can be obtained by burning-curve or shielded ignition experiments; and (4) to obtain information for establishing specifications for the pure metal and alloy specimens.

Burning-curve and shielded ignition experiments have been conducted in a 700-watt tube furnace which has a water-cooled shell to reduce the heating of the glove box atmosphere. The quartz furnace tube is protected from the heat and occasional spattering of igniting metal by an inner zirconia tube. The furnace temperature is controlled by a cam programmer so that a constant rate of temperature increase is obtained. Usually, a rate of ten degrees per minute is employed for burning curves, but other definite rates can be readily controlled.

Preliminary burning-curve and shielded ignition experiments were performed on foils of one weight per cent aluminum-plutonium alloy, which were used for burning-propagation studies (ANL-6068, page 144). Complete analyses were not available, the samples were from different sources, and the supply of each was somewhat limited. Therefore, no definite conclusions can be reached other than that both burning-curve and shielded ignition experiments do provide useful data. The reproducibility and comparability of ignition temperatures obtained by the two methods are fair. The ignition temperatures in air are close to those in oxygen, but may be slightly lower. There seems to be only a minor change of ignition temperature for a change of specific area from approximately 1.3 to 8.8 sq cm/gram. Further study of the aluminum alloys of plutonium will be of interest when well-characterized samples are available.

Burning-curve experiments in oxygen and air also have been completed with plutonium rod samples approximately 6 mm in diameter and 6 mm in length. Each sample was not completely oxide-free, but had a thin, adherent oxide. For the runs in oxygen, the flow rate was 1250 cc/minute while in air the flow rate was 6000 cc/minute. Samples of high purity, low purity, and binary alloys containing 1.96 atom per cent carbon and 2.19 atom per cent iron were obtained from Hanford. Samples of high purity, intermediate purity, and low purity were obtained from Metallurgy Division, ANL. Analyses of the mentioned plutonium samples are given in Table 35.

Table 35

CHARACTERIZATION OF PLUTONIUM SAMPLES

	Samples obtained from MET, ANL[a]			Samples obtained from Hanford[b]			
Sample Designation	ALP	AIP	AHP	HLP	HHP	C	Fe
Purity	Low	Intermediate	High	Low	High	-	-
Additives Composition (a/o)	None	None	None	None	None	Carbon 1.52	Iron 2.77
Density (g/cc)	-	-	-	19.08	19.50	18.99/19.19	19.01/19.12
Hardness (DPH with 20-kg load)	-	-	-	219	279	233/261	260/279
Specific Impurities (ppm):							
C	-	-	60	360	90	710/840	85
H	-	-	-	15	80	5	3
O	-	-	90	615	610	50	100
N	-	-	-	10	15	85	-
Al	150	100	20	-	-	-	-
Ca	250	<5	<5	-	-	-	-
Co	15	-	<5	-	-	-	-
Cr	250	150	<20	155	16	17	76
Cu	75	10	25	50[c]	10[c]	10[c]	20[c]
Fe	500	150	30	1000	50	110	6620
Mg	250	50	<5	228	44	24	237
Mn	50	20	25	200[c]	100[c]	200[c]	200[c]
Ni	500	200	<20	158	31	38	77
Pb	100	5	<1	50[c]	20[c]	20[c]	10[c]
Si	-	-	55	9	<1	2	6
Zr	100	20	-	-	-	-	-
Total Metallic Impurities (ppm)	2500	710	210	1850	270	420	625[e]
Total Impurities Including C,H,O,N (ppm)	4000[d]	1260[d]	360	2850	1065	560[e]	815[e]

---

[a] The cooperation of L. Kelman and R. J. Dunworth (Metallurgy Division, ANL) is gratefully acknowledged.

[b] Preparation supervised by O. J. Wick, R. W. Stewart and P. G. Pallmer, General Electric Company, Hanford Atomic Products Operation, Richland, Washington.

[c] By a factor of 2, others plus or minus 15 per cent. Unlisted contaminants below spectrographic limits of detection.

[d] Estimates of C, H, O, N contents to be 1500 for low purity and 550 for intermediate purity.

[e] Not including the concentration of the alloy additive.

Various selected plutonium samples had 0.055-inch holes drilled half way into the samples. The temperature measurements of a drilled sample are more sensitive than those on undrilled ones, and the various plutonium transformation phases can therefore be observed. However, the indicated ignition temperature obtained from the burning curve, by means of the usual tangent method, gives similar results for both the undrilled and drilled samples.

In oxygen, the Hanford low-purity plutonium gave the highest ignition temperature, 621 C, while the 1.96 atom per cent carbon-plutonium alloy ignited at 447 C. In one experiment, the 1.96 atom per cent carbon-plutonium alloy ignited at 208 C. However, this low ignition temperature has not been reproduced in subsequent experiments and there is no present information to explain this anomalous behavior. Other than this occasion, the reproducibility appears to be satisfactory.

In air the indicated ignition temperatures obtained from the burning curves appear to be slightly lower than in oxygen. Ignitions in air are not nearly as bright as ignitions in oxygen. In oxygen the temperature will rise quickly above 1400 C and the sample melts. In air, the temperature rises more slowly to approximately 1100 C, cools to about 600 C and then continues to thermocycle. This phenomenon has also been reported for uranium burning curves in air (see ANL-5974, page 31).

The burning-curve ignition temperatures and the total impurities in the different plutonium samples are summarized in Table 36.

Table 36

IGNITION TEMPERATURES OF PLUTONIUM SAMPLES DETERMINED BY BURNING-CURVE METHOD ON RIGHT CYLINDERS 6 X 6 MM

Sample Designation	Total Impurity Content (ppm)	Ignition Temperature (C)	
		In Air	In Oxygen
AHP	360	530	559,555
HHP	1065	-	520
AIP	1260[b]	-	515
HLP	2850	-	619,617,621
ALP	4000[b]	-	537,518
2.8 a/o Fe	815[c]	485,476	520
1.5 a/o C	560[c]	-	208,455,447

---

[a] For further specifications, see Table 4, page 42.

[b] Estimates of C, H, O, N contents to be 550 ppm for intermediate purity and 1500 ppm for low purity samples.

[c] Not including the concentration of the additive. If included, the total impurity would be 7450 ppm for 2.8 a/o Fe and 1340 ppm for 1.5 a/o C samples.

It is regrettable that some of the analyses are incomplete. There appears to be no reasonable explanation for the high ignition temperature for the Hanford low-purity plutonium. Otherwise, there would appear to be a gradual increase of ignition temperature with increasing purity below approximately 1000 ppm. The ignition temperature of plutonium appears not to be strongly influenced by iron content, but is strongly influenced by carbon content. It will be necessary, therefore, to exercise careful control of the carbon content during the fabrication of the alloys for future studies.

4. Metal Powder-ignition Experiments

(L. W. Mishler, M. Tetenbaum)

Ignition-temperature measurements on uranium powders were studied as a function of particle size and powder charge. The uranium powders manufactured by a special process by the National Lead Company, Fernald, Ohio, showed a remarkable degree of smoothness and sphericity for various size ranges. Figure 47 shows micrographs of four sizes of these spherical particles and two sizes of irregular particles produced by the hydriding-dehydriding process. These irregular particles were identical to those used in previously reported experiments (see ANL-6101, page 130). The burning-curve technique was used to measure the ignition temperatures of the uranium charges contained in a graphite crucible (~3/8-inch ID, hemispherical bottom) and heated at a rate of approximately 15 degrees C per minute.

The ignition-temperature values obtained from these studies confirmed the strong dependence of ignition temperature on specific area, and to a lesser degree upon sample weight. The dependence on sample weight is illustrated in Figure 48. The data for irregularly shaped uranium particles in the range -100 +140 and -325 mesh are also included. The lower ignition temperature would be expected because of the greater specific area due to roughness. The mass effect is intimately related to the heat loss associated with the particular geometry used in these experiments. The effect of variation of sample geometry on the ignition temperature will be investigated.

Since conduction in fine particles is low compared with that of larger particles, ignition temperatures for the former should approach a constant value at a lower mass than for the corresponding case with larger particles. This appears to be borne out with -200 +230, -230 +325, and -325 mesh powders.

Data obtained for ignition of uranium powder charges greater than 0.5 gram are shown to compare favorably with the values predicted by theoretical calculations which are described in Section 6 below, as shown in Figure 49.

FIGURE 47

PHOTOGRAPHS OF SPHERICAL AND IRREGULAR URANIUM POWDERS

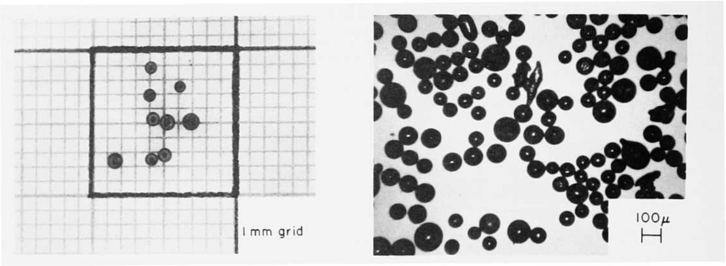

−14 +20 mesh spherical

−200 +230 mesh spherical

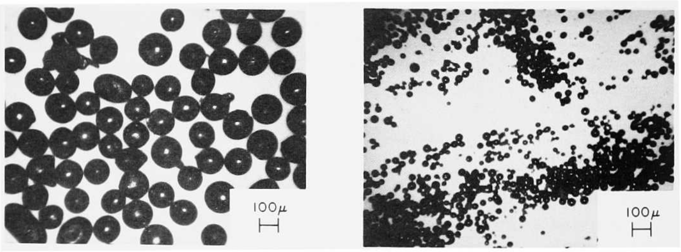

−100 +140 mesh spherical

−325 mesh spherical

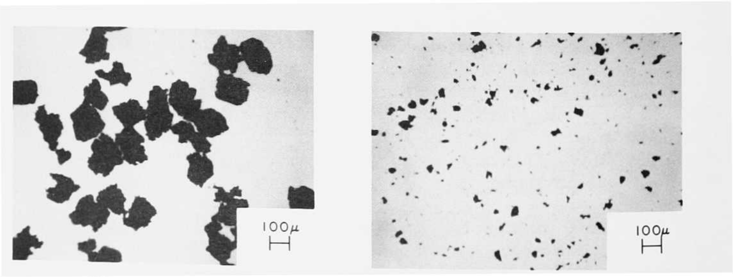

−100 +140 mesh irregular

−325 mesh irregular

FIGURE 48

IGNITION TEMPERATURE OF SMOOTH URANIUM SPHERES DERIVED FROM BURNING CURVES IN OXYGEN ATMOSPHERE

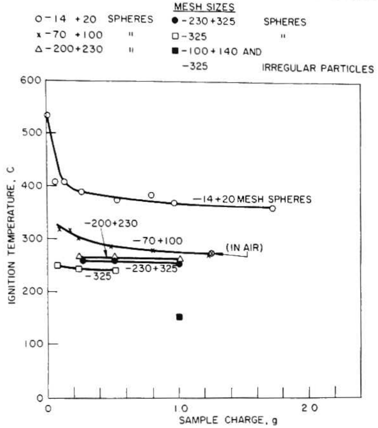

FIGURE 49

COMPARISON OF THEORETICAL AND EXPERIMENTAL IGNITION TEMPERATURES IN OXYGEN FOR URANIUM

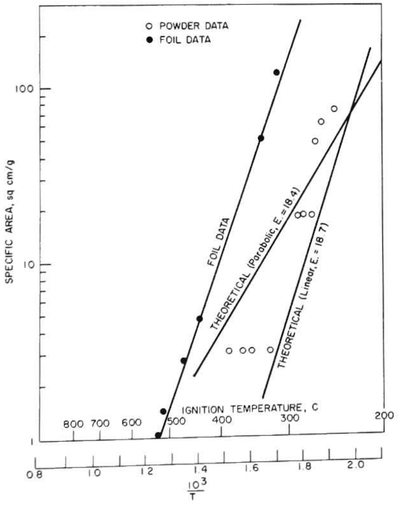

Ignition temperatures obtained from uranium foils (ANL-6068, page 129) are included in this figure for comparison. It is apparent that uranium foils ignite at somewhat higher temperatures than powders of equivalent specific area. This suggests that heat loss from the surface of uranium foils is greater than heat loss by conduction through a powder mass.

The ignition behavior of small charges (~7 to 14 mg) of -325 mesh, irregularly shaped uranium powder was examined by means of a Leitz heating stage combined with microscopic examination. The uranium powder charge under study was arranged on the heating stage in the shape of a mound and heated at a rate of approximately 25 to 50 degrees C per minute. Ignition in oxygen was characterized by a brilliant flash of light and instantaneous disruption of the powder mound. Ignition in air was characterized by a less intense flash of light than in pure oxygen. The mound of powder remained intact for several seconds after ignition, then slowly expanded and ruptured. These experiments confirmed that burning takes place from the inside of the sample to the outside. The general condition necessary for ignition is that the rate of exothermal heat development inside the sample mass be greater than the rate at which the heat can be transferred to the surroundings.

5. Combustion of Various Metals

(H. A. Porte)

Although intensive study of the ignition and combustion behaviors of a few metals is essential, it is felt that the relative importance of particular properties and characteristics can be appraised more quickly by study of metals with wider variations of their properties. This study has included measurements of burning-propagation rates and shielded ignition temperatures of metals chosen from available supplies on the basis of known and more widely differing oxidation kinetics, and physical and thermochemical properties. After it is determined which properties have the greatest effects, it is hoped that a more complete theory of ignition and combustion can be developed.

a. Burning-propagation Rates

The burning-propagation rates of various metals in oxygen have been obtained. A summary of the propagation rates is presented in Table 37, which includes representative uranium and zirconium data. Some of the metals tested would not sustain combustion in oxygen and these metals are also included in the table. As previously determined for uranium and zirconium, a decrease in foil thickness caused an increase in propagation rate. However, the variation of propagation rate with thickness differs for the various metals, as shown in Figure 50.

Table 37

COMPARISON OF BURNING-PROPAGATION RATES IN OXYGEN FOR VARIOUS METALS

Samples in form of either foil or wire. See ANL-5959, page 71, for method

Metal	Thickness (mm)	Width (mm)	Diameter (mm)	Burning-propagation Rate (cm/sec)
Aluminum	0.015	~3.0		-[a]
Cadmium	0.005	~3.0		-[a]
Cobalt	0.30	~3.0		-[a]
Cobalt	0.025	2.9		5.09
Chromium	0.05	2.9		3.56
Chromium	0.013	2.8		5.37
Copper	0.05	~3.0		-[a]
Copper	0.007	3.1		8.32
Hafnium	0.13	~3.0		6.40
Hafnium	0.07	3.0		9.27
Indium	0.05	~3.0		-[a]
Iron	0.28	3.0		0.87
Iron	0.030	3.0		2.74
Iron	0.007	3.2		6.96
Iron			0.23	5.09
Lead	0.17	~3.0		-[a]
Magnesium	0.13	2.8		9.32
Magnesium	0.007	3.2		109
Molybdenum	0.13	3.2		0.96
Molybdenum	0.08	3.1		1.96
Molybdenum	0.05	3.0		2.75
Molybdenum			0.25	2.13
Nickel	0.01	~3.0		-[a]
Niobium	0.030	3.0		12.6
Niobium	0.010	3.1		26.5
Niobium			0.05	49.5
Rhenium			0.52	-[a]
Tantalum	0.25	3.2		1.15
Tantalum	0.13	3.1		2.01
Tantalum	0.05	3.0		4.32
Tantalum	0.007	3.0		39.9
Thorium	0.23	3.0		8.75
Thorium	0.13	3.1		19.4
Tin	0.01	~3.0		-[a]
Titanium	0.29	3.2		6.11
Titanium	0.12	3.1		14.3
Titanium	0.025	3.3		53.3
Titanium	0.007	3.1		138
Tungsten	0.13	~3.0		-[a]
Uranium	0.25	3.0		3.75
Uranium	0.13	3.0		6.04
Uranium	0.03	3.0		24.5
Uranium	0.01	3.0		60.6
Uranium			0.48	5.96
Vanadium	0.28	3.0		1.51
Zinc	0.02	~3.0		-[a]
Zirconium	0.27	3.0		8.24
Zirconium	0.13	3.0		11.1
Zirconium	0.05	3.0		17.3
Zirconium	0.02	3.0		42.8
Zirconium	0.007	4.2		177
Zirconium			0.39	19.9

---

[a] Combustion not sustained, therefore no burning propagation rate measurable.

FIGURE 50

VARIATION OF BURNING PROPAGATION RATES IN OXYGEN WITH THICKNESS FOR VARIOUS METALS

(All samples ~ 3.0mm in width)

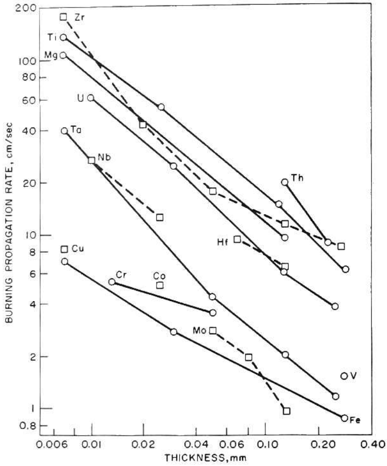

b. Ignition Temperatures

The ignition temperatures (in oxygen) of various metals as measured by the shielded method have been determined and are reported in Table 38, together with previously determined ignition temperatures for uranium (by the burning-curve method) and zirconium. The metals which would not ignite below their melting points were aluminum, cadmium, indium, lead, tin, and zinc. In addition, cobalt, chromium, hafnium, nickel, rhenium, tungsten, and thicker copper and titanium foils would not ignite below 1000 C.

It has previously been demonstrated (ANL-5974, page 28) that for uranium a plot of log specific area versus $1/T_{ign}$ yields a straight line with a slope of $E/2.303$ R, where E is the activation energy obtained from oxidation rate data. The theory predicting this type of relationship has been derived by DeHollander.[20]

The ignition temperature of recently acquired 0.007-mm zirconium foil indicates that the ignition temperature-specific area relationship is more analogous to that of uranium than heretofore suspected. For convenience a plot of both the zirconium and uranium ignition data

---

[20] DeHollander, W. R., HW-44989 (1956)

Table 38

IGNITION TEMPERATURES IN OXYGEN FOR VARIOUS METALS

Shielded experiments using samples in form of wires (25 mm long) or foils (25 x 3 mm), except for uranium, for which burning-curve experiments were used on designated size samples

Metal	Thickness (mm)	Diameter (mm)	Specific Area (sq cm/g)	Ignition Temperature (C)
Aluminum	0.015			> 650
Cadmium	0.005			> 275
Cobalt	0.30			>1000
Cobalt	0.025		90	>1000
Chromium	0.05			>1000
Chromium	0.013		225	>1000
Copper	0.05			>1000
Copper	0.007		319	815 - 846
Hafnium	0.13			>1000
Hafnium	0.07		22	>1000
Indium	0.05			> 125
Iron	0.28		10	840 - 869
Iron	0.030		86	680 - 700
Iron	0.007		363	582 - 605
Iron		0.23	22	817 - 846
Lead	0.17			> 285
Magnesium	0.13		92	605 - 625
Magnesium	0.007		1640	605 - 625
Molybdenum	0.13		16	680 - 705
Molybdenum	0.08		25	675 - 702
Molybdenum	0.05		40	655 - 680
Molybdenum		0.25	16	750 - 777
Nickel	0.01		225	>1000
Niobium	0.030		79	868 - 890
Niobium	0.010		233	580 - 605
Niobium		0.05	94	820 - 846
Rhenium		0.52		>1000
Tantalum	0.25		5.3	845 - 876
Tantalum	0.13		9.7	820 - 849
Tantalum	0.05		25	775 - 800
Tantalum	0.007		172	653 - 675
Thorium	0.22		8.4	>1000
Thorium	0.12		15	975 - 1010
Tin	0.01			> 190
Titanium	0.29			>1000
Titanium	0.12		38	950 - 994
Titanium	0.025		178	940 - 976
Titanium	0.007		630	817 - 847
Tungsten	0.13		8	>1000
Uranium	$3\frac{1}{2}$-mm cube (BMI)		1.1	530
Uranium	0.45 x 8 x 7		2.6	470
Uranium	0.24 x 13 x 14		4.7	385
Uranium	0.13 x 13 x 13		8.5	380
Uranium	0.03 x 13 x 14		49	335
Uranium	0.01 x 15 x 17		121	315
Vanadium	0.28		13	641 - 667
Zinc	0.02			> 410
Zirconium	0.94		4.4	935
Zirconium	0.27		12	833
Zirconium	0.13		25	786
Zirconium	0.02		155	665
Zirconium	0.007		441	643

FIGURE 51

SPECIFIC AREA DEPENDENCE OF URANIUM AND ZIRCONIUM IGNITIONS

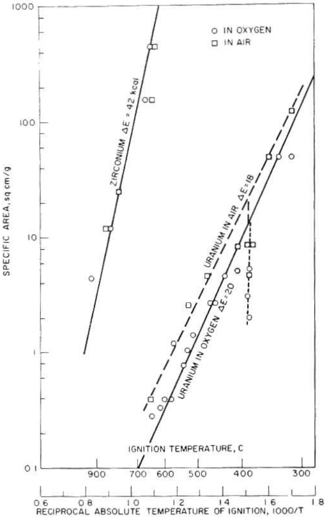

FIGURE 52

SPECIFIC AREA DEPENDENCE OF THE IGNITIONS OF VARIOUS METAL FOILS IN OXYGEN

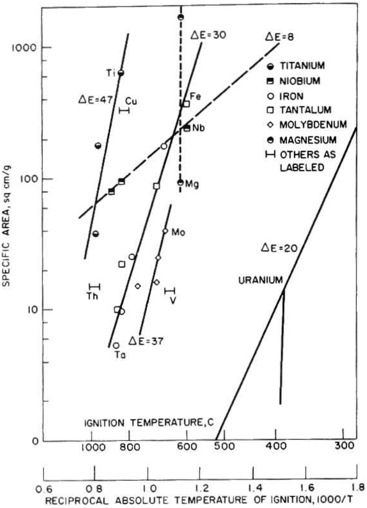

are presented in Figure 51. The agreement between the data and the activation energies obtained from isothermal oxidation studies make similar relationships reasonable for other metals.

In Figure 52 the log specific area is plotted versus $1/T_{ign}$ for various metals. The solid lines through the data were constructed with slopes to correspond to activation energies obtained from oxidation rate data.[21] The agreement is indicative that the rate-controlling process is the same as that for isothermal oxidation. Dotted lines have been drawn for the data pertinent to the metals magnesium and niobium. The mechanisms for oxidation and ignition are believed to be different for magnesium, since it has been established[22] that magnesium vaporizes prior to burning. Therefore, it was not surprising to find that the ignition temperature was independent of specific area. Recent

---

[21] Kubaschewski, O. and Hopkins, B. E., Oxidation of Metals and Alloys, Butterworths Scientific Publications, London, England (1957), page 162.

[22] Coffin, K. P., NACA-TN-3332 (1954).

data[23] on the oxidation of niobium indicates a very low activation energy for the linear oxidation in the temperature range from 450 to 650 C. Further study may demonstrate agreement between this ignition data and isothermal oxidation data.

The ignition temperatures obtained for copper, thorium, and vanadium were only at a single specific area. By drawing lines of the proper slope through these points it should be possible to predict a specific area-ignition temperature relationship for these metals. In a similar manner it should be possible to predict the variation of ignition temperature with specific area for any metal if (a) the oxidation rate activation energy is available and (b) the mechanism of the reaction does not change in the vicinity of the ignition temperature.

The equation describing the variation of ignition temperature with specific area as plotted in Figure 52 is

$$\log S = \log I + (E/2.303 \, RT_{ign})$$

or

$$T_{ign} = E/[2.303 \, R \log (S/I)] \quad ,$$

where

S is the specific area (sq cm/g),

E is the activation energy obtained from oxidation rate data (cal/mole),

R is the gas constant (cal/mole-degree),

T_{ign} is the ignition temperature (K), and

I, the intercept at $1/T = 0$, may be considered as an empirical ignition constant.

The quantity I is analogous to the term A in the Arrhenius equation describing the variation of oxidation reaction rate with temperature:

$$\log K = \log A - (E/2.303 \, RT) \quad .$$

Further considerations may reveal the relationship between them.

A list of A and I values for the various metals is presented in Table 39. From the I values of the various metals, ignition temperatures were calculated for (a) specific area = 1, where the metals are in bulk form, and (b) specific area = 1000, where the metals are in

---

[23] Gulbransen, E. A. and Andrew, K. F., J. Electrochem. Soc. 105, 4 (1958).

Table 39

IGNITION AND OXIDATION RATE CONSTANTS
FOR VARIOUS METALS

Metal	Rate Law Temperature Range[a] (C)	Activation Energy,[a] E (kcal/mole)	Arrhenius Rate Constant,[a] A [(g O_2/sq cm)^n/sec]	Ignition Intercept,[b] I (sq cm/g)
Copper	p 500- 900(Air)	37.7	2.7×10^{-1}	1.2×10^{-5}
Iron	p 500-1100(Air)	33.0	3.7×10^{-1}	3.0×10^{-6}
Molybdenum	p 350-450	36.5	3.6×10^{-2}	1.5×10^{-7}
Niobium	p 200-375	27.4	2.6×10^{-5}	2.5[d]
Tantalum	p 250-450	27.4	3.5×10^{-4}	5.9×10^{-5}
Thorium	1 350-450	22.0	7.8×10^{-1}	2.5×10^{-3}
Titanium	1 830-950	47.0	5.	3.9×10^{-7}
Uranium	1 125-295[c]	19.9	1.7×10^{2}	3.9×10^{-6}
Vanadium	p 400-600	30.7	1.3×10^{-3}	8.2×10^{-7}
Zirconium	c 400-900[c]	42.7	9.9×10^{-4}	3.5×10^{-8}

---

[a] Kubaschewski and Hopkins (unless otherwise indicated):
1 = linear (n = 1); p = parabolic (n = 2); c = cubic (n = 3).

[b] Calculated from the equation $\log \text{spec area} = \log I + (E/2.303\ RT_{ign})$ using specific areas and ignition temperatures from Table 38, and activation energies from this table (unless otherwise indicated).

[c] ANL-5974.

[d] Activation energy of 8.0 kcal/mole used in calculating I.

the form of thin foils. These ignition temperatures are listed in Table 40. The important feature of these lists is not the absolute magnitude of the ignition temperatures, but rather the relative orders of the metals which can be considered as a measure of the pyrophoricity of the metals in the bulk and foil form. It is interesting that uranium remains the most pyrophoric in both bulk and foil, while all of the other metals change their positions in the lists.

Table 40

CALCULATED IGNITION TEMPERATURES OF VARIOUS METALS IN BULK AND FOIL FORMS

Data on Figure 52 extrapolated to common specific areas

Bulk Metal
(Specific Area = 1 sq cm/g)

Increasing Pyrophoricity ↑

Metal	Ignition Temperature (C)
U	527
Mg	615
V	825
Mo	890
Zr	973
Fe	1119
Ta	1135
Ti	1322
Cu	1392 (>m.p.)
Th	1567
Nb	∞

Metal Foil
(Specific Area = 1000 sq cm/g)

Increasing Pyrophoricity ↑

Metal	Ignition Temperature (C)
U	246
Nb	401
V	468
Mo	542
Ta	558
Fe	576
Th	588
Mg	615
Zr	623
Cu	771
Ti	822

6. Theoretical Calculations of Ignition Temperatures of Powders

(M. Tetenbaum)

The object of these calculations was to demonstrate the possibility of systematic trends in metal powder ignition behavior with such factors as reaction rate constants, Arrhenius activation energies, heats of formation, density, specific area, position in the Periodic Table, etc. The theoretical treatment outlined below is essentially that of Murray, Buddery, and Taylor[24] with some modifications.

By means of bulk oxidation data, heats of formation, and allowing for surface area, ignition temperatures can be calculated by converting the isothermal expressions derived to a rising temperature basis. The isothermal heat evolved corresponds to a rise in temperature of the powder mass, since no allowance is made for heat losses. Ignition takes place when the temperature of the powder mass, T, is some value above the container temperature T_c. Generally, the powder mass has been

---

[24] Murray, P., Buddery, J. H., and Taylor, Mrs. J. R., AERE M/R-1428 (1954).

found to be 50 to 100 degrees higher than the container temperature at ignition, and since the ΔT vs T_c curve rises very steeply in the neighborhood of the ignition temperature, a difference in the arbitrary value taken for ΔT should therefore have only a slight effect on the calculated value of the ignition temperature. Taking an arbitrary value of 50 degrees for ΔT, the following expressions can be derived for different rate processes.

Linear

$$\log \frac{531\ \phi\ \rho\ sr}{A\ (\Delta H)E} = -\frac{E}{4.56\ T_i} + \log \left[\left(\frac{RT_i}{E}\right)^2 - 2\left(\frac{RT_i}{E}\right)^3\right]$$

Parabolic

$$\log \frac{2125\ \phi^{\frac{1}{2}}\ \rho\ sr}{A^{\frac{1}{2}}\ (\Delta H)E^{\frac{1}{2}}} = -\frac{E}{9.15\ T_i} + \log \left[\left(\frac{2RT_i}{E}\right)^{\frac{3}{2}} - \frac{3}{2}\left(\frac{2RT_i}{E}\right)^{\frac{5}{2}}\right]$$

Cubic

$$\log \frac{2880\ \phi^{\frac{1}{3}}\ \rho\ sr}{A^{\frac{1}{3}}\ (\Delta H)E^{\frac{1}{3}}} = -\frac{E}{13.71\ T_i} + \log \left[\left(\frac{3RT_i}{E}\right)^{\frac{4}{3}} - \frac{4}{3}\left(\frac{3RT_i}{E}\right)^{\frac{7}{3}}\right]$$

where s = specific heat of metal [cal/(g)(deg)],

ρ = density of metal (g/cc),

r = radius of spherical particle (cm),

ϕ = container heating rate (C/min),

ΔH = heat of formation of oxide (cal/g mole of O_2),

E = energy of activation (cal/mole),

A = frequency factor [$(\text{g/sq cm})^n$/min; linear, $n = 1$; parabolic, $n = 2$; cubic, $n = 3$], and

T_i = container temperature when ignition takes place (K).

The expressions containing T_i can be plotted for various values of T and T_i obtained for any value of r.

The results of theoretical ignition temperature calculations for several Group IV and Group VI elements, and for the triad iron, cobalt, and nickel in the first transition series of the Periodic Table are summarized in Table 41.

Table 41

CALCULATED IGNITION TEMPERATURES FOR GROUPS OF METALS

ΔH - Heat of formation of oxide per gram mol oxygen
E - Energy of activation
A - Frequency factor
K - Reaction rate constant: linear, n = 1; parabolic, n = 2; cubic, n = 3
T_i - Calculated ignition temperature based on heating rate of 10 C/min

Metal	Rate Process	Source[a]	ΔH (kcal/mole)	E (kcal/mole)	A [(g/sq cm)^n/min]	K at 300 C [(g/sq cm)^n/min]	Density (g/cc)	Specific Area of 10-micron Radius Particle (sq cm/g)	T_i (C)
Ti	Parabolic	Gulbransen	225	29.3	1.2×10^{-3}	8.0×10^{-15}	4.5	668	538
Zr	Parabolic	Gulbransen	259	28.6	1.1×10^{-2}	1.3×10^{-13}	6.4	469	410
Zr	Cubic	ANL-5974	259	42.7	5.9×10^{-2}	3.3×10^{-18}	6.4	469	390
Hf	Parabolic	Smeltzer[b]	266	36.0	6.0×10^{-2}	1.2×10^{-15}	13.3	225	695
Th	Parabolic	Cubicciotti	330	31.0	3.5	5.5×10^{-12}	11.2	268	300
U	Parabolic	Murray, et al.[c]	265	18.4	1.2×10^{-9}	1.1×10^{-9}	18.9	159	188
U	Linear 1st Stage	ANL-5974	265	18.7	3.1×10^{2}	2.5×10^{-5}	18.9	159	198
U	Linear 2nd Stage	ANL-5974	265	20.5	2.1×10^{4}	3.2×10^{-4}	18.9	159	160
Cr	Parabolic	Gulbransen	181	66.3	1890	1.2×10^{-22}	6.9	434	810
Mo	Parabolic	Gulbransen	120	36.5	2.13	2.1×10^{-14}	10.2	295	488
W	Parabolic	Gulbransen	135	54.0	0.31	7.6×10^{-22}	19.3	156	914
Fe	Parabolic	Stanley	130	33.0	22.2	6.3×10^{-12}	7.9	379	385
Co	Parabolic	Gulbransen	114	23.4	1.2×10^{-3}	1.4×10^{-12}	8.9	338	458
Ni	Parabolic	Kubaschewski	114	45.0	1.92	1.3×10^{-17}	8.9	337	718

---

[a] Reaction rate constants for most elements (exceptions are noted) obtained from tabulation by Kubaschwski and Hopkins, Oxidation of Metals and Alloys, Butterworths Scientific Publications, London, England, (1953) page 162.

[b] Smeltzer and Simnad, Acta Met. 5, 328 (1957).

[c] Murray, P., Buddery, J. H., and Taylor, Mrs. J. F., AERE M/R-1428 (1954)

It is apparent from Table 41 that uranium is more pyrophoric than the Group IV metals, despite its low specific area value. In general, the metal powders show a systematic trend of increasing ignition temperature values with decreasing reaction rate constants. These trends, based on theoretical considerations, are fairly consistent with the order of ignition temperatures obtained on foils of similar specific area for the variety of metals listed in Table 42. The discrepancies for thorium and molybdenum are probably due to the considerable extrapolation required. It is expected that further considerations of heat losses, sample size and sample geometry will resolve the differences between ignitions of powders and foils. In addition, experiments will be designed to test the assumptions involved in deriving the above equations.

Table 42

COMPARISON OF ORDER OF OBSERVED AND CALCULATED IGNITION TEMPERATURES OF VARIOUS METALS

	Calculated[a] for 10-μ Radius Powder		Observed[b] for Foils	
Metal	Specific Area (sq cm/g)	Ignition Temp. (C)	Specific Area (sq cm/g)	Ignition Temp. (C)
U	159	198	121	315
Th	268	300	268[c]	686[c]
Fe	379	385	363	582-605
Zr	469	390	441	643
Mo	295	488	300[c]	585[c]
Ti	668	538	630	817-847
Ni	337	718	225	>1000
Cr	434	810	225	>1000

---

[a] See Table 41.

[b] See Table 38.

[c] Extrapolated from lower specific area using data from Table 38, on the basis of relationship $\log(\text{Spec. Area}) = \log I + (E/2.303\ RT_{ign})$.

B. Metal-Water Reactions

(L. Baker, R. C. Liimatainen, M. Kilpatrick*)

1. Laboratory Studies - Condenser-discharge Method

(L. Baker, R. Warchal)

The condenser-discharge experiment is an attempt to obtain fundamental rate data under experimental conditions similar to those during a serious accident in a nuclear reactor. Either a nuclear runaway or a sudden loss of coolant during operation of a water-cooled reactor could result in contact between very hot fuel and cladding metals with water or steam and might involve fine particles. The condenser-discharge experiment simulates the limiting case of a nuclear incident in that the heating time is very short and very fine metal particles are produced.

In the condenser-discharge experiment, metal wires are rapidly melted and dispersed in a water-filled cell by a surge current from a bank of condensers. The energy input to the wire indicates reaction temperature; the transient pressure measures reaction rate, the amount of hydrogen generated gives the extent of reaction, and the particle size of the residue indicates the surface area exposed to reaction.

Analysis of the results of a run is based on one of the usual laws of metal oxidation and a simple heat transfer model. In this way, it has been possible to obtain rate constants which, in turn, may be applied toward a detailed analysis of particular reactor conditions.

a. Runs with Uranium

A series of runs with 60-mil uranium wires was reported in a previous quarterly (ANL-6029, page 125). Further runs have been completed using 30-mil specimens. The results are summarized in Table 43. The total extent of reaction, determined from the hydrogen analysis, is plotted as a function of the energy input to the wire and the calculated initial temperature in Figure 53. The previous results obtained with 60-mil wires are also plotted on the figure. It was assumed that the following reaction was the only one to occur:

$$U + 2H_2O \longrightarrow UO_2 + 2H_2 \quad .$$

The gas collected from several runs was analyzed on the mass spectrometer and found to be pure hydrogen. The preliminary results indicate that the extent of reaction is independent of the original wire size. This suggests that a linear rate law may be applicable.

---

* Consultant, Illinois Institute of Technology.

Table 43

URANIUM-WATER REACTION DATA:
CONDENSER-DISCHARGE METHOD

Run	Energy Input (cal/g)	Calc Temp (C) and Physical State	% Reaction	Appearance of Residue
134	26	662, Solid β	0.50	Intact
135	39	840, Solid γ	0.85	Intact
142	53	1133, 30% Liq	3.8	Coarse particles
141	65	1270, Liq	6.8	Coarse particles
140	72	1430, Liq	9.6	Some fines
137	74	1500, Liq	10.2	Some fines
138	75	1530, Liq	8.8	Some fines
155	80	1630, Liq	10.9	Some fines
139	90	1930, Liq	17.8	Mostly fines
153	91	1980, Liq	16.8	Mostly fines
152	93	2030, Liq	16.2	Mostly fines
154	96	2100, Liq	20.1	Mostly fines
157	98	2150, Liq	17.9	Mostly fines
151	99	2200, Liq	19.4	Mostly fines
156	115	2630, Liq	22.7[a]	Fine particles
158	116	2650, Liq	31.0[a]	Fine particles
149	124	2850, Liq	29.0[a]	Powder
148	138	3300, Liq	38.6[a]	Powder

---

[a] Runs had explosive pressure rise.

FIGURE 53
RESULTS OF CONDENSER DISCHARGE RUNS,
URANIUM-WATER REACTION

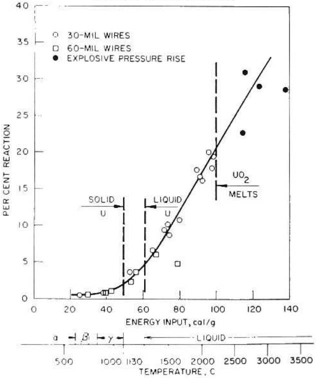

FIGURE 54
PER CENT REACTION AS A FUNCTION OF TIME AND INITIAL URANIUM TEMPERATURE
CONDENSER DISCHARGE METHOD

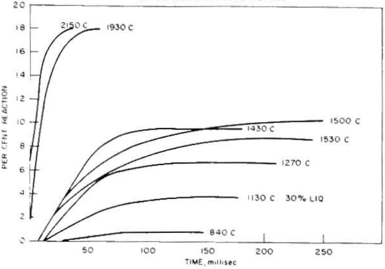

Pressure-time traces were obtained for most of the runs by means of a quartz crystal pressure transducer and an oscilloscope. Electrical noise generated by the discharge obscured results for several of the runs. Clear indications of an explosive pressure rise were obtained in the four most energetic runs. The transient pressure measurements for the remainder of the runs are shown in Figure 54. Runs having initial temperatures in the region between 1900 and 2200 C showed quite rapid rates of pressure rise. Significant reaction occurred in a few milliseconds. More energetic runs, having explosive pressure rises, were essentially completed in one millisecond. The transition between slow reaction rates and explosive rates is not as striking with uranium as it was with zirconium. The point of transition does, however, coincide approximately with the melting point of the uranium dioxide. The induction period reported previously for the 60-mil runs was also found for 30-mil specimens, although the values are only approximate because of the electrical interference. The induction period might result from initial absorption of hydrogen.

b. Nature of the Solid Products of the Reaction

Residues from the uranium runs did not have the spherical shape characteristic of residues from runs with zirconium. The larger particles resulting from uranium runs appeared as though they had been broken open by some internal pressure. The finer particles were irregular flakes or chips. The high-speed motion pictures (4000 frames/sec) indicated that the particles were formed as spheres and broke up at some later time. Further studies, using backlighting and slower film speeds, are under way to determine the point at which the change takes place. It may then be possible to develop a method to determine an average particle weight. The mean size of spheres formed at the high temperature could then be calculated indirectly. Particle size results must precede a complete analysis of the data on the computer.

2. Laboratory Studies - Pressure-pulse Method

(D. Mason, P. Martin)

The pressure-pulse method has been developed to study the reaction of molten metals with water vapor under conditions as nearly isothermal as possible. The metal is heated in vacuum by means of an induction heater. When the desired temperature is attained, a system of electronically operated valves is used to contact water vapor with the metal for a specified period of time. The apparatus and procedure of operation are described in a previous report (ANL-6068, page 153).

Isothermal rate data obtained by this method should provide a check on the results of both the condenser-discharge and the in-pile studies. The method should give the best determination of the form of the rate law to be used to interpret the results of the other methods.

A series of preliminary runs has been completed. Liquid zirconium samples have been reacted with water vapor at about 20 mm pressure. A temperature range of about 1850 to 2100 C has been studied. Some attack of the liquid zirconium on the thoria crucibles has been found.

Temperature measurement is accomplished by means of the two-color pyrometer described in a previous quarterly report (ANL-6101, pages 144 and 145).

a. Zirconium Runs

Table 44 shows the results of the zirconium runs for which accurate temperature data are available. Figure 55 is an Arrhenius plot of the data. The spread in the data may be due partly to unknown amounts of thorium present in the zirconium samples. (Analysis of one sample showed the presence of about seven per cent thorium.)

Table 44

RESULTS OF REACTION OF WATER VAPOR (20 mm Hg) AND LIQUID ZIRCONIUM

(Pressure-pulse Method)

Run	Area (sq cm)	Hydrogen Evolved (cc STP)	Hydrogen Evolved (cc STP/sq cm)	Zr Oxidized (mg/sq cm)	Time (sec)	Temp. (C)
L15	1.3	0.53	0.4	0.9	0.11	1870
L18	1.2	0.71	0.6	1.2	0.11	1960
L17	1.0	0.77	0.7	1.5	0.11	2050
L19	1.1	1.32	1.3	2.6	0.11	2100
L28	0.9	1.00	1.1	2.3	0.48	1915
L26	1.1	1.46	1.4	2.8	1.04	1920
L25	1.0	1.58	1.7	3.4	1.04	1940
L23	0.8	1.28	1.6	3.3	1.04	2030
L27	0.8	1.50	1.9	3.8	1.04	2030

FIGURE 55
ARRHENIUS PLOT OF DATA FOR THE REACTION OF WATER VAPOR AT 20 mm Hg WITH LIQUID ZIRCONIUM. PRESSURE PULSE METHOD

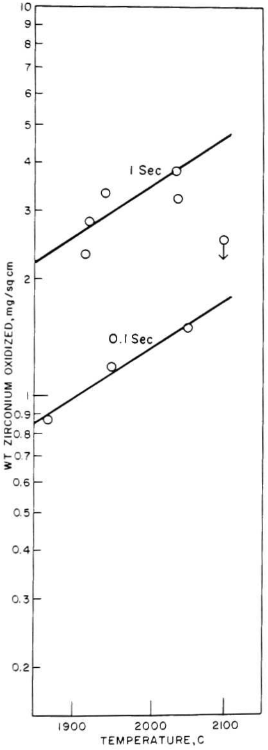

In Figure 55, lines corresponding to a 30-kilocalorie activation energy are shown for the liquid zirconium data. This value has been obtained from the condenser-discharge data.

Figure 56 is a plot of total reaction vs contact time for data extrapolated to the melting point, 1850 C. The parabolic law slope is drawn through the points.

b. Future Work

Runs at high water vapor pressures and longer periods of time are required for verification and extension of the present zirconium data. Since the thoria crucibles have caused much trouble (dissolution in the zirconium and evolution of gas, giving rise to uneven surfaces), graphite crucibles will be tried.

A preliminary aluminum-water run indicated that significant reaction occurred. Necessary modifications to the apparatus are nearly completed and some aluminum runs are to be attempted soon. It is planned to investigate a larger portion of the liquid range up to temperatures where the vapor pressure is quite significant.

3. In-pile Testing in the TREAT Reactor

(R. C. Liimatainen, R.O. Ivins, M. Deerwester, F. Testa)

The purpose of the in-pile testing program in TREAT is to obtain data on metal-water reactions initiated by a nuclear reactor transient. This is accomplished by exposing a small reactor fuel pin to conditions simulating either a power excursion or a loss of coolant incident. Another important purpose of the program is to determine how the fuel pins break up under the influence of reactor excursions of sufficient energy to cause either partial or complete melting.

FIGURE 56
REACTION OF LIQUID ZIRCONIUM AT THE MELTING POINT OF 1850 C WITH WATER VAPOR AT 20 mm Hg, PRESSURE PULSE METHOD

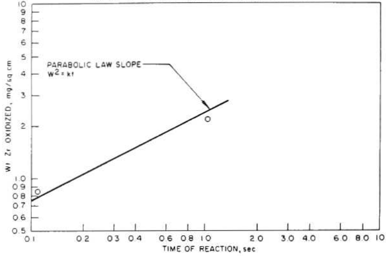

The previous report (ANL-6101, page 147) described the experimental method and the results of the first two series, consisting of eight experiments. Unclad uranium pins were used. The present report describes three series of transients made with fuel pins clad with Zircaloy-2. Additional transients were made to test the behavior of pressure transducers in the transient radiation field. A preliminary correlation of the experimental data available to date is presented.

a. Results of Transients Made with Zircaloy-2-clad Pins

Table 45 summarizes the conditions and results of the metal-water experiments. Transient CEN-9, not listed, was a blank run made in a helium atmosphere with a 90 Mw-sec burst, having a 530-Mw peak power and a 100-msec period. The 20 per cent enriched, Zircaloy-2-clad pin melted completely. The measured thermal neutron dose was 1.53×10^{14} nvt. The number of nvt is determined by activating both aluminum-covered and cadmium-covered 1-mil thick gold foils; the difference between the two is the thermal neutron value.

Figures 57 through 63 show photographs of the pins after the transient. The scale of one-half inch is shown on the figures to allow estimate of the size of the fragments and particles produced. Each fuel element initially had a hole punctured in the bottom end of the Zircaloy-2 jacket, either 3 or 15 mils in diameter, to achieve dispersion of the molten core while the clad still remained intact as a solid. In transients where the core melted but the clad did not, from 0.3 to 14 per cent of the core sprayed out into the water from the simulated ruptured fuel element.

Table 45

SUMMARY OF DATA ON METAL-WATER TRANSIENTS IN TREAT

The pins for these experiments were 20 per cent enriched with U^{235}, Zircaloy-2-clad 20 mils thick, with the dimensions 0.2 inch diameter by 0.5 inch length

CEN Transient No.	14	13	15	10	16	18	17	11	12
Conditions									
Megawatt-seconds	56	60	60	81	90	132	133	153	175
Megawatt peak	270	305	300	378	482	550	580	644	1085
Period, milliseconds	102	104	102	110	96	104	103	100	77
nvt x 10^{-14}, thermal neutron dose by Au foil	0.62	0.66	0.86	1.24	1.37	2.03	2.45	-	-
Size of pin hole, mil	3	3	15	15	15	15	15	3	15
Results									
Max pin surface temp, C	450	980	670	-	1200	1530	770	1430	1400
Max pressure, psia	20	20	270	40	152	59	13	615	660
Per cent of metal reacted by H_2 analysis	0.9	2.0	1.7	2.0	9.1	7.4	7.3	10.1	8.6
Fission energy input, cal/gm by Mo^{99} analysis	55	83	62	-	101	151	180	-	-
Observation of pin after transient									
Clad	not melted but fractured	not melted but bulged	not melted but fractured	partially melted and distorted	completely melted	completely melted	completely melted	completely melted	completely melted
Core	partially melted	partially melted	partially melted	melted	completely melted	completely melted	completely melted	completely melted	completely melted

FIGURE 57

BULGED PIN AND FRAGMENTS
FROM TRANSIENT CEN-13

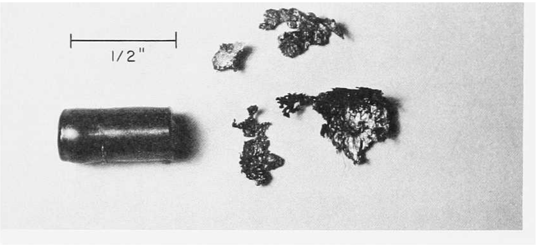

FIGURE 58

FINE-SPRAYED PARTICLES
FROM TRANSIENT CEN-13

FIGURE 59

UNUSED PIN, ZIRCALOY-2 JACKET AND MELTED URANIUM ALLOY OF PIN FROM TRANSIENT CEN-10

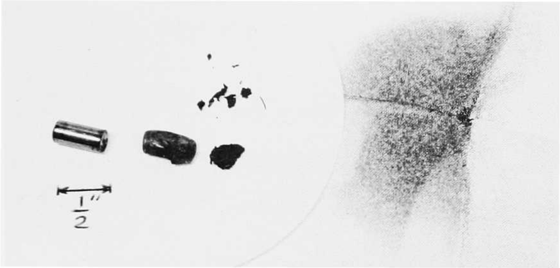

FIGURE 60

UNUSED PIN AND MELTED PIN FROM TRANSIENT CEN-18

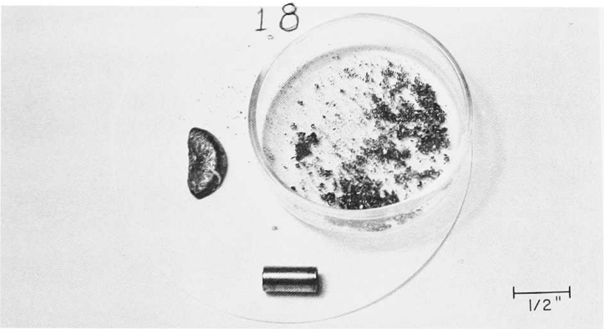

FIGURE 61

LARGE PIECES OF COMPLETELY MELTED PIN FROM TRANSIENT CEN-12 AND UNUSED PIN

FIGURE 62

FINE PARTICLES OF PIN FROM TRANSIENT CEN-12

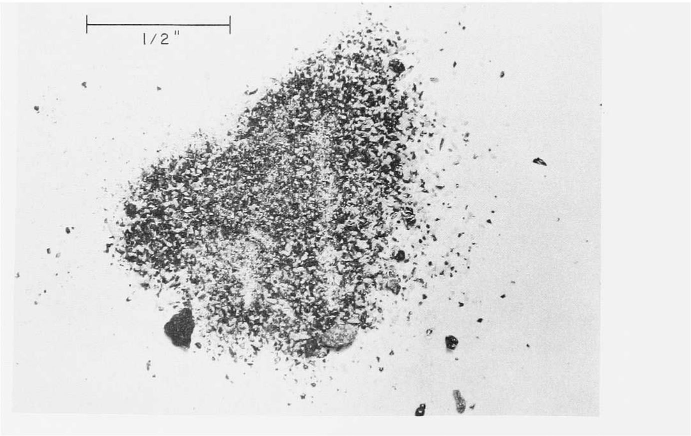

FIGURE 63

PORTION OF PIN FUSED TO AUTOCLAVE COVER FROM CEN-12

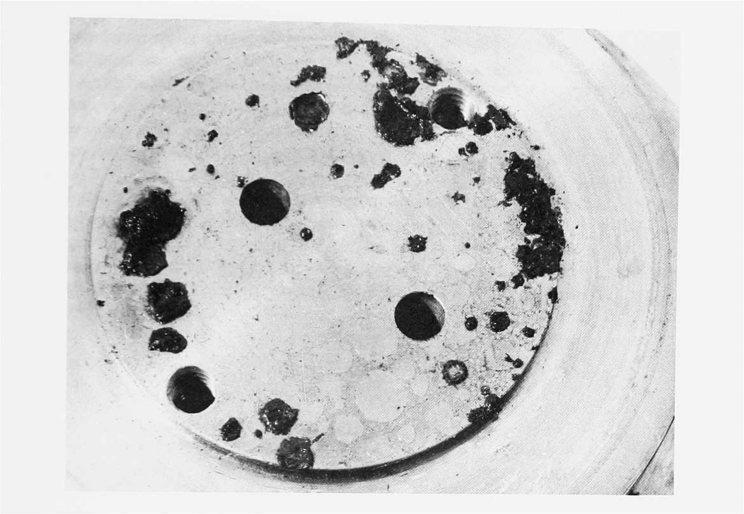

In Run CEN-13, the 60 Mw-sec transient caused the jacket of the pin to bulge as shown in Figure 57; also, the pin hole was enlarged. Both fragments of about one-quarter inch mean width (Figure 57) and particles (Figure 58) were produced. The total amount of fragments plus particles corresponded to 14 per cent of the original weight of the fuel pin. Run CEN-10, an 81 Mw-sec burst, caused considerable distortion of the pin, as shown in Figure 59; also, some fine particles of a powdery nature were produced, as shown in the right portion of the photograph. In CEN-18, the 132-Mw-sec burst resulted in complete melting of both the core and the jacket, as shown in Figure 60, together with the production of the particles shown.

In CEN-12, the most energetic run to date (175 Mw-sec), about 20 per cent of the original mass of the pin was converted into particles in the size range of 5- to 10-mil diameter (see Figure 62). This partial conversion of the metal fuel pin into particles results in a significant increase of the surface area available for reaction relative to the original area of the pin. Figure 61 shows the fragments produced and an unused pin for size reference.

When the autoclave containing the pin and the water from CEN-12 was dismantled, it was evident that a fairly violent event had taken place. The inner ceramic crucible was shattered (the gray pieces in Figure 61 are fragments from the crucible); also, the top of the autoclave showed drops of solidified metal, as shown in Figure 63. Evidently, drops of molten metal had been propelled upward about 5 inches from their original location and splattered and solidified on the walls of the autoclave. The oscillograph record from CEN-12, shown in Figure 64, also gives evidence of sharp temperature rises. The pressure trace, however, was smooth, with no indication of a shock or pulse. The pressure pickups in most of the runs in these series were located on the bottom of the autoclave and thus were exposed directly to the liquid phase. However, no pressure spikes have occurred to date.

FIGURE 64
CEN-12 OSCILLOGRAPH RECORD

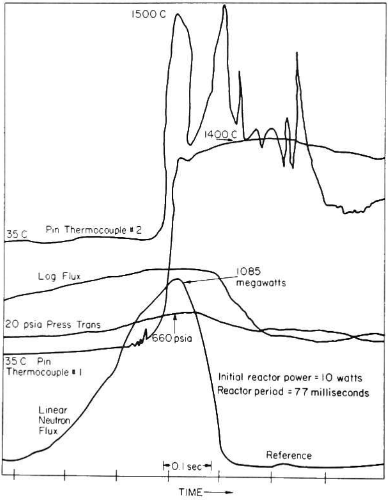

b. <u>Effect of Radiation Field on Pressure Transducers</u>

Two tests were made purely to check the behavior of pressure transducers in the transient neutron-gamma radiation field in the reactor. Unbonded strain gage pressure pickups were exposed to a 140-Mw-sec transient with a 795-Mw peak power on a 77-msec period and showed a behavior similar to that described in the previous report (ANL-6101, page 149). The output of the transducer responded to the neutron flux level while the pressure was constant at one atmosphere. The observed changes in output were 18 and 9 per cent of full scale for a 1000 and 500-psi transducer, respectively. On more severe transients, radiation outputs greater than 50 per cent of full scale have been observed with strain gage pickups.

One transient was made to test a variable reluctance pressure pickup. When exposed to a 520-Mw-sec, 1460-Mw peak, 66-msec transient, the change in output was only 2 per cent of the full scale 100-mv output. The pickup was used with a carrier amplifier-demodulator unit. The small change in output is attributed to the change in ambient temperature that occurs during the transient. This small change in output is considered to be quite encouraging, since this is the first time that essentially a negligible influence of transient radiation on a pressure pickup has been observed in our work. For comparison, from previous tests, an unbonded strain gage would have shown an output caused by radiation of 30 to 50 per cent of its range.

c. Correlation of Results of In-pile Studies

Two correlations of the experimental data available to date are given in Figures 65 and 66. These relationships are submitted as progress reports; hence, the location of the curve relating the two variables is to be considered tentative. As more experimental results are obtained, it is hoped that the accuracy and precision will be improved and that such factors as type of pin, reactor period, etc., can be taken into account in the correlations. The next step in generalizing the data will be by means of an analog computer.

The problem of obtaining a relationship between the total energy of the reactor burst and the fission energy actually imparted to the pin in the autoclave is important for the following reasons:

(1) It is necessary for future application of the in-pile data to reactor hazard analysis.

(2) It is necessary for analog computer evaluation of the data.

(3) It is necessary for comparison with condenser-discharge results.

Three methods have been used to determine the energy input to the pin. The first is an indirect method by gold foil activation. From the measured neutron dose, and the known fission cross section and computed flux depression, the number of fissions is calculated. The second and third analytical methods are direct determinations of the fission products Ba^{140} and Mo^{99}, respectively. Figure 65 gives the linear correlation obtained. The equation of the line, as determined by a weighted least squares, is $Q = 1.2\ E$, where Q is the energy input to the pin in cal/g uranium and E is the energy of the reactor transient in megawatt-sec. A weight of 1.0 was assigned to the indirect gold foil analysis, a weight of 1.5 to the barium determination, and a weight of 2.0 to the molybdenum method.

FIGURE 65

CORRELATION BETWEEN PIN AND REACTOR ENERGY

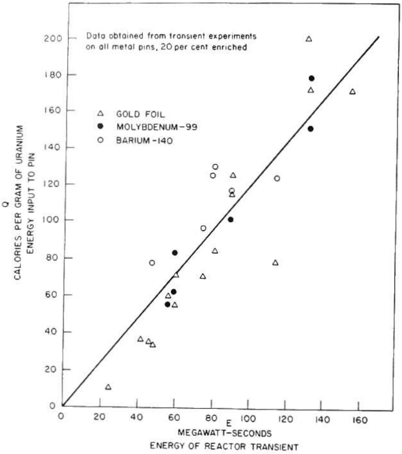

FIGURE 66

METAL-WATER EXPERIMENTS IN TREAT

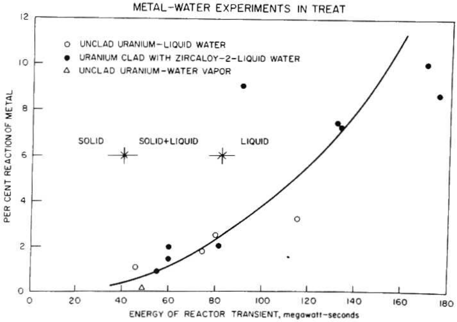

In connection with the burn-up analyses some interesting results were obtained on the extent of volatilization of barium and molybdenum fission products. During Run CEN-12, a 175-megawatt-second transient in which the pin completely melted, 43 per cent of the barium was volatilized from the fuel pin and plated out on the walls of the autoclave. In CEN-18, a 132-megawatt-second transient which also resulted in complete melting of the pin, less than one per cent of the molybdenum was volatilized from the metal.

Figure 66 shows the correlation between extent of reaction and the integrated reactor power. The use of a single line to represent all runs in Figure 66 ignores important variables such as whether the pins were clad or not and does not account for minor changes in reactor period. Three thermal regions are noted on the plot. The divisions are based on observations of the metal pins after the transients. Below 40 Mw-sec the pin retains its cylindrical shape; in the range from 40 to 81 Mw-sec the pin is partially melted. Beyond 81 Mw-sec complete melting results. It is in the region beyond 81 Mw-sec that relatively large amounts of fragments and particles are produced; this gives rise to increased extents of reaction.

It is of interest to make an interpretation of the two correlations of calories per gram energy input and per cent reaction versus the megawatt-seconds to obtain an estimate of the importance of heat losses. Table 46 gives the results at two different temperatures. From thermodynamic data for uranium metal, an energy input of 62 calories per gram is required to heat and melt a pin starting from room temperature if there are no heat losses. During the transient, an energy input of 82 Mw-sec or 98 cal/gram is required to achieve melting, thus giving a 37 per cent heat loss.

Table 46

CALCULATED HEAT LOSSES FROM PIN
BASED ON FISSION ENERGY INPUT

Energy Required (cal/gram)	Pin Temperature (C)	Energy Input to Pin		Per Cent Heat Loss
		(Mw-sec)	(cal/gram)	
62	1130 (melted)	82	98	37
90	1800	170	204	58

These numbers will be applied later in putting the condenser-discharge and TREAT data on the same basis for checking any scale-up effects of the electrically heated wires versus the pins used in the TREAT work.

IV. REACTOR CHEMISTRY

Data are being obtained on the neutron-capture cross sections of uranium-236 as a function of neutron energy.

Work continues on development of a Boiling Slurry Reactor concept (described in ANL-6101, page 160). Problems being examined include preparation of spherical thoria-urania particles and determination of physical properties of thoria-urania materials.

The Reactor Decontamination Program is directed principally to boiling water reactors. It is concerned with the consequences of a fuel element rupture; how much and what types of fission products will be expected to be deposited on the internal surfaces of the reactor system, and what methods are available for removing these deposited activities should this become necessary.

A stainless steel loop simulating the action of a boiling water reactor has been operated with yttrium-90 and cesium-137 tracer activities. Activity deposited is monitored internally on metal samples removed following operation, and externally with a gamma scintillation spectrometer coincident with operation. The latter allows study of the time parameter. Runs to date have been made principally at 200 psig with steam velocities of 0.8 and 1.2 feet per second of from 4.5 to 144-hour duration. A minimum of activity deposition occurs consistently at elevations of 35 to 45 inches above the liquid level.

Laboratory studies are being directed toward corrosion behavior of the alkaline permanganate-citrate procedure toward turbine and other materials, and the selection and evaluation of adequate foaming agents for the transportation of liquid decontaminants with foam techniques. Recent experiments have shown that an overpressure of either hydrogen or oxygen (considerably in excess of that to be expected in reactor operation) during the contamination cycle reduces the decontamination obtained with the alkaline permanganate-citrate procedure.

A program of research directed toward the selection and evaluation of materials for nuclear superheaters has been initiated. Fundamental studies have begun of the corrosion of metals in superheated steam at temperatures up to 560 C and pressures up to 65 atm. Initial phases of the work will concentrate on the effects of simulated radiolytic hydrogen and oxygen in the steam phase.

A. Determination of Nuclear Constants
(C. E. Crouthamel)

Neutron Cross Sections of Uranium-236
(D. Stupegia and R. Heinrich)

The neutron-capture cross sections of uranium-236 are being determined as a function of neutron energy. Neutrons are available in the energy range from about 0.4 to 1.5 Mev, from the Li^7 (p,n) Be^7 reaction produced by bombardment of a lithium target with protons from the Van de Graaff accelerator. The irradiation targets are 1-cm diameter discs of sintered uranium dioxide, each weighing about 0.25 gram and containing 95.16 per cent U^{236}.

Four neutron irradiations of U^{236} targets have been carried out for neutron energies between 0.56 and 0.80 Mev. The activated targets have been gamma-analyzed with the 256-channel analyzer, using a 4-inch by 4-inch NaI detector. The decay of the activation product, 6.7-day U^{237}, was followed through several half-lives. In each case the gamma count of the unirradiated sample must be subtracted from that of the irradiated sample, channel by channel, to get the net resultant counting rate of the activation product for each channel.

In order to carry out the counting calibration, a known amount of U^{237}, having been determined by a 4π-beta count, is introduced into uranium dioxide pellet samples (natural uranium), having the same size and shape as the U^{236} irradiation targets. These standards are then gamma counted by the same procedure as are the irradiation targets, and the absolute amount of U^{237} produced in an irradiation can be determined by a simple comparison with the standard. Work is progressing on the details of the 4π-beta counting of U^{237}.

Since the calibration is not complete, no exact cross sections are available. Approximate calculations show that the values in the neutron range from 0.56 to 0.80 Mev are between 5 and 10 barns. No values appear to be available in the literature.

B. Slurrex Chemistry Supporting Program
(C. E. Crouthamel)

1. Preparation of Spherical Thoria-Urania Particles
(W. G. Knapp)

The method of preparing spherical thoria-urania slurry fuel material by spraying nitrate-stabilized thorium hydroxide sol, containing the required percentage of uranyl nitrate, into a column containing ammonia vapor has been developed to the point where specific application of the method is now planned. Particle size of the material is determined by parameters of the atomization of the liquid. The droplets emitted from the atomizer quickly assume a spherical shape during free fall in the column. The reaction with ammonia to solidfy the liquid sol to a gel takes place very rapidly, so that the thorium-uranium mixture is "frozen" in the spherical shape before it deposits in the column.

There are still details of the atomization which will be studied in an effort to improve control over particle sizes, and particularly to narrow the range about a given size. Other atomizers besides the air-liquid style now used will be tried.

The spherical gel material is washed thoroughly with aqueous ammonium hydroxide, followed by a rinse with alcohol. The ammonium hydroxide wash serves to harden the particles further and to leach out the ammonium nitrate produced from the reaction of ammonia with the nitrate salts of thorium and uranium used for the preparation. The alcohol rinse is used to prepare the material for drying. Use of alcohol prevents, to a large degree, caking of the material during drying.

The material has been air dried and oven dried, the former being preferred. It is then calcined at temperatures up to 1000 C. Sieving to remove extra coarse or extra fine material is the final step in the preparation of the spherical slurry fuel material.

2. Properties of Thoria-Urania Materials

(D. C. Stupegia)

The sizes, shapes, and densities of thoria and thoria-urania particles are being studied by this group. These properties determine the flowing characteristics of the materials and give information for predicting their behavior when slurried in the Slurrex reactor. The effects of particle size, shape, and density upon properties of significance to the Slurrex operation have been mentioned in the previous report (ANL-6101). This report also included a discussion of the method being used for determining particle size distributions. Other investigations of particle properties will now be discussed.

a. Hardness and Abrasiveness

When a flowing slurry contacts its containing vessel, the walls of the vessel will be abraded and the particles themselves will be degraded in size. It is therefore useful to be able to measure quantitatively the hardness and abrasiveness of the particles, and to correlate these properties with size, shape, and density. These effects can be observed in an apparatus in which the particles are jetted and made to impinge upon a metal foil. Such an apparatus was developed at Oak Ridge and a copy of it has been built here. With this equipment, called a jet abrasion tester, one can get a measure of the abrasiveness of a powdered material by observing the time required for the jetted particles to penetrate a steel foil. Further, one can measure the size-degradation of the particles caused by the impingement.

b. Specifications for Slurry Fuels

A list of specifications to be met by thoria-urania fuels for use in a Slurrex reactor has been prepared. Work has been done by this group to determine whether materials prepared by our group could meet certain of these requirements.

Measurements were made to test two of the specifications, namely, those concerning particle-size degradation during autoclaving, and the leaching of uranium out of the particles by nitric acid. Thoria-urania powder prepared by spraying a mixture of thorium hydroxide sol and uranyl nitrate solution was subjected to both tests; that prepared by boiling thorium oxide with aqueous ammonium uranyl carbonate was given only the leaching test.

(1) Uranium Leaching Test

The specification is as follows: "Uranium oxide shall be distributed uniformly throughout the thoria particles. Newly fired material, when subjected to a one hour refluxing in 8 M nitric acid should place less than 3 per cent of the uranium in solution. Repeated refluxing of the washed material should place less than 0.5 per cent of the remaining uranium in solution."

The first material, made by the spraying method, was prepared as follows: mixed thorium hydroxide sol and uranium solution were sprayed into ammonia gas. The resulting gel particles were washed with ammonium hydroxide and then with methanol, and dried at 110 C. Powder passing through a NBS No. 325 sieve was fired at 650 C for 4 hours, and then at 1050 C for 12 hours. This product contained 7.2 per cent uranium and its density was 7.1 g/cc. The results of the leaching test are as follows:

(1) uranium placed in solution by first reflux: 0.85 per cent
(2) uranium placed in solution by second reflux: 0.04 per cent.

It is seen, therefore, that the sprayed material meets the leaching specification.

Thoria-urania prepared by boiling thorium oxide with aqueous ammonium uranyl carbonate was also subjected to the leaching test. The first leaching removed 19 per cent, and the second removed 9 per cent of the uranium. This material clearly did not meet the specification.

It should be noted that the results of this test do not prove that the uranium is or is not uniformly distributed in the thoria particle. One may presume only that if a large amount of uranium is removed, then a probable cause was that the uranium was deposited mainly on the surface of the particle.

(2) Autoclaving Test

The specification is as follows: "The stability of the particles is to be such that after aqueous autoclaving for 48 hours at 300 C, material dried at 200 C shall meet the particle-size specification."

Particle-size distributions were determined before and after autoclaving of the sprayed thoria-urania. A 4.0-gram sample in 25 ml of 0.001 M $Na_4P_2O_7$ was heated in an autoclave at 330 C for 65 hours. These conditions are slightly more severe than required by the specification. The mean particle size and the standard deviation of the weight distribution before and after autoclaving are given in Table 47.

Table 47

PARTICLE SIZE BEFORE AND AFTER "AUTOCLAVING"
SPRAYED THORIA URANIA

Conditions: 4.0-g sample in 25 ml 0.001 M $Na_4P_2O_7$
Autoclaved 65 hr at 330 C

	Mean Particle Size (microns)	Standard Deviation (microns)
Before Autoclaving	20.3	11.5
After Autoclaving	14.9	10.3

These distributions are shown in Figure 67. It is seen that the decrease in average particle size resulted mainly from a degradation of particles in the range of 22 to 50 microns. After autoclaving there is a larger weight fraction in the range from 6 to 12 microns. It is not possible to state exactly whether the size degradation is due to the breakup of primary thoria-urania spheres, or agglomerates of these. Furthermore, without more information on the effects of particle size on slurry characteristics, no exact conclusions can be drawn as to whether this material would be suitable for a slurried fuel.

FIGURE 67
PARTICLE-SIZE DISTRIBUTION OF THORIUM DIOXIDE-URANIUM TRIOXIDE

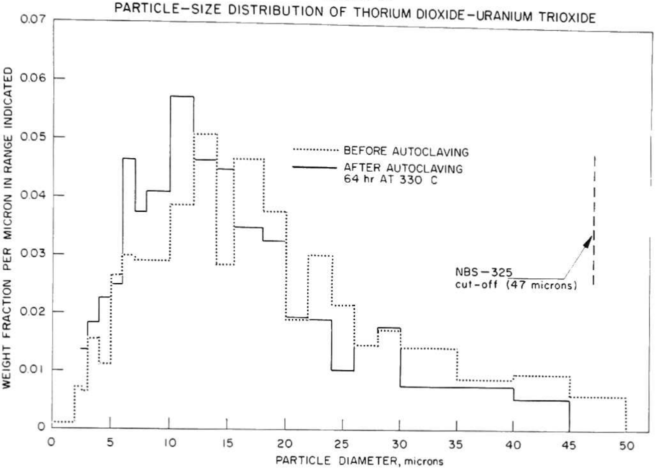

C. Reactor Decontamination

(W. B. Seefeldt)

1. Loop Operations

(D. Grosvenor, C. Bally)

A stainless steel loop which simulates the action of a boiling water reactor has been installed in a shielded cell. The equipment was described in ANL-5858, page 66. The unit is primarily intended to study the deposition characteristics of various fission products in the vapor phases of the system. To accomplish this, mixed or single fission products are introduced in various forms into the water of the circulating loop. The subsequent distribution and deposition of activities from the vapor phase onto surfaces are monitored on metal sample strips inserted into the disengaging section for that purpose. In addition, a scintillation detector is located on the outside of the disengaging section at an elevation of about 8 inches below the steam exit to monitor the deposition of gamma activities at that point.

In the first runs that were made with activity, yttrium-90 was used as the tracer. The results of these runs were reported in ANL-6068 and ANL-6101. Seven additional runs have been made, four with yttrium-90 and three with cesium-137. Runs up to and including Y5B were made at

600 psig. Because of equipment difficulties associated with leakages, the operating pressure for subsequent runs was reduced to 200 psig. Operation at 600 psig will be resumed at a later date. All 200-psig runs were operated with steam velocities of 0.8 ft/sec, with the exception of Run Cs-3, in which steam velocity was 1.2 ft/sec. Run lengths varied from 4 to 68 hr. Equipment modifications have reduced leakage problems considerably.

Much of the data obtained has been related to the elevation in the equipment of the point of observation above a reference point. Figure 68 is a sketch of the disengaging section, showing the reference elevation together with the elevations of related components. This reference is used in all accompanying graphs and texts unless otherwise indicated.

Activity deposition data for several runs are shown graphically in Figure 69 and tabulated in Table 48. The curves obtained by plotting the logarithm of deposited activity vs elevation (Figure 69) are similar to those obtained for earlier runs. The same minimum values previously obtained in an elevation range from 35 to 45 inches were obtained in these 48 to 68-hour runs as well. These minimum values were again in the range of 100 to 200 cpm/sq cm for runs with yttrium-90, while the single result obtained with cesium-137 tracer showed a minimum value of about 6 cpm/sq cm.

FIGURE 68

DISENGAGING SECTION OF LOOP SHOWING ELEVATIONS OF COMPONENTS RELATIVE TO REFERENCE

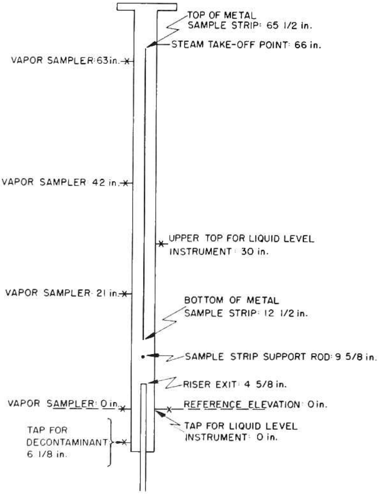

FIGURE 69

BETA ACTIVITY OF 304 SS SAMPLE STRIP

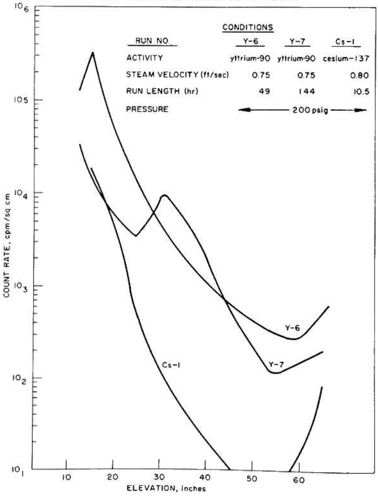

Table 48

TABULATED RESULTS FOR CONTAMINATION RUNS IN BOILING WATER LOOP

Sample Strip: SS304 preoxidized at 600 psi

Run No.	Y5A	Y5B	Y6	Y7	Cs1	Cs2
Operational Data						
Pressure, psig	600	600	200	200	200	200
Steam Rate, ft/sec	0.56	0.56	0.75	0.75	0.8	0.8
Run Length, hr	2.5	30.3	49	4	10.5	68
Activity Identification	Y^{90}	Y^{90}	Y^{90}	Y^{90}	Cs^{137}	Cs^{137}
Quantity, cpm/g ($\times 10^{-10}$)	1.65	4.20	1.69	3.15	4.79	6.06
Steam and Water Data						
Time of Sampling, hr after start of run	1	30	48.5	3.75	No Samples Taken	64
Liquid level at time of sampling, in. above lower liquid level tap (reference point[b])	8.8	3.9	3.1	10.2		14.4
Disengaging Factor[a] (β) (Weight Basis) at						
a. At max elevation[b] 65.5 in.	2.66×10^3		3.5×10^4	1.9×10^4		3.71×10^{4}[c] (γ)
b. At elevation[b] 34.4 in.	2.60×10^3	2.58×10^3	6.6×10^3	1.5×10^4		3.34×10^4 (γ)
c. At elevation[b] 13.5 in.	2.17×10^3	2.40×10^3	2.58×10^2	3.08×10^3		8.45×10^2 (γ)
Activity Deposited on Sample Strip						
a. in liquid phase, cpm/sq cm			3.3×10^5	3.4×10^4	4×10^4 (β)	
b. min in vapor phase			1.90×10^2	0.84×10^2	6 (β)	
c. vapor phase at max elevation (63 in.)[b]			2.2×10^3	2.53×10^2	170 (β)	

---

[a] "Disengaging factor" is defined as the ratio of activity in the liquid phase to that in the steam phase. This factor is often called a "decontamination factor" in the literature but is not so called herein to avoid confusion with the "decontamination factors" reported which are the ratios of activities on solid surfaces before and after various chemical treatments.

[b] Elevation above reference point (see Figure 68).

[c] Sample taken at 42 hr with liquid level of 15.7 in. gave a disengaging factor of 6.67×10^3.

The rise in activity above an elevation of 45 inches remains unexplained. The most likely possibilities include the effect of heat loss from the sample strip to its holder at the top of the loop, and the position of the steam exit line relative to the top of the metal sample strip (see Figure 68).

An effort was made to correlate the ratio of deposited activities to the count level in the circulating loop liquid as a function of time. Three ratios were so examined:

1. deposited activity in liquid phase (cpm/sq cm) to liquid count (cpm/g);
2. minimum deposited activity in vapor phase to liquid count; and
3. deposited activity in vapor phase at maximum elevation to liquid count.

A plot of the first of those listed is shown in Figure 70. Similar efforts made with the other two ratios did not show any reasonable relationship, indicating that other parameters are influencing the amount of activity depositing and that the time factor may not be of major importance in the deposition of activity in the vapor phase in this equipment. This point will be examined more carefully in the future runs.

FIGURE 70

DEPOSITION OF ACTIVITY ON SAMPLE STRIP IN LIQUID PHASE

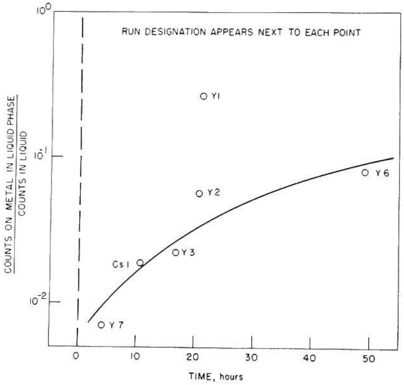

With the beginning of runs involving cesium-137 tracer, it was possible to utilize a single-channel spectrometer for monitoring activity deposition in the disengaging section as a function of time. The crystal head is located 8 inches below the steam takeoff line and is shielded with about 1000 pounds of lead from general background radiation levels. The counts were obtained with a threshold setting of 0.5 Mev. The crystal head location is such that it sees three activities:

1. that deposited on the metal sample strip inside the disengaging section,

2. that contained in the flowing steam, and
3. that deposited on the pipe wall.

Preliminary results indicated that a high percentage (perhaps 90 per cent) of the total activity seen is represented by the last item. A plot of count rate vs time is shown for each of the three cesium runs made to date in Figure 71. After 6 hr of operation in Run Cs-1, a rapid drop in liquid level occurred, accompanied by a rise in the count rate through the same period, from 463 to 4400 cpm/hr. The curve suggests a relationship

FIGURE 71

DISENGAGING SECTION COUNT RATE FOR RUNS Cs-1, Cs-2, Cs-3

RUN NO.	Cs-1	Cs-2	Cs-3
STEAM VELOCITY	0.8 ft/sec	0.8 ft/sec	1.2 ft/sec
ACTIVITY	CESSIUM-137	CESSIUM-137	CESSIUM-137
PRESSURE	200 psig	200 psig	200 psig

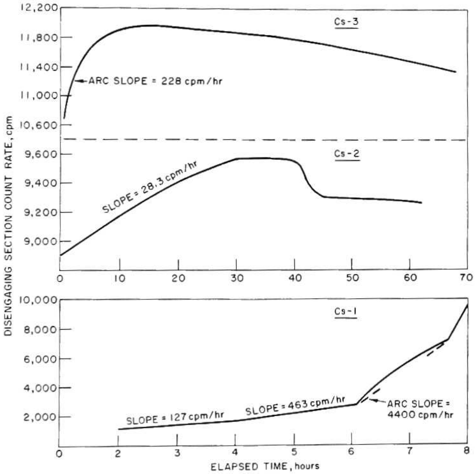

between the rate of rise of the count rate and liquid level. The steam-water mixture enters the $2\frac{1}{2}$-inch disengaging section through a $\frac{1}{2}$-inch stainless steel riser pipe. The expulsion velocity exceeds by a large factor the average steam velocity in the disengaging section. The depth of liquid above the exit pipe provides a baffling action of the rising steam and water, the effectiveness of which is determined by actual depth.

Examination of data from the three cesium runs reveals an inconsistent pattern regarding the rate of rise of the count rate and the liquid level. Some of these results are shown in Table 49. Disengaging factor data have been re-examined to determine whether liquid level has affected these results.

Table 49

RATE OF CHANGE OF COUNTING RATE ON DISENGAGING SECTION AS A FUNCTION OF LIQUID LEVEL

Run No.	Average Liquid Level (inches[a])	Rate of Change of Count Rate (cpm/hr)
Cs-1	7.8	127
Cs-1	9.5	463
Cs-2	9.5	28
Cs-2	15.9	0
Cs-3	14.5	228
Cs-3	16.0	0

[a] Reference point is shown in Figure 68.

The largest disengaging factor obtained to date (second set of samples on Run Cs-2) did coincide with one of the highest liquid levels used to date. However, a factor nearly as large was obtained on Run Y6 with a liquid level 11 inches below that used in Run Cs-2. In the last two runs the count rate decreased slightly with continued exposure beyond 30 to 35 hours and continued to decrease to the termination of the run at 68 hours. The reasons for the beginning of these decreases in the middle of the run is not clear as control of the experiment before and after the 30 to 35 hour mark was equally good.

Certain limitations exist with the present equipment relative to the application of data to boiling water reactors. Deposition data is being obtained on the disengaging section which in a reactor plant comparable to the EBWR would correspond to the vapor spaces in the primary reactor vessel. Application of these data to reactor piping and turbine may be seriously questioned. The primary value of the unit as it now stands is the obtaining of good comparative information regarding the relative deposition characteristics of a wide range of fission products together with how these characteristics vary with surface condition and metal type.

An additional parameter which appears to be significant is the amount of heat loss from a surface. At the present time it appears that the amount of deposition of cesium-137 on the side walls is greater than that which occurs on the metal sample strip on the inside. Considerable heat is lost through the former while the latter is very nearly adiabatic.

Following the cesium-137 runs, mixed fission product activity in the form of long-cooled irradiated metallic uranium will be introduced into the loop. This will be followed by short-cooled metallic uranium and portions of EBWR fuel plates.

2. Laboratory Program

(S. Vogler, H. Tyler)

Laboratory studies are being made to evaluate decontamination methods that may be useful in boiling water reactor systems. Efforts to date have been focused on the decontamination of stainless steel type 304 with liquid reagents.

A recommended procedure for the decontamination of metallic surfaces contaminated by high-pressure steam (~600 psig) involves the use of alkaline permanganate and ammonium citrate or citric acid. Current investigations are aimed at exploiting the use of foam with these reagents in an effort to achieve decontamination with smaller volumes of solution than are necessary with liquid-phase decontamination.

Preliminary corrosion tests on both stainless steel and mild steel have indicated adequate corrosion resistance, especially for stainless steel. The following additional items need to be investigated and evaluated:

1. corrosion behavior of other representative metals;
2. selection and evaluation of an adequate foaming agent; and
3. handling of waste solutions.

Corrosion Behavior

The turbine of a steam generator unit is a complex piece of machinery composed of many different metals, whose uses may be determined by operating conditions. In order to evaluate corrosion resistances properly, it is first proposed to identify metals used in typical turbines. This may be accomplished by determining the turbine components used by major fabricators, i.e., General Electric (Dresden), Westinghouse (Shippingport), Allis Chalmers (EBWR). For example, the EBWR turbine contains the following metals:

1. ASTM-A-113SSC (structural steel)
2. AISI-4140 (steel)

3. Stainless steel type 403 (13 per cent chromium)

4. 1 per cent chromium-$\frac{1}{2}$ per cent molybdenum steel

5. Low carbon steel

6. 13 per cent chromium steel - nonhardening

7. Leaded bronze.

Samples of each of these materials will be subjected to corrosion tests with the contemplated reagents under the most adverse conditions. As the decontamination procedure is of short duration, the testing time need not extend beyond 24 hours. In addition several corrosion tests will be run to determine if coupling of dissimilar metals results in an increased corrosion.

Selection of Foaming Agent

Tests to date have been made with two types of surfactants: an alkyl aryl sulfonate, and an ethylene oxide condensation product with nonyl phenol. The ethylene oxide condensation product is known to react with potassium permanganate. Samples of several different types of surfactants, including fluorinated compounds, are being gathered for laboratory testing. These surfactants will be evaluated on the basis of foam generation, foam stability, and chemical stability to the decontaminating reagents with the aim of selecting the surfactant best suited to the purpose.

Handling of Waste Solutions

A problem of a secondary nature is concerned with the handling of the waste solutions accumulated as a result of decontamination. For example, with dilute solutions evaporation might be one way to reduce waste handling. In order to achieve this in the presence of surfactants, some method of defoaming is probably necessary. In addition, other methods of concentrating the activity of waste solutions, such as scavenging and ion exchange, might be applicable.

Effect of Hydrogen or Oxygen in Reactor Water

Several experiments have been performed to determine if excess hydrogen or oxygen present in the water during the contamination stage would result in a different film than that obtained when water alone is used. Excess hydrogen or oxygen might be expected in an operating reactor because of radiation decomposition of the water. Typical oxygen contents of the steam in the EBWR are 10 to 20 ppm.

In order to magnify the situation, large excesses of oxygen and hydrogen were used. Three experiments were run. One was in the normal manner. In the other two, either oxygen or hydrogen at 80 psi was added to the evacuated sealed autoclave containing the water and irradiated uranium. Then the autoclave in each case was heated so as to yield steam at 600 psig. In all cases the tests continued for $6\frac{1}{2}$ days at pressure. After the tests, the stainless steel liners were cut up for test specimens. Preliminary results indicated that the decontamination tests with specimens obtained in the presence of excess gas gave poorer results than the specimen obtained in water alone.

It is probable that the 80-psi overpressure used in these experiments produced a more severe environment relative to subsequent decontamination than that occurring in boiling water reactors, where an oxygen level of 5 to 20 ppm is typical.

These preliminary results on the effect of the presence of oxygen in the steam substantiate observations made in the Vallecitos Boiling Water Reactor.[25]

D. Structural Materials for Nuclear Superheaters

(E. H. Dewell)

Current efforts, both in the United States and abroad, to increase the steam temperatures of commercial power reactors have created a need for data on the effects of steam and other gases on materials of construction at high temperatures. Although conventional power stations have been operating for many years at temperatures well above those which are present goals in the reactor field, the experience has been limited to a few materials, namely, the austenitic stainless steels and some low chrome steels. Experience is further limited to high-purity steam, whereas the steam in a nuclear superheater is likely to contain both hydrogen and oxygen.

As a part of this program, a high-pressure steam loop is being built to observe the reactions of metals and alloys with steam and other gases at high temperatures and pressures.

1. Materials Requirements

Ideal materials should meet the usual requirements for nuclear applications (low cross section, freedom from excessive radiation damage) and must, in addition, show exceptionally high-temperature strength and

---

[25] Evans, T. F., Danielson, D. W., Gaul, G. G., Corrosion and Contamination in the Vallecitos Boiling Water Reactor. Paper to be presented at the Sixth Annual Meeting of the American Nuclear Society, June 12 to 15, 1960, Chicago, Illinois.

corrosion resistance. At the present time, the latter engineering requirements are the most severe and have forced designers to use materials which are less than ideal from a neutron-economy standpoint, particularly in thermal reactors.

The performance of a given superheater material will depend principally on four factors:

a. The Gas Environment

The composition of the steam phase in an operating superheater is open to question at the present time. Radiolytic reactions will probably produce both hydrogen and oxygen as decomposition gases, but the net decomposition rate must be considered unknown.

Early experiments in the program will be designed to show up differences in behavior of samples exposed to pure steam and those exposed to steam containing simulated gases.

b. The Alloy Composition

Designers have specified austenitic stainless steels for current superheat projects, mostly because of lack of alternative choices. The need for lower cross-section alloys is acute and the development of economical nuclear superheat depends strongly on the eventual availability of such alloys. The basic metallurgical properties of the materials are of obvious importance.

c. The Gas-Metal Interface

The nature of the corrosion film which forms on the surface usually determines the corrosion rate of the material. The film structure in turn depends upon both the alloy substrate and the composition and physical parameters of the gas phase, e.g., temperature, pressure, and velocity.

d. The Nature and Intensity of the Radiation Field

The influence of pile radiation is important for two reasons: it influences the gas phase composition by radiolytic processes, and it alters the structure of both the corrosion film and the base metal by solid-state radiation damage.

All four of these factors will be investigated during the course of the program. The gas environment has been chosen as the logical beginning point.

2. Gas-phase Reactions

Steam passing through a nuclear superheater will undergo a series of radiolytic and thermal reactions to give a steady-state steam composition which can be represented by the net effect of a series of terms:

net decomposition = radiolytic decomposition - radiolytic recombination - thermal recombination.

It is not possible to prevent radiolytic decomposition of an in-pile sample by any known process. In many cases, however, decomposition is unimportant, because it is partially or completely offset by radiolytic or thermal recombination reactions. There is no way to predict the net decomposition which can be expected in a nuclear superheater, but the magnitude of the thermal recombination term in the above expression can be investigated by a series of capsule tests. Such tests are planned as the first experiments under the program.

At high temperatures, mixed hydrogen and oxygen gases can react smoothly with each other to form steam.[26, 27] The reaction takes place in a variety of modes - under some conditions it is a purely surface-catalyzed process and under somewhat different conditions it is both a surface reaction and a homogeneous reaction in the bulk gas phase. Some work has been done on the kinetics of hydrogen-oxygen reactions when these are diluted with steam, but the composition range expected in a superheater has apparently not been investigated.

The velocity of the reaction between hydrogen and oxygen is not only important to the operating reactor; it is also important to the steam-phase corrosion studies which are a part of this program. If the reaction is rapid, the steam composition in the corrosion loop will be difficult to control. Provision for continuous additions of both hydrogen and oxygen will be required along with apparatus for continuous monitoring of their respective concentrations.

---

[26] Lewis, B. and von Elbe, G., Combustion, Flames, and Explosions of Gases, University Press, Cambridge (1938).

[27] Hinshelwood, C. N. and Williamson, A. T., The Reaction between Hydrogen and Oxygen, Clarendon Press, Oxford (1934).

V. ROUTINE OPERATIONS

(H. G. Swope)

A. Waste Processing

(H. G. Swope, J. Harast, K. Bremer, G. Teats, and C. Ryberg)

The total volume of liquid radioactive wastes processed from January through March, 1960 was as follows:

Process	Gallons
Evaporation and Concentration	19,590
Ion-exchange (Cation, only)	1,900
Flocculation	1,640
Filtration	2,800
Absorption on Vermiculite	27
Total	25,957

B. High-level Gamma Irradiation Facility

(H. G Swope, J. Harast, B. Kullen, N. Ondracek, R. Juvinall, R. Jarrett and H. Byerly)

Data for samples irradiated in Rack M-1 during January, February, and March, 1960 are summarized in Table 50.

Table 50

SUMMARY OF IRRADIATIONS PERFORMED IN RACK M-1 DURING JANUARY, FEBRUARY, AND MARCH, 1960

Month	No. of Samples[a]	No. of Special Dosimetry Samples	Total Urn Units[b]	
			Day	Night
January	513	172	801	1721
February	720	251	1110	2165
March	1275	473	2372	2846
Totals	2508	896	4283	6732

---

[a] Equivalent to a No. 2 sized can.

[b] One urn unit = 2×10^6 rads.

The large Rack M-2 has been used almost continuously during this period, with dosages of 27 night units and two dosimetry urn units.

Repairs were required on Rack M-1. The main gear drive was replaced as well as the gears under three rack positions.